Tetrahydropyridine LIMK inhibitors: Structure activity studies and biological characterization

Anthony Champiré, Rayan Berabez, Abdennour Braka, Aurélie Cosson, Justine Corret, Caroline Girardin, Amandine Serrano, Samia Aci-Seche, Pascal Bonnet, Béatrice Josselin, et al.

European Journal of Medicinal Chemistry 271 (2024) 116391

Contents lists available at ScienceDirect

European Journal of Medicinal Chemistry

journal homepage: www.elsevier.com/locate/ejmech

Research paper

Tetrahydropyridine LIMK inhibitors: Structure activity studies and biological characterization

Anthony Champiré [a,1], Rayan Berabez [a,1], Abdennour Braka [a], Aurélie Cosson [b], Justine Corret [b], Caroline Girardin [b], Amandine Serrano [b], Samia Aci-Sèche [a], Pascal Bonnet [a], Béatrice Josselin [c], Pierre Brindeau [c], Sandrine Ruchaud [c], Rémy Leguevel [d], Deep Chatterjee [e,f], Sebastian Mathea [e,f], Stefan Knapp [e,f], Régis Brion [g,h], Franck Verrecchia [g], Béatrice Vallée [b], Karen Plé [a], Hélène Bénédetti [b,**], Sylvain Routier [a,*]

[a] ICOA, Université d'Orléans, CNRS UMR 7311, 45067, Orléans, France
[b] Centre de Biophysique Moléculaire, CNRS UPR4301, 45071, Orléans, France
[c] Sorbonne Université / CNRS UMR 8227, Station Biologique, 29688, Roscoff, France
[d] Plate-forme ImPACcell, UAR BIOSIT, Université de Rennes 1, 35043, Rennes, France
[e] Structural Genomics Consortium, Buchmann Institute for Molecular Life Sciences Goethe- University, 60438, Frankfurt am Main, Germany
[f] Institute for Pharmaceutical Chemistry, Max von Lauestrasse 9, Goethe-University, 60438, Frankfurt am Main, Germany
[g] CRCI²NA, INSERM, UMR 1307, CNRS, UMR 6075, Université de Nantes, 44035, Nantes, France
[h] Centre Hospitalier Universitaire de Nantes, 44000, Nantes, France

ARTICLE INFO

Keywords:
LIMK inhibitors
Synthesis
Molecular modeling
Co-crystallization
Kinase
Cytoskeleton
Cofilin
Cell migration

ABSTRACT

LIM Kinases, LIMK1 and LIMK2, have become promising targets for the development of inhibitors with potential application for the treatment of several major diseases. LIMKs play crucial roles in cytoskeleton remodeling as downstream effectors of small G proteins of the Rho-GTPase family, and as major regulators of cofilin, an actin depolymerizing factor. In this article we describe the conception, synthesis, and biological evaluation of novel tetrahydropyridine pyrrolopyrimidine LIMK inhibitors. Homology models were first constructed to better understand the binding mode of our preliminary compounds and to explain differences in biological activity. A library of over 60 products was generated and *in vitro* enzymatic activities were measured in the mid to low nanomolar range. The most promising derivatives were then evaluated *in cell* on cofilin phosphorylation inhibition which led to the identification of **52** which showed excellent selectivity for LIMKs in a kinase selectivity panel. We also demonstrated that **52** affected the cell cytoskeleton by disturbing actin filaments. Cell migration studies with this derivative using three different cell lines displayed a significant effect on cell motility. Finally, the crystal structure of the kinase domain of LIMK2 complexed with **52** was solved, greatly improving our understanding of the interaction between **52** and LIMK2 active site. The reported data represent a basis for the development of more efficient LIMK inhibitors for future *in vivo* preclinical validation.

1. Introduction

Cell migration is a fundamental cellular property involved in many physiological processes such as embryogenesis, wound-healing, immune defense, but also in disease pathology such as the growth of tumors, their spread *in vivo* and the subsequent development of metastases. Cell movement is regulated by adopting different motility modes [1]. Migration is a cyclic process in which a cell extends protrusions at its front and retracts its trailing end. It is spurred into action by migration-promoting agents that induce polarization. During classical amoeboid cell motility, actin polymerization supplies the pushing force for protrusion of the leading edge to establish the direction of migration. Cofilin, an actin depolymerizing factor, plays an important role in this process to initiate actin filament depolymerization to recycle actin

* Corresponding author.
** Corresponding author.
E-mail addresses: helene.benedetti@cnrs.fr (H. Bénédetti), sylvain.routier@univ-orleans.fr (S. Routier).
[1] These authors contributed equally to this work.

https://doi.org/10.1016/j.ejmech.2024.116391
Received 16 February 2024; Received in revised form 3 April 2024; Accepted 3 April 2024
Available online 9 April 2024

monomers and to control the temporal and spatial extent of actin filament dynamics [2]. Cofilin is inactivated by phosphorylation of its N-terminal Ser 3 by LIMK1 or LIMK2 which are themselves activated by phosphorylation mediated by the kinases ROCK, PAK or MRCK, that are effectors of the Rho family of GTPases (Rho, Rac, Cdc42) [3]. Controlling cofilin phosphorylation is a promising approach to regulate actin polymerization and thus is an interesting therapeutic target to inhibit cancer cell invasion of organs, and metastasis [4–6]. Therefore, molecules able to inhibit cofilin dependent pathways could be good candidates to develop prophylactic and therapeutic anticancer strategies.

To date, and compared to efforts for designing molecules targeting MEK, ERK and ROCK (Rho associated kinases), LIM kinases have been poorly exploited as therapeutic targets, and only a few inhibitors have successfully reached pre-clinical trials [7–9]. A selection of LIMK inhibitors is shown in Fig. 1. As highlighted by the different chemical structures, there is no LIMK specific pharmacophore required for designing potent LIMK inhibitors and all three canonical kinase inhibitor binding modes (type-I, type-II and type-III) can be exploited for inhibitor design [10]. Bristol Myers Squibs (BMS) reported the first family of potent type-I inhibitors using a non-fused *N*-aryl pyrrazoles (**BMS3** and **BMS5/LIMKi3**) which exhibit activities on the two LIMK homologues in the nanomolar range [11–13]. There are also polycyclic molecules such as the pyridocarbazole **Pyr1** [14,15] which has been extensively studied and went to preclinical trials for leukemia, breast cancer and schizophrenia. A larger family containing pyrrolopyrimidine derivatives, mostly developed by Lexicon Pharmaceuticals and Amakem, have also been described, with the dual LIMK/ROCK inhibitor **LX7101** being the only compound to enter clinical trials for glaucoma [16–18]. However, no data have been published after the announcement of the clinical trial. This inhibitor seems to have multiple side effects due to its dual activity, as ROCK regulates several different signaling pathways [19]. One allosteric inhibitor **TH-257**, initially reported by Lexicon [20] was further modified and characterized as a chemical probe [10].

After an intensive **Pyr1** study, Cellipse published an *in vivo* study showing the anti-leukemic activity of **CEL_Amide** synergistically with TKi inhibitors and confirmed the preclinical and clinical interest of LIMK1/2 inhibitors in cancer treatment [21,22]. More recently, a LIMK2 PROTAC, **TH-257-PEG3-VH032**, suggested that LIMKs are implicated in melanoma tumor growth and metastasis in mice [23].

At the start of our medicinal chemistry program, our efforts were concentrated on the modification of the pyrrolo[2,3-*d*]pyrimidine scaffold **II** disclosed by Lexicon as the necessary pharmacophore to strongly interact with hydrogen bonds at the hinge region. They used a piperazine or piperidine core as a central unit to position a second aromatic moiety *via* an amide or a urea, eventually leading to the discovery of **LX7101** [17,18]. The bioisosteric replacement of an N atom *versus* a CH in the central ring attached at position *C*-4 of the pyrrolopyrimidine ring system was not conclusive as the derivative **1** was reported to exhibit only sub-micromolar activity on LIMK2 (Fig. 2). We hypothesized that the loss of both the electronic conjugation at *C*-4 and the electronic enrichment of the pyrimidine ring were detrimental to precisely position the urea group in the active site.

We thus decided to use a tetrahydropyridine core, generating a large library of type **I** inhibitors [24]. The alkene introduced into the tetrahydropyridine was able to restore the electronic density and adopt a more planar conformation and was beneficial for the global interaction of the molecules within the LIMK binding site. Over sixty final products were prepared and *in vitro* enzymatic activities for LIMK1 and LIMK2 were measured for all compounds. A homology-based docking model was built to facilitate Structure-Activity Relationship (SAR) studies. Co-crystallization of the best compound formally established binding mode and highlighted key interactions in the binding site, and its selectivity was measured on a representative panel of 100 kinases. *In cell* biological assays were performed to determine cytotoxicity, cell penetration, the effects on cofilin phosphorylation and cytoskeleton remodeling, and the ability of our best compounds to inhibit cell migration (wound healing assay) using several cell lines in order to evaluate the potential of this innovative lead series.

2. Chemistry

2.1. Library building

Our initial synthetic efforts were directed toward the preparation of a set of secondary tetrahydropyridine derivatives able to furnish the desired urea **III**. We first started with the methyl pyrrolopyrimidine derivative **2**, prepared from 2-cyanoacetamide according to the large-scale optimized synthesis described by Wu in 2007 [25]. Chlorination with $POCl_3$ led to derivative **3** in a 81 % yield (Scheme 1). The cross coupling procedure with the *N*-Boc protected tetrahydropyridine borane **5** and the *C*-6 substituted or non-substituted base **3** or **4** (commercially available) required the use of Na_2CO_3 and 10 % of $Pd(PPh_3)_4$ as catalyst under a microwave irradiation at 120 °C to form **6** or **7** in a satisfying yield (67−72 %) [26]. A final deprotection step led to the stable hydrochloric acid salts **8** or **9** in a nearly quantitative manner.

For additional substitution in position *C*-3, compound **6** was chlorinated or iodinated using nearly stoichiometric amounts of *N*-chlorosuccinimide (NCS) or *N*-iodosuccinimide (NIS) (Scheme 2). Derivatives **10** and **11** were easily purified giving the desired products in 61 % and 90 % yield respectively. The iodine derivative **11** was subjected to a palladium cross coupling reaction with cyclopropylboronic acid but our efforts using this direct pathway failed. Consequentially, the indole NH in compound **11** was tosylated using NaH as base to furnish the protected derivative **12** in a 82 % yield. The cross-coupling reaction was successfully carried out in a toluene/water mixture under microwave irradiation (60 % yield). As classical conditions with PPh_3 led to impurities, a switch to PCy_3 as the palladium ligand increased the reaction yield. The deprotected chlorine derivative **15** was obtained with HCl in 1,4-dioxane treatment from **10.** A two-step deprotection sequence was performed with compound **13** by first treating it with KOH in water to remove the tosyl protecting group, followed by Boc deprotection with either TFA and neutralization to give the free base **14**, or treatment with

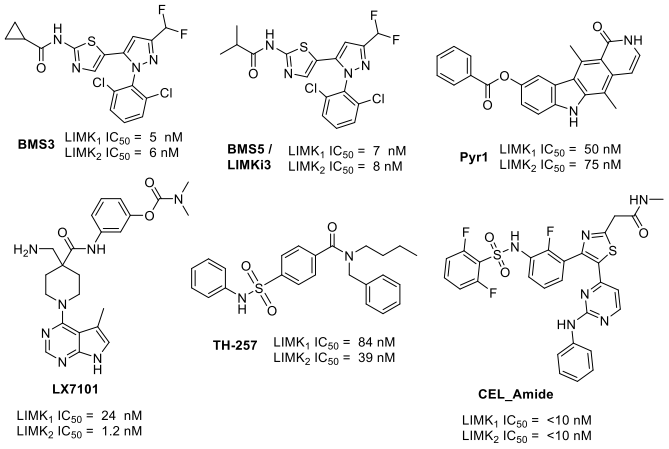

Fig. 1. Several potent LIMK kinase inhibitors.

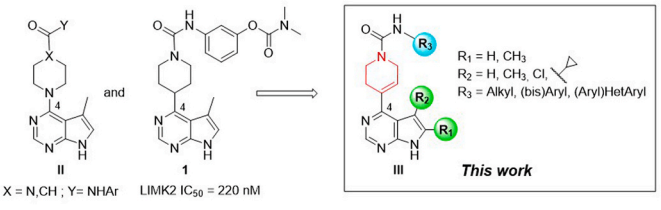

Fig. 2. Pharmacophore structures **II** and **III** leading to LIMK inhibition.

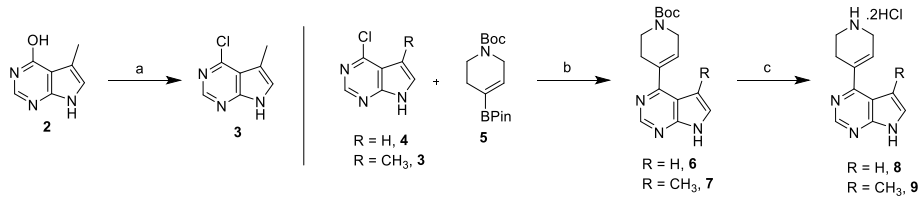

Scheme 1. Reagents and conditions: a) $POCl_3$, reflux, 40 min, 81 %; b) $Pd(PPh_3)_4$ (0.1 equiv.), 2 M aq. Na_2CO_3 (3.0 equiv.), THF, μW, 120 °C, 75 min, **6**: 72 %, **7**: 67 %; c) 4 M HCl 1,4-dioxane solution (15.0 equiv.), rt, 1 h, **8**: 96 %, **9**: 96 %.

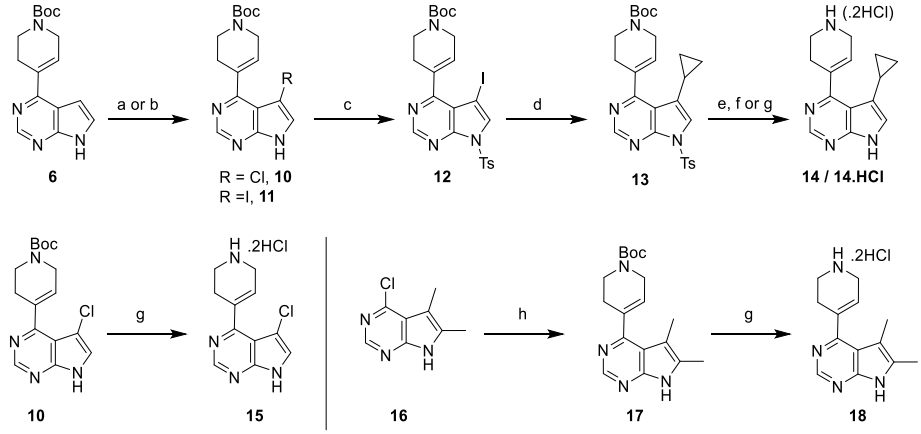

Scheme 2. Reagents and conditions: a) NCS (1.05 equiv.), anhydrous DMF, 70 °C, 4 h, **10**: 61 %; b) idem with NIS (1.05 equiv.), **11**: 90 %; c) TsCl (1.1 equiv.), NaH 60 % in oil (1.2 equiv.), THF, rt, 16 h, 82 %; d) $CyPrB(OH)_2$ (2.3 equiv.), K_3PO_4 (3.5 equiv.), Pd $(OAc)_2$ (0.1 equiv.), PCy_3 (0.2 equiv.), toluene/water 10/1, μW, 140 °C, 1 h, 60 %; e) KOH (9.0 equiv.), THF/water 5/1, reflux, 24 h; f) TFA (35 equiv.) rt, 2h then neutralization with 2 M aq. NaOH, **14**: 85 % (2 steps); g) 4 M HCl 1,4-dioxane solution (8.0 equiv.), rt, 1 h, **14.HCl**: 98 % (2 steps); **15**: 95 %; **18**: quant.; h) $Pd(PPh_3)_4$ (0.1 equiv.), 2 M aq. Na_2CO_3 (3.0 equiv.), THF, μW, 120 °C, 1.5h, quant.

HCl in 1,4-dioxane to give **14.HCl**. Finally, the *C*-2 and *C*-3 bis methylated pyridopyrimidine intermediate **17** was prepared on a multigram scale from chloride **16** [24] and was subjected to the cross-coupling reaction and deprotection with HCl to afford the tetrahydropyridine pyrrolopyrimidine **18**.

In the last step, the urea function was incorporated in the final products with derivatives **8**, **9**, **14, 14.HCl, 15** and **18** in basic media using one of three methods (Table 1). The first method (A) consisted of reaction of the amine derivative with commercially available isocyanates in the presence of diisopropylethylamine (DIPEA) at 0 °C. This led to the synthesis of 19 derivatives (**19**, **21**–**25**, **27**, **31**–**33**, **35**, **36**, **44–47,** and **57–59**) with yields ranging from 35 to 80 %. The second method (B) required the *in situ* preparation of a *p*-nitrophenylcarbamate starting with a chosen aniline followed by the addition of a solution containing the dihydropyridine salt in solution with an excess of DIPEA. This second strategy led to 22 products (**20**, **26**, **28**–**30**, **34**, **40–43**, **48–56,** and **60–62**) in moderate to good yields (45–82 %). Finally, for derivatives **37–39**, we synthesized the urea using an isocyanate generated under Curtius rearrangement conditions (C), but this third method led to more complex purifications, and overall lower yields.

3. *In vitro* evaluation

3.1. LIMK assays

Each final compound was evaluated for its capacity to inhibit both LIMK1 and LIMK2 enzymes, and the inhibition constants Ki were measured using LanthaScreen™ Eu Kinase Binding Assay from Thermo Fisher Scientific Service. Structure activity relationships could be analyzed from the synthesized library (Table 2). More than half of the compounds inhibited LIMK1 more effectively than LIMK2, with the majority exhibiting a Ki value below 50 nM for either LIMK1 or LIMK2. A modest selectivity of LIMK1 *vs.* LIMK2 (Ki ratio higher than 4) was observed for several compounds.

In general, compounds substituted by a hydrogen or a methyl group in position *C*-5 of the pyrrolopyrimidine ring and with a monoaryl urea (substituted or unsubstituted), gave LIMK1/LIMK2 inhibition constants in the submicromolar range (entries 1–15). Several exceptions could be noted, first with derivatives **23** and **24** bearing a chlorine or bromine atom in the meta position of the phenyl urea with Ki values around 50 nM for LIMK1 and 100 nM for LIMK2 (entries 5, 6). Furthermore, the introduction of a dimethylcarbamate moiety in the same position of the aryl urea increased the inhibition of both enzymes (compound **30**, entry 12) showing an excellent inhibition of 46 and 12 nM for LIMK1 and LIMK2 respectively.

The absence of a substituent at *C*-5 lead to a slight loss of activity compared to the methylated analogues (compounds **19** and **20** *vs.* **23** and **30**). Replacing the methyl group by a chlorine atom as a bioisostere of the methyl group in the *C*-5 position was also detrimental (entries 36–38), with a slight decrease in activity on LIMK1 and stabilization of activity on LIMK2 (compounds **54–56** vs. **23**, **24** and **30**). Compound **56**, possessing a carbamate residue, remained the best candidate in this mini-series, with activities of 58 and 9 nM on LIMK 1 and 2 respectively (entry 38), with a surprising preference for LIMK2. The switch from a methyl to a cyclopropyl substituent in the R_2 position of the pyrrolopyrimidine core was then performed. We chose this group because it has the size, lipophilicity and electronic character between an alkyl group and a halogen atom. This modification resulted in significantly improved Ki values for LIMK2 compared with the methyl analogues. The chlorinated and brominated derivatives **46** and **47** (entries 28 and 29) were almost three times more active on LIMK2 than compounds **23** and **24** (entries 5, 6), with almost identical inhibition of LIMK1. This impact was confirmed by observing the effect of compound **48**, which inhibited LIMK2 as low as 3 nM. Finally, the di-substitution of the

Table 1
Urea synthesis and compound library.

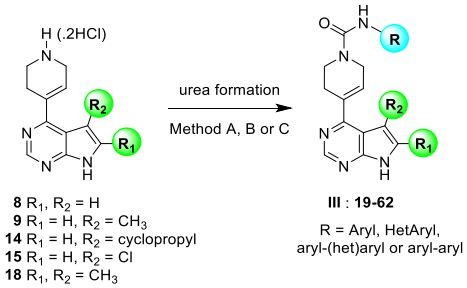

Entry	Starting material	R	Method[a]	Cpd (Yield)[b]	Entry	Starting material	R	Method[a]	Cpd (Yield)[b]
1	**8**		A	**19** (71 %)	23	**9**		B	**41** (72 %)
2	**8**	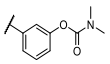	B	**20** (45 %)	24	**9**	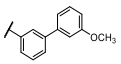	B	**42** (78 %)
3	**9**		A	**21** (80 %)	25	**9**	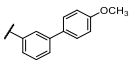	B	**43** (72 %)
4	**9**		A	**22** (60 %)	26	**14**		A	**44** (38 %)
5	**9**		A	**23** (47 %)	27	**14**		A	**45** (56 %)
6	**9**		A	**24** (70 %)	28	**14**		A	**46** (67 %)
7	**9**		A	**25** (46 %)	29	**14**		A	**47** (50 %)
8	**9**		B	**26** (70 %)	30	**14.HCl**	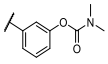	B	**48** (59 %)
9	**9**		A	**27** (35 %)	31	**14.HCl**		B	**49** (48 %)
10	**9**		B	**28** (78 %)	32	**14.HCl**		B	**50** (70 %)
11	**9**		B	**29** (78 %)	33	**14.HCl**		B	**51** (58 %)
12	**9**	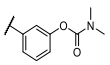	B	**30** (57 %)	34	**14.HCl**	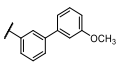	B	**52** (67 %)
13	**9**		A	**31** (72 %)	35	**14.HCl**	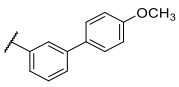	B	**53** (67 %)
14	**9**		A	**32** (76 %)	36	**15**		B	**54** (82 %)
15	**9**		A	**33** (47 %)	37	**15**		B	**55** (60 %)
16	**9**		B	**34** (60 %)	38	**15**	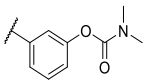	B	**56** (70 %)
17	**9**		A	**35** (59 %)	39	**18**		A	**57** (72 %)

(*continued on next page*)

Table 1 (*continued*)

Entry	Starting material	R	Method[a]	Cpd (Yield)[b]	Entry	Starting material	R	Method[a]	Cpd (Yield)[b]
18	**9**	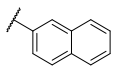	A	**36** (60 %)	40	**18**	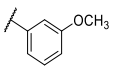	A	**58** (55 %)
19	**9**	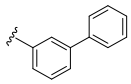	C	**37** (34 %)	41	**18**		A	**59** (75 %)
20	**9**	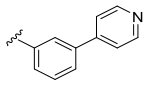	C	**38** (15 %)	42	**18**	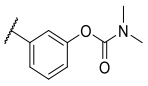	B	**60** (58 %)
21	**9**	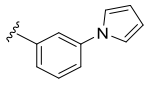	C	**39** (49 %)	43	**18**	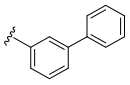	B	**61** (48 %)
22	**9**	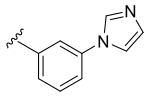	B	**40** (45 %)	44	**18**	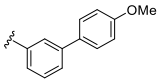	B	**62** (50 %)

[a] ***Method A***: DIPEA (3.0 equiv.), RNCO (1.1 equiv.), CH_2Cl_2, 0 °C, 30 min; ***Method B***: DIPEA (1.1 equiv.), RNH_2 (1.0 equiv.), 4-NO_2PhOCOCl (1.2 equiv.), THF, 0 °C, 30 min then **8**, **9**, **14**, **14.HCl**, **15** or **18** (1.2 equiv.), DIPEA (2.1 equiv.), THF, 50 °C, 2 h; ***Method C***: Curtius rearrangement: RCOOH (1.0 equiv.), Et_3N (1.2 equiv.), ethyl chloroformate (1.5 equiv.), THF, 0 °C, 1 h, 0 °C then NaN_3 (1.5 equiv.), 0 °C, 1.5 h then toluene reflux, 1 h and addition of **9** (1.0 equiv.), DIPEA (2.2 equiv.), CH_2Cl_2, 0 °C.

[b] Isolated yields.

pyrrolopyrimidine core was investigated by introducing CH_3 groups at both the *C*-5 and *C*-6 positions. The electronic enrichment of the ring and the contribution of lipophilicity in these positions had a beneficial effect on inhibition for both kinases. Activities were enhanced irrespective of the urea substitution employed (entries 39–44). The best inhibition in this monoaryl urea series was observed with the brominated and dimethylcarbamate derivatives **59** and **60**, with slightly improved efficiency compared to the monomethyl pyrrolopyrimidine core (**30**).

Pyridine, thiophene and naphthalene residues were also used to generate ureas **34**–**36**, but the observed activities showed no significant amelioration (entries 16–18) except for the naphthene derivative, which led to affinities less than 100 nM on both kinases. Armed with this positive result, we then disassociated the two aromatic rings by generating a first biaryl compound **37** (entry 19). The result was unequivocal, with Ki values of 13 and 25 nM on LIMK 1 and 2 respectively. This compound (**37**) was 6–9 times more active than the mono phenyl derivative **21** on both kinases. We then changed the second phenyl residue for a pyridine ring (**38**, entry 20), a pyrrolidine (**39**, entry 21) and finally an imidazole (**40**, entry 22) and no significant decrease in inhibition was observed showing that the presence of one or more heteroatoms was tolerated. We next introduced ortho, meta and para electron-donating groups (OMe) on the second aromatic ring (entries 23–25). Substitution in the ortho position favored LIMK2 vs. LIMK1 inhibition, while substitution in the para position had no real effect compared to the unsubstituted derivative **37**. The meta methoxy derivative **42** exhibited activity on LIMK1 comparable to our initial bis-aryl derivative **37,** with a threefold improvement for the inhibition of LIMK2. This suggests that the electron character of the second aryl group and the congestion in this region of the catalytic pocket is essential. To further explore our SAR studies, we once again switched the R_2 group for a cyclopropyl and introduced different (heteroaryl)phenyl ureas. All bis (het)arylated products **49**–**53** showed Ki between 5 and 28 nM for LIMK1 and LIMK2. We can note that the presence of the cyclopropyl group diminishes the impact of the methoxy group substitution of the second aromatic ring as all derivatives in this series (**51**–**53**, entries 33–35) show similar Ki values.

3.2. ROCK assays

We then further characterized our library by determining ROCK1 and ROCK2 inhibition at 1 μM by using the Z′-LYTE™ Kinase Assay from Thermo Fisher Scientific Service (Table 2). As previously mentioned, these two kinases are directly upstream of LIMKs, and we wished to avoid, if possible, dual inhibition as ROCK regulates several different signaling pathways and could generate harmful side-effects, as suspected for LX7101. Our goal was to obtain selective LIMK1 and LIMK2 inhibitors with regards to ROCK1/2. Although the values varied, a trend could be discerned. Products bearing an H or a chlorine atom in the *C*-5 position of the pyrrolopyrimidine were much less selective than the other series (entries 1, 2, 36–38). Among the most active LIMK inhibitors in the *C*-5 methyl pyrrolopyrimidine series, products substituted with a bisaryl urea (entries 19, 23–25) or a phenylcarbamate (entry 12) showed good to moderate ROCK inhibition. Compounds **37** and **41** should be highlighted as they were potent LIMK inhibitors with low ROCK inhibition (less than 30 % at 1 μM). The same observation was made examining C-5 cyclopropyl-substituted compounds **49** and **51**–**53** that were highly active and selective for LIMKs. The best LIMK selectivity was achieved by the bismethylated pyrrolopyrimidine compounds **57**–**62**. The majority were very potent and selective LIMK inhibitors with little to no ROCK inhibition, whatever the nature of the urea.

4. Probe synthesis and *In vitro* LIMK/ROCK inhibition assays

With this data in hand, we then prepared several fluorescently labeled probes to visualize cell penetration. We chose to make two compounds using the bisaryl urea motif and focused our attention on the active compounds **42** and **52** possessing a methyl or a cyclopropyl pyrrolopyrimidine tetrahydropyridine scaffold. For these derivatives, SAR analyses and molecular modeling indicated that the *meta* methoxy group of the second aryl ring was well tolerated and solvent exposed. We thus hoped that incorporating a small linker and a fluorophore in this position would only minimally affect activity toward LIMK1 and LIMK2.

The first step of the linker synthesis was a Mitsunobu reaction with the commercially available 3-(Boc-amino)-1-propanol and 3-bromophenol **63** to afford the bromide derivative **64** in 76 % yield (Scheme 3). Suzuki-Miyaura coupling of **64** with 3-nitrophenylboronic acid under microwave irradiation followed by the reduction of the nitro group gave the desired bisaryl aniline derivative **65** in 79 % overall yield. Coupling of this derivative to the pyrrolopyrimidine base **9** or **14.HCl** furnished the Boc protected compounds **66** and **67** in 58 and 41 % yields

Table 2
Ki values of our compound library on LIMK1/2 and % inhibition of ROCK1/ROCK2 at 1 μM.

Entry	Compound Number	Substitution on type III compound	Ki (nM) LIMK1	Ki (nM) LIMK2	% inh. ROCK1[a]	% inh. ROCK2[a]
1	**19**	R = 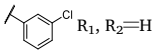	93	213	99	71
2	**20**	R = 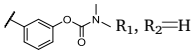	137	39	87	70
3	**21**	R = 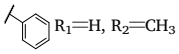	82	234	81	59
4	**22**	R = 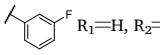	124	319	86	69
5	**23**	R = 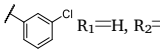	51	105	72	70
6	**24**	R = 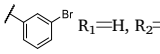	52	106	94	78
7	**25**	R = 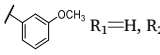	128	264	60	45
8	**26**	R = 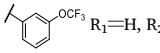	85	150	54	39
9	**27**	R = 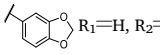	481	693	79	59
10	**28**	R = 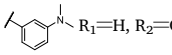	116	428	34	26
11	**29**	R = 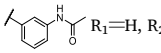	186	181	98	95
12	**30**	R = 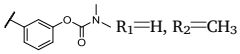	46	12	66	31
13	**31**	R = 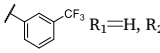	142	161	71	59
14	**32**	R = 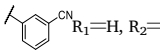	244	268	46	30
15	**33**	R = 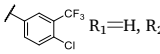	114	116	79	69
16	**34**	R = 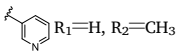	1420	2850	55	39
17	**35**	R = 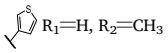	50	186	96	87
18	**36**	R = 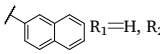	75	91	73	56
19	**37**	R = 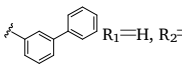	13	25	23	21
20	**38**	R = 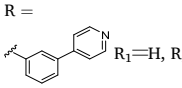	54	128	17	18
21	**39**	R = 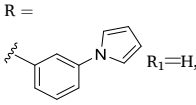	41	101	74	65
22	**40**	R = 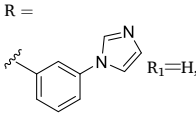	190	180	40	25

(*continued on next page*)

Table 2 (*continued*)

Entry	Compound Number	Substitution on type III compound	Ki (nM) LIMK1	Ki (nM) LIMK2	% inh. ROCK1[a]	% inh. ROCK2[a]
23	**41**	R = 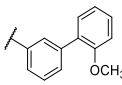 R_1=H, R_2=CH_3	27	14	30	17
24	**42**	R = 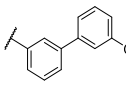 R_1=H, R_2=CH_3	15	8	63	22
25	**43**	R = 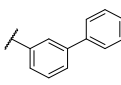 R_1=H, R_2=CH_3	12	25	48	46
26	**44**	R = 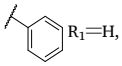 R_1=H, R_2 = CycPr	90	136	45	21
27	**45**	R = 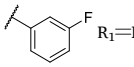 R_1=H, R_2 = CycPr	109	86	37	10
28	**46**	R = 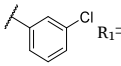 R_1=H, R_2 = CycPr	61	32	54	31
29	**47**	R = 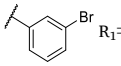 R_1=H, R_2 = CycPr	63	32	73	37
30	**48**	R = 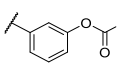 R_1=H, R_2 = CycPr	32	3	28	19
31	**49**	R = 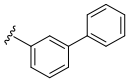 R_1=H, R_2 = CycPr	28	10	9	8
32	**50**	R = 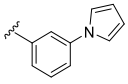 R_1=H, R_2 = CycPr	13	10	36	35
33	**51**	R = 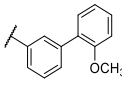 R_1=H, R_2 = CycPr	21	7	28	19
34	**52**	R = 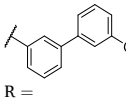 R_1=H, R_2 = CycPr	22	5	19	12
35	**53**	R = 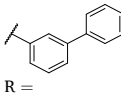 R_1=H, R_2 = CycPr	20	21	20	11
36	**54**	R = 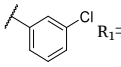 R_1=H, R_2=Cl	113	104	91	84
37	**55**	R = 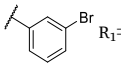 R_1=H, R_2=Cl	99	75	96	78
38	**56**	R = 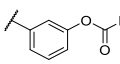 R_1=H, R_2=Cl	58	9	77	61
39	**57**	R = 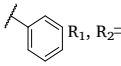 R_1, R_2=CH_3	17	108	4	−5
40	**58**	R = 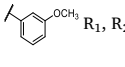 R_1, R_2=CH_3	15	79	3	−1

(*continued on next page*)

Table 2 (*continued*)

Entry	Compound Number	Substitution on type III compound	Ki (nM) LIMK1	Ki (nM) LIMK2	% inh. ROCK1[a]	% inh. ROCK2[a]
41	**59**	R = 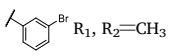	7	23	0	7
42	**60**	R = 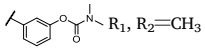	31	18	3	−4
43	**61**	R = 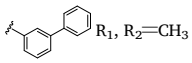	9	17	2	−6
44	**62**	R = 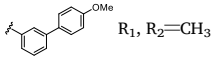	4	27	1	0

[a] Measured at 1 μM compound concentration. Experiments were performed in duplicate (n = 2). CycPr = cyclopropyl residue.

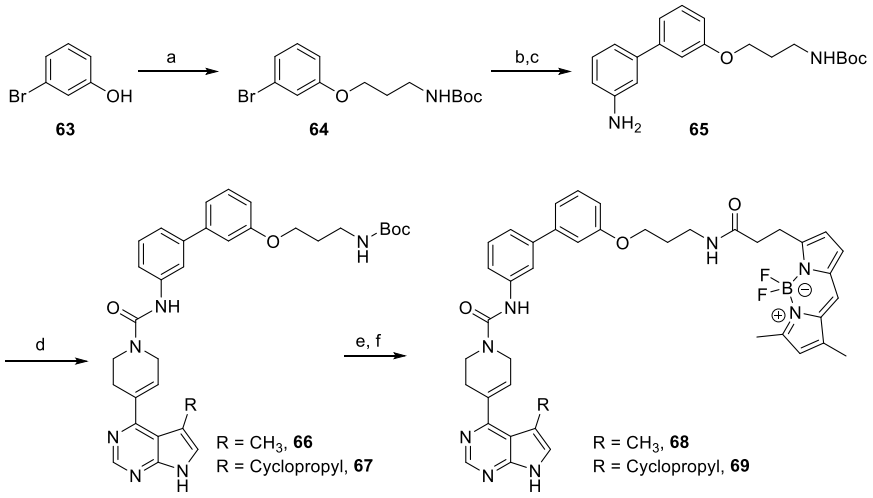

Scheme 3. Reagents and conditions: a) 3-(Boc-amino)-1-propanol (1.0 equiv.), DIAD (1.1 equiv.), PPh_3 (1.1 equiv.) THF, μW, 120 °C, 1 h, 77 %; b) 3-nitrophenylboronic acid (2.0 equiv.), $Pd(PPh_3)_4$ (0.05 equiv.), K_2CO_3 (3.0 equiv.), DME, EtOH, H_2O (3/2/1), μW, 160 °C, 15 min, 79 %; c) H_2, Pd/C (10 %), EtOAc, 24 h, quant.; d) Urea formation **method B**: DIPEA (2.1 equiv.), RNH_2 (1.0 equiv.), 4-NO_2PhOCOCl (1.2 equiv.), THF, 0 °C, 30 min then **9** or **14.HCl** (1.2 equiv.), DIPEA (2.1 equiv.), THF, 50 °C, 1 h, **66**: 58 %; **67**: 41 %; e) 4 M HCl 1,4-dioxane solution (8.0 equiv.), rt, 1 h; f) DIPEA (6.0 equiv.), HOBt (3.0 equiv.), Bodipy FL (1.1 equiv.), EDC (3.0 equiv, **68**: 28 % (2 steps), **69**: 24 % (2 steps).

respectively. Protecting group removal and amide formation with BodipyFL led finally to the desired compounds **68** and **69** in modest yields, 28 % and 24 % respectively over two steps.

These compounds were also evaluated for LIMK inhibition (Fig. 3). Even though affinity for LIMKs decreased, with Ki values in the 200 nM range, very high selectivity for LIMKs with respect to ROCKs was observed.

With our inhibitor library of 62 derivatives in hand, and based on the observed *in vitro* biological activity, eleven molecules were then selected as sufficiently promising to continue in our studies with LIMK1/2 inhibition below 40 nM and ROCK activity less than 30 % at 1 μM.

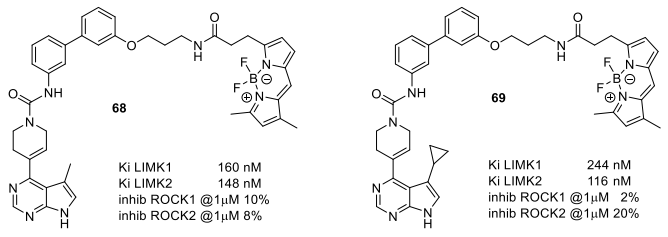

Fig. 3. Biological activity of fluorescent LIMK inhibitors **68** and **69**.

5. Biological evaluation

5.1. Cell penetration

Using the two fluorescent probes synthesized previously, we first established if our compounds were able to penetrate cells. Hela cells were incubated with 10 μM of fluorescent inhibitor for 30 min and then washed three times with PBS and fixed with CytoFix/CytoPerm™ from BD Biosciences. As depicted in Fig. 4, the fluorescent inhibitors enter HeLa cells and exhibit a diffuse labeling throughout the cytoplasm.

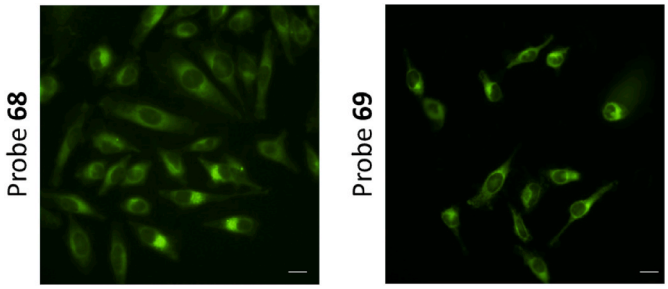

Fig. 4. Cell staining upon incubation with fluorescent inhibitors. Left panel: inhibitor with a methyl as R_2 substituent (**68**). Right panel: inhibitor with a cyclopropyl as R_2 substituent (**69**).

5.2. Cytotoxicity

Cytotoxicity on the HeLa cell line was measured using the CellTiter Glo® Luminescent cell viability assay from Promega after incubating the molecules at different concentrations for 48 h. The majority of the tested compounds had low toxicity with an EC_{50} higher than 25 μM (EC50 corresponds to the concentration of the inhibitor leading to the death of half of the cell population). The pyrrolopyrimidine series substituted in C-5 with a cyclopropyl appeared to be slightly more toxic with an EC50 for some compounds between 12 and 17 μM (Table 3). We also tested the toxicity of our compounds on a broader panel of cancer cell lines to have an overview of their effect on cell viability (Appendix A, Table 1). No significant differences were observed according to the cell line, except for compound **41** which was quite toxic on CaCo2 (EC_{50} = 5 μM) and compounds **61** and **62** which were more toxic across most of the cell lines. Furthermore, we evaluated our compounds on a wild type cell line of fibroblast to assess biosafety. The results show that all of our compounds have low toxicity on this wild type cell line (EC50 > 25 μM).

5.3. Inhibition of cofilin phosphorylation by LIMKs

Further characterization of our compounds was performed by evaluating their ability to inhibit cofilin phosphorylation by LIMKs in HeLa cells (Table 3). Cofilin, an actin depolymerizing factor, is LIMKs main substrate and phosphorylation on its Ser3 leads to its inhibition. HeLa cells were incubated with 25 μM of inhibitors for 2 h according to a well-established protocol from Prudent et al. [27]. Cells were then lysed and the lysates were analyzed by western blotting using anti-phospho-Ser3-cofilin and anti-cofilin antibodies. DMSO, **LX7101** and **LIMKi3** were used in each experiment as negative and positive controls (an example is given in Fig. 5). Bands were quantified and the ratio phospho-cofilin versus cofilin was normalized with values obtained with DMSO.

Seven molecules were more potent than **LIMKi3** and four more effective than the clinically evaluated **LX7101** (Table 3 and Appendix A Fig. 1). The four best compounds belonged to the *C*-5 cyclopropyl pyrrolopyrimidine series, three of them possessing a methoxy substituent on the second aromatic ring. In this bisaryl series, the meta-methoxy had the best inhibition of cofilin phosphorylation. The *C*-5, *C*-6 dimethyl pyrrolopyrimidine series was disappointing as these compounds were less efficient than **LIMKi3** for cofilin phosphorylation inhibition in spite of their promising Ki values. This could be because the *in vitro* LanthaScreen™ Eu Kinase Binding Assay, which measures the competition of binding of the tested compounds with a reference tracer on purified enzymes, does not consider the physiological parameters linked to the cell environment. Overall, the highest inhibition was observed with derivatives **48** and **52**, this last compound exhibiting a remarkable 96 % inhibition of cofilin phosphorylation.

5.4. Kinase selectivity

Compound **52** was then tested for selectivity on a representative panel of 100 kinases *via* a kinome scan performed by the DiscoverX (Eurofins) company. At the concentration of 1 μM, only eight kinases were inhibited at more than 50 % including LIMK1 and LIMK2 (95.8 % and 100 % respectively) (Appendix A Fig. 2 and Table 2). Interestingly, PDGFRb (84 %) involved in tumor angiogenesis, FAK (100 %) involved in cell migration, as well as KIT (70 %) and mutated KIT-D816V (92.7 %) key mediators for tumorigenesis, were also inhibited by **52.**

Derivative **52** was therefore our best candidate for further evaluation as it showed good inhibition and selectivity for LIMKs, was able to efficiently inhibit cofilin phosphorylation (96 %) and penetrated the cell plasma membrane with low toxicity.

Table 3
Cell toxicity and inhibition of cofilin phosphorylation.

Entry	Cmpd	Substitution on type III compound	% inhib. Phospho Cofilin[a]	Cell toxicity (EC_{50} in μM)[b]
Ref	**LIMKi3**	–	73 (±8)	25 (±3)
Ref	**LX7101**	–	85 (±3)	55 (±5)
1	**37**	R = 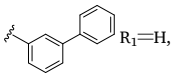 R_1=H, R_2=CH_3	78 (±8)	22 (±9)
2	**41**	R = 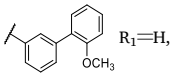 R_1=H, R_2=CH_3	73 (±10)	28 (±2)
3	**48**	R = 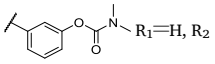 R_1=H, R_2 = CycPr	88 (±8)	47 (±2)
4	**49**	R = 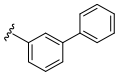 R_1=H, R_2 = CycPr	82 (±8)	12 (±3)
5	**51**	R = 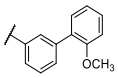 R_1=H, R_2 = CycPr	87 (±1)	14 (±2)
6	**52**	R = 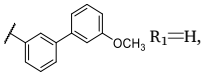 R_1=H, R_2 = CycPr	96 (±2)	26 (±5)
7	**53**	R = 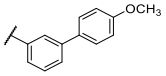 R_1=H, R_2 = CycPr	86 (±8)	12 (±7)
8	**59**	R = 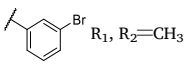 R_1, R_2=CH_3	69 (±13)	70 (±6)
9	**60**	R = 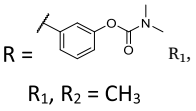 R_1, R_2 = CH_3 R_2=CH_3	72 (±10)	>100
10	**61**	R = 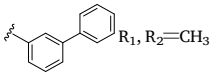 R_1, R_2=CH_3	60 (±13)	29 (±15)
11	**62**	R = 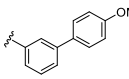 R_1, R_2=CH_3	63 (±14)	24 (±6)

HeLa cells were used for both experiments: cofilin phosphorylation inhibition and cell toxicity. Experiments were performed in triplicate (n = 3). Standard deviations are in parentheses. Values of cell toxicity are expressed in EC_{50} (μM) corresponding to the concentration of inhibitor leading to 50 % cell death. CycPr = cyclopropyl residue.

5.5. Cytoskeleton imaging

Cell cytoskeleton imaging was also performed to assess the effect of compound **52** on actin filaments and microtubules. At 1 μM, **52** already had a strong impact on the cytoskeleton, as actin filaments were disturbed whereas microtubules were only slightly affected (Fig. 6).

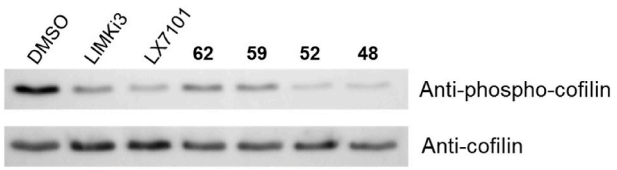

Fig. 5. Cofilin phosphorylation of selected compounds. HeLa cells were incubated for 2 h with 25 μM of inhibitor, and then lysed. Lysates were analyzed by Western Blot using anti-phospho-Ser3-cofilin and anti-cofilin antibodies.

When the concentration was increased to 25 μM this effect was enhanced. **LX7101** also affected the cell cytoskeleton but in a lesser extent at both concentrations.

5.6. Cell migration

We next conducted wound healing experiments to assess the impact of compound **52** on the migration ability of cervical carcinoma HeLa cells and of two osteosarcoma cell lines U-2 OS and KHOS; osteosarcomas being very aggressive and known to metastasize rapidly. Cell viabilities (48 h) were measured beforehand and gave an IC_{50} of 9.5 μM on U-2 OS, and 6.2 μM on KHOS cell lines (Appendix A Fig. 3, cytotoxicity on HeLa cells was reported in Table 3).

Using live cell imaging, we monitored cell migration as relative wound density (RWD) at hourly intervals for 48 h (Fig. 7 Appendix A). The experiment was conducted at a 0.5 % concentration of fetal bovine serum (FBS) in order to substantially decrease interference of dividing cells (proliferation) with the migration results. We tested compound **52** at two concentrations of 2.5 and 5 μM, alongside a DMSO control and a positive control treatment with the actin polymerization inhibitor cytochalasine D at 0.1 μg/mL. Full migration kinetics are shown on Appendix A Fig. 4. Approximately 100 % wound closure is obtained on control groups treated with DMSO after 30h for KHOS cells and 24h for U-2 OS cells. HeLa cells showed a slower migration rate with a wound closure under 50 % at 48h for the DMSO control (Appendix A Figure 4). We then compared relative wound density at endpoints for each treated cell line. For all three cell lines, compound **52** significantly impaired cell migration in a dose-dependent manner. At 5 μM, the RWDs, when compared to the DMSO control values, were decreased by 27.5 % for HeLa, 22 % for KHOS and 41 % for U-2 OS cell lines. The effects obtained at 2.5 μM, although less pronounced, were statistically significant.

These results indicate that compound **52** demonstrated a clear inhibitory effect on cell migration of three different cancerous cell lines from osteosarcoma and cervical carcinoma origin, suggesting its potential as a promising candidate for anti-angiogenic applications.

6. Molecular modeling and co-crystallization studies

6.1. Homology models

To better design new compounds and understand our observed SAR, molecular modeling, using in-house generated homology structures was performed. First, the reference molecules, including known pyrrolopyrimidine derivatives, were docked in the LIMKs model structures to establish the required interactions and to identify the possible sites of chemical modulation. The docking pose obtained for a representative molecule of the pyrrolopyrimidine derivatives (CHEMBL583464) is represented in Fig. 8.

Using these models, we highlighted the necessity of keeping the pyrrolopyrimidine core, which makes hydrogen bonds with the residue Ile408 (Ile416 in LIMK1) from the hinge part of LIMK2. This behavior is well known in the majority of type I kinase inhibitors which interact with the hinge region. The pyrrolopyrimidine core interaction is stabilized by a hydrophobic interaction with Leu337 (Leu345 in LIMK1) and

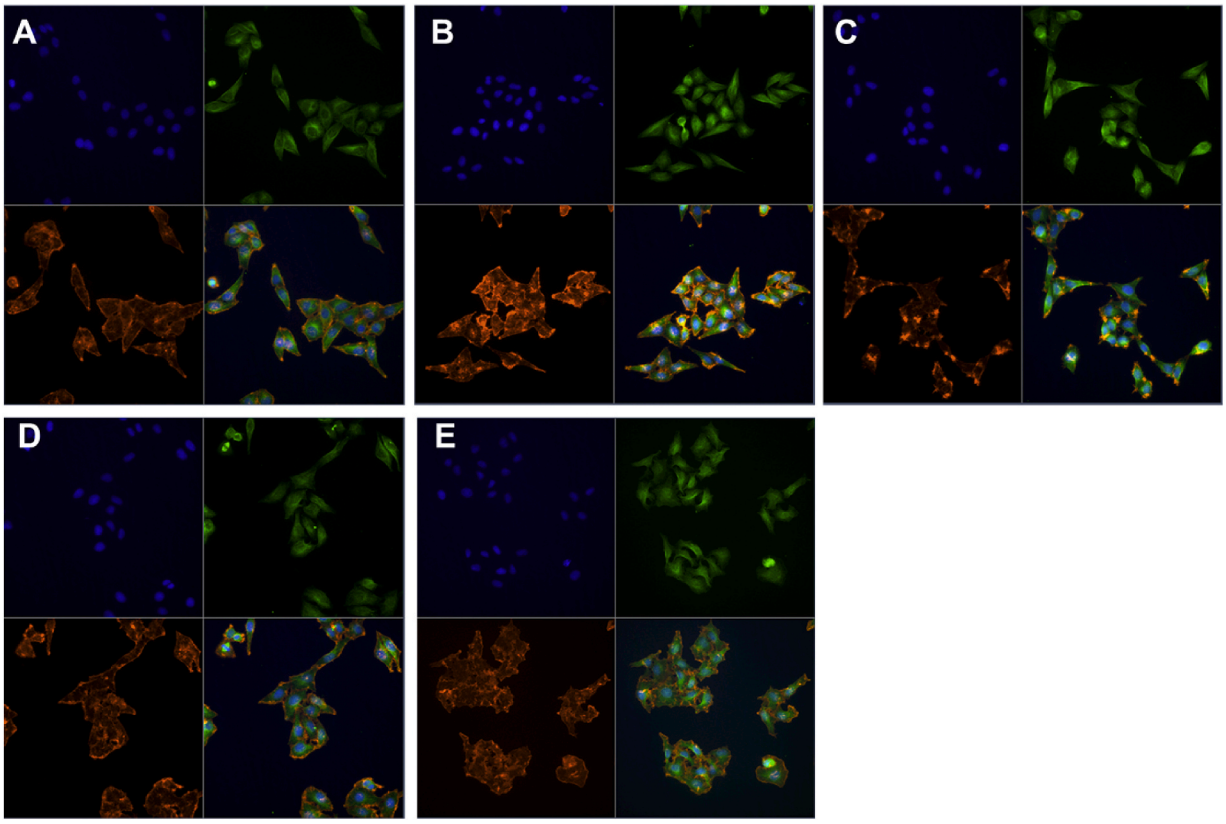

Fig. 6. Cell cytoskeleton imaging with compound **52**. HeLa cells were incubated for 2 h with 1 μM or 25 μM of inhibitor then fixed and labeled. A. DMSO. B. 1 μM **52**. C. 25 μM **52**. D. 1 μM **LX7101**. E. 25 μM **LX7101**. Blue channel: Nuclei. Green channel: Microtubules. Red channel: Actin filaments. Bottom right panel: Merged.

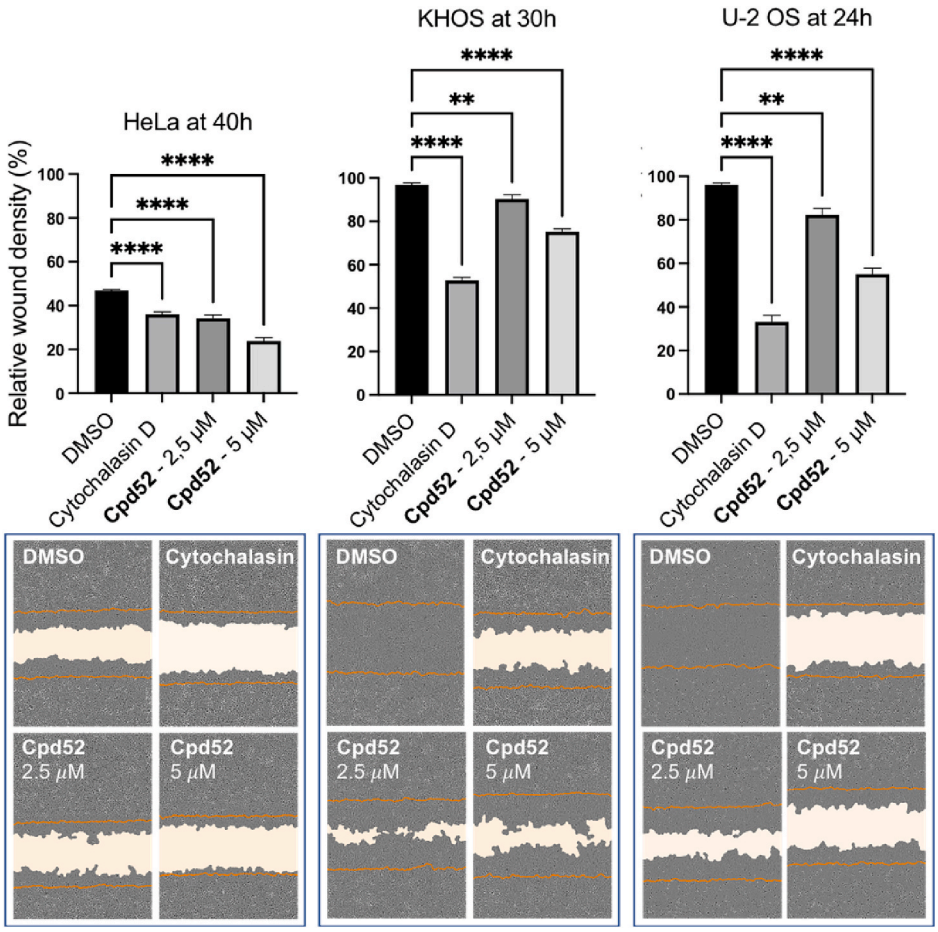

Fig. 7. Effects of compound **52** on cell migration. Scratch wound cell migration assays were conducted on HeLa, KHOS and U-2 OS cells after treatment with 2.5 or 5 µM of compound **52**, 0.1 µg/mL cytochalasine D or 0.05 % DMSO. Images were acquired every hour for 48 h by real-time live-cell microscopy (IncuCyte, Essen Bioscience) and images were analyzed to determine the relative wound density (RWD) (IncuCyte software). Percentages of RWD are shown as bar graphs for data extracted at 48 h for HeLa cells, 30 h for KHOS and 24 h for U-2 OS cells; 100 % represents full wound closure. Data are RWD% mean ± S.E.M (n = 8); **P ≤ 0.01, ****P ≤ 0.0001 (One-way ANOVA statistical analysis). Lower panels show representative images taken at each endpoints for the 3 cell lines. Orange lines represent the initial scratch wound boundaries at time 0; the light area shows the un-colonized part of the scratch.

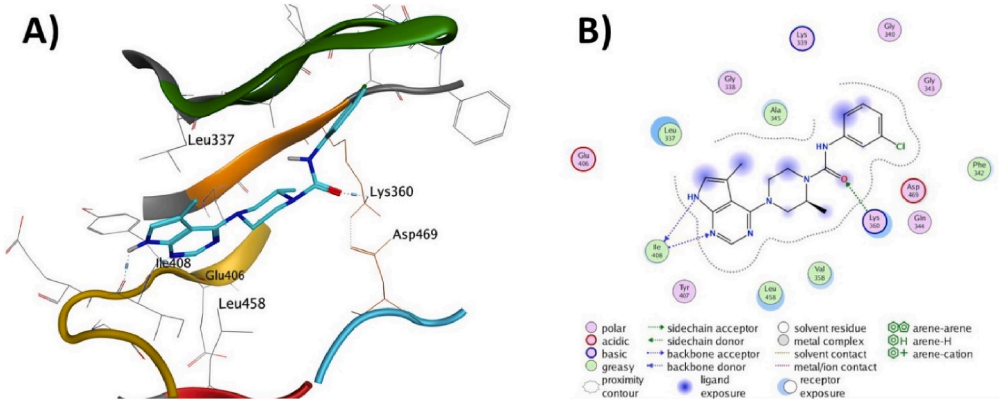

Fig. 8. Docking pose obtained for reference molecule CHEMBL583464. A) 3D representation of the molecule (blue licorice) bound in the active site of LIMK2 (represented as ribbons with side chains in sticks). B) 2D plot of interaction between molecule CHEMBL583464 and LIMK2.

Leu458 (Leu467 in LIMK1). We also observed a hydrogen bond between the urea group and the catalytic Lys360 (Lys368 in LIMK1).

As the pyrrolopyrimidine motif was deemed crucial for the desired interaction, we then turned to the modification of the central piperazine by a tetrahydropyridine core. We first ensured that this substitution did not modify the interactions previously identified by molecular docking, that is the hydrogen bonds with Ile408 and Lys360 (Fig. 9, A). Then, a docking model was used to evaluate the binding mode and the interactions formed by the inhibitors featuring the urea group. We observed a notable increase in affinity for compounds where the R-group is a biphenyl derivative. Indeed, our docking model showed the formation of π-stacking interactions between the second aromatic ring and

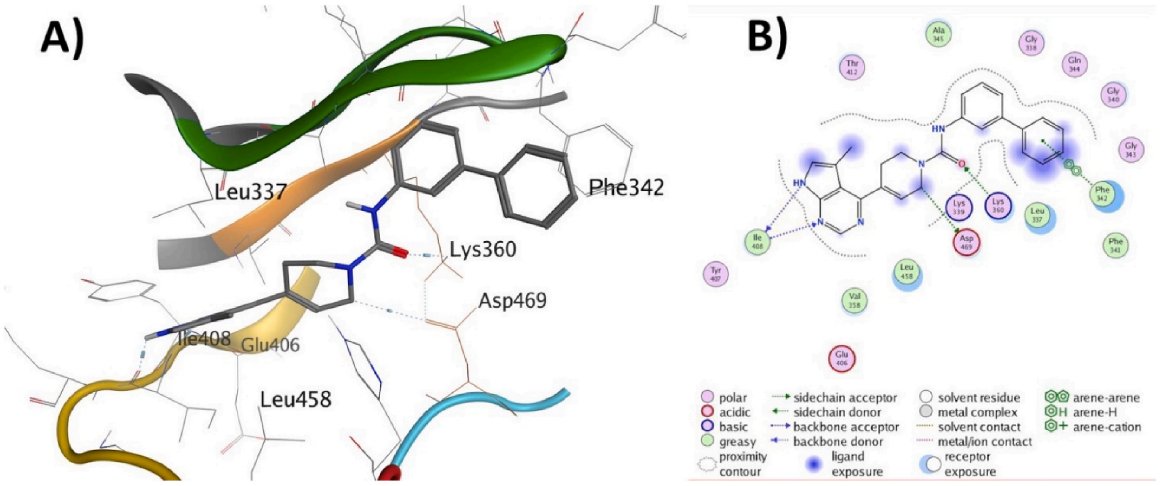

Fig. 9. Docking pose obtained for compound **37**. A) 3D representation of the molecule (licorice) bound in the active site of LIMK2 (represented as ribbons with side chains in sticks). B) 2D plot of interaction between **37** and LIMK2.

the Phe342 residue of LIMK2 (Fig. 9, B).

6.2. Crystallography

During our study, the crystallographic structure of LIMK2 complexed with our most active biphenyl derivative, **52** was solved (PDB 8S3X, Appendix A Table 3), and is shown in Fig. 10.

We observed that the pyrrolopyrimidine motif adopts the same binding mode that was described by our docking model: two hydrogen bonds with the backbone atoms of the Ile408 residue and hydrophobic interactions with Leu458 and Leu337 residues. As predicted, the Phe342 residue in the X-ray structure is also located in proximity of the second ring of the biphenyl moiety. We did notice, however, a difference between the docking model and the solved complex around the urea motif. Indeed, in the crystallographic complex, the urea makes hydrogen bonds with Gly338 and Asp469, leaving the catalytic Lys360 free to move. Hence, the catalytic Lys360 seems to be very flexible in the crystallographic structure as the atoms of the side chain were not solved. This difference is probably since, in the target structure used in the docking model, Asp469 is engaged in a hydrogen bond with Lys360, stabilizing it and positioning the Lys360 in an ideal location to interact with the urea motif. An interesting structural feature shown by the crystallographic structure is the presence of the Cys365 residue close to the methoxy group of **52**. This may suggest the possibility to transform this molecule in covalent inhibitor by adding a reactive warhead on the methoxy group.

7. Conclusion

In this study we have developed a new tetrahydropyridine pyrrolopyrimidine family of LIMK inhibitors with promising activity and selectivity. The central tetrahydropyridine core was added to the different pyrrolopyrimidine bases *via* a Suzuki-Miyaura cross-coupling reaction, and structural variation was further achieved with substitution of the urea moiety to give a library of over 60 final derivatives. In silico docking models were elaborated and continuous *in vitro* testing effectively guided the structure activity studies to design more efficient molecules. Our best compounds were then evaluated *in cell* for cytotoxicity and inhibition of cofilin phosphorylation leading to the identification of the best compound **52**. Cytoskeleton imaging in the presence of **52** showed a strong effect on actin filaments. Kinase selectivity of this compound was excellent on a 100-panel screen with only 5 kinases being inhibited at >80 % at 1 μM (including LIMK1 and LIMK2). Wound healing experiments on Hela as well as two osteosarcoma cell lines demonstrated that for all three cell lines, **52** significantly impaired cell migration, one key function of metastatic development, in a dose-dependent manner. In the development of these new LIMK inhibitors, we have shown that the tetrahydropyridine ring is a stable bioisoster of a

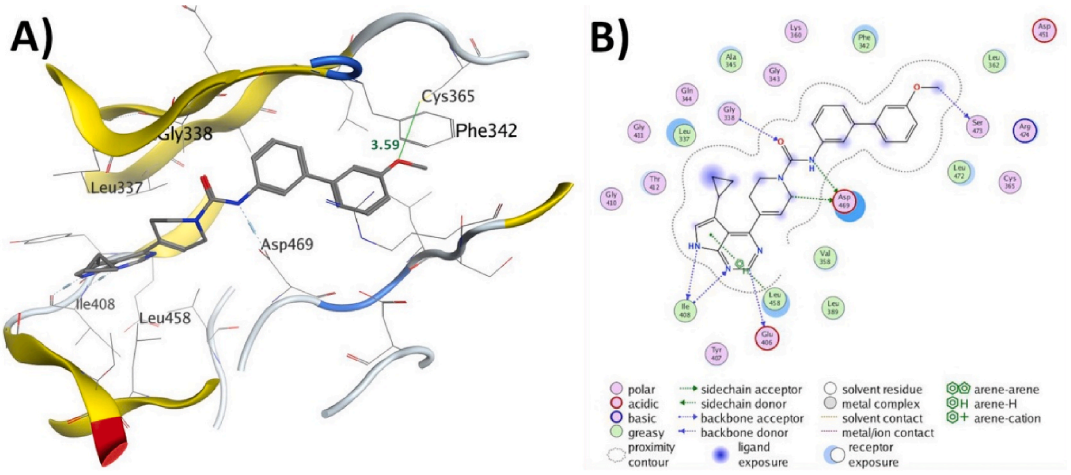

Fig. 10. Crystallographic structure of the LIMK2-**52** complex A) 3D representation of the molecule (licorice) bound in the active site of LIMK2 (represented as ribbons with side chains in sticks). B) 2D plot of interaction between **52** and LIMK2.

pyrimidine ring, with a good fit in the active site. This was first confirmed by docking experiments in homology models, then with a resolved crystallographic structure of the kinase domain of LIMK2 with **52**. This series of molecules is being further explored toward their use in preclinical studies.

8. Experimental section

8.1. Chemistry

Chemicals and analytical grade solvents were purchased from commercial suppliers and used without further purification unless otherwise stated. The Bodipy-FL probe was made in-house according to Richert et al. [28] ^{1}H NMR and ^{13}C NMR spectra were recorded with a Bruker Avance II 250 MHz or an Avance III HD Nanobay 400 MHz spectrometer in $CDCl_3$, MeOH-d_4 or DMSO-d_6. The chemical shifts are reported in parts per million (δ scale), and all coupling constant (*J*) values are in Hertz (Hz). The following abbreviations were used to denote the multiplicities: s (singlet), d (doublet), t (triplet), q (quartet), m (multiplet), and dd (double doublet). Some methylene groups in the tetrahydropyridine core are visible only as correlation spots in the HSQC spectra. IR absorption spectra were obtained with a Perkin–Elmer PARAGON 1000 PC instrument, and values are reported in cm^{-1}. HRMS were recorded with a Bruker maXis Q-Tof mass spectrometer. Optical rotations were recorded on a Jasco P2000 polarimeter at 20 °C. Compound purity was evaluated by LC-MS using an Ultimate 3000 UHPLC system equipped with a DAD and coupled to an MSQ Plus mass spectrometer (Thermo Fisher Scientific). Monitoring of the reactions was performed with silica gel TLC plates with a fluorescent indicator. Spots were visualized with UV light at 254 nm and 356 nm. Column chromatography was performed with silica gel 60 (0.063–0.200 mm, Merck). Reactions requiring anhydrous conditions were performed under argon. Heating blocks were used for conventionally heated reactions. Microwave irradiation was carried out in sealed 2–5 mL vessels placed in a Biotage Initiator system using a standard absorbance level (300 W maximum power). The temperatures were measured externally with an IR probe on the surface of the vial, and could be read directly from the instrument screen. The reaction time was measured from when the reaction mixture reached the desired temperature for temperature-controlled experiments. Pressure was measured by a non-invasive sensor integrated into the cavity lid.

8.1.1. General methods

8.1.1.1. ***Method A****: urea synthesis using isocyanates.* To a solution of the desired amine (1.0 equiv.) in anhydrous CH_2Cl_2 (0.07 M) under argon was added DIPEA (1.0–3.0 equiv.). The solution was cooled to 0 °C and the corresponding isocyanate (1.1 equiv.) was added. The reaction mixture was stirred at 0 °C for 1 h then at rt for 18 h or until completion (TLC monitoring). The solvent was then removed under reduced pressure and the residue was purified by silica gel column chromatography to afford the desired product.

8.1.1.2. ***Method B:*** *urea synthesis using 4-nitrophenyl chloroformate.* To a solution of the desired aniline (1.0 equiv.) in THF (0.07 M) at 0 °C was added DIPEA (1.1–2.1 equiv.) and 4-nitrophenyl chloroformate (1.2 equiv.). The mixture was stirred at 0 °C until total disappearance of the starting material (TLC monitoring, 30 min). Then, amine (1.2 equiv.) and DIPEA (2.1 equiv.) were added and the reaction mixture was stirred at 50 °C until completion (TLC monitoring, 2h). The solvent was removed under reduced pressure and the residue was purified by silica gel column chromatography to afford the desired product.

8.1.1.3. ***Method C:*** *urea synthesis using the Curtius rearrangement.* To a solution of acid (1.0 equiv.) was added Et_3N (1.2 equiv.) in THF (0.05 M) at 0 °C. Ethyl chloroformate (1.5 equiv.) was added and the reaction was stirred for 1–2 h at 0 °C (TLC monitoring). A solution of NaN_3 (1.5 equiv.) in H_2O (0.3 M) was then added at 0 °C and stirred for 1.5 h or until complete by TLC. The reaction was quenched with ice and quickly extracted with EtOAc, dried with $MgSO_4$, filtered and the solvent was removed under reduced pressure without heating. The crude acylazide was dissolved in toluene (0.05 M) and stirred for 1 h at reflux. Toluene was removed under reduced pressure. To this freshly prepared isocyanate was added a solution of amine (1.0 equiv.) and DIPEA (2.2 equiv.) in anhydrous CH_2Cl_2 (0.07 M) at 0 °C. The reaction mixture was stirred at 0 °C for 1 h then at rt for 18 h or until completion (TLC monitoring). The solvent was then removed under reduced pressure and the residue was purified by silica gel column chromatography to afford the desired product.

8.1.1.4. ***Method D: Suzuki-Miyaura cross-coupling reaction.*** To a solution of chlorinated heterocycle (1.0 equiv.) in THF (0.25 M) were added boronate ester (1.1 equiv.) followed by a 2 M aqueous solution of Na_2CO_3 (3.0 equiv.). The solution was degassed for 20 min and Pd $(PPh_3)_4$ (0.1 equiv.) was added. The mixture was then heated under microwave irradiation at 120 °C for 1.5 h and extracted with CH_2Cl_2. The organic layers were dried over $MgSO_4$, filtered and concentrated under vacuum. The residue was purified by silica gel column chromatography to afford the desired product.

8.1.2. Compound description

*8.1.2.1. 4-Chloro-5-methyl-7H-pyrrolo [2,3-d]pyrimidine (**3**).* 5-Methyl-3*H*-pyrrolo[2,3-*d*]pyrimidin-4(7*H*)-one **2** [18] (2.0 g, 13.4 mmol) was dissolved in $POCl_3$ (50 mL) and stirred at reflux for 1.5 h. After cooling, the mixture was slowly poured into a vigorously stirred ice-water bath and stirred for 30 min. The mixture was carefully neutralized to pH 7 with solid NaOH. Then, the mixture was extracted with CH_2Cl_2 (3 x 150 mL) The combined organic layers were dried over $MgSO_4$, filtered and concentrated under reduced pressure. The residue was purified by flash silica gel column chromatography using a gradient solvent system of PE/EtOAc from 100/0 up to 70/30. Finally, the product was precipitated in a mixture of acetone/PE to give compound **3** (3.6 g, 81 %) as a beige solid. ^{1}H NMR (250 MHz, $CDCl_3$) δ 9.49 (brs, 1H), 8.60 (s, 1H), 7.11 (dd, $J = 2.3$ Hz, $J = 1.2$ Hz, 1H), 2.50 (d, $J = 1.2$ Hz, 3H). ^{13}C spectral data corresponded to the literature values found in Seela, F., Thomas, H., Synthesis of Certain 5-Substituted 2′-Deoxytubercidin Derivatives. *Helv. Chim. Acta* **1994**, *77*, 897–903. CAS: 1618-36-6.

*8.1.2.2. tert-Butyl 4-(7H-pyrrolo [2,3-d]pyrimidin-4-yl)-3,6-dihydropyridine-1(2H)-carboxylate (**6**).* The reaction was carried out as described in **method D** using commercially available 4-chloro-7*H*-pyrrolo[2,3-*d*]pyrimidine (0.60 g, 3.91 mmol) and *N*-Boc-1,2,3,6-tetrahydropyridine-4-boronic acid pinacol ester **5** (1.3 g, 4.30 mmol) in THF (10 mL). The crude reaction mixture was purified by silica gel column chromatography using a gradient solvent system of CH_2Cl_2/acetone from 90/10 up to 50/50. To remove final impurities, the product was precipitated in a mixture of acetone/pentane to afford compound **6** (0.85 g, 72 %) as a pale-yellow solid. R_f (CH_2Cl_2/acetone 70/30) 0.43. Mp: 159–161 °C. IR (ATR diamond, cm^{-1}) *ν*: 3120, 2971, 2831, 1690, 1583, 1558, 1423, 1345, 1169, 1112, 839. ^{1}H NMR (400 MHz, MeOD-d_4) δ 8.63 (s, 1H), 7.42 (d, $J = 3.7$ Hz, 1H), 6.74 (brs, 1H), 6.72 (d, $J = 3.6$ Hz, 1H), 4.21–4.15 (m, 2H), 3.66 (t, $J = 5.7$ Hz, 2H), 2.78–2.71 (m, 2H), 1.49 (s, 9H). ^{13}C NMR (101 MHz, MeOD-d_4) δ 158.4 (C), 156.5 (C), 153.4 (C), 151.2 (CH), 136.3 (C), 130.9 (CH), 127.9 (CH), 115.9 (C), 101.8 (CH), 81.4 (C), 44.9 (CH_2), 41.5 (CH_2), 28.7 (3 x CH_3), 27.6 (CH_2). HRMS (EI-MS) *m/z* calcd for $C_{16}H_{21}N_4O_2$ $[M+H]^+$: 301.1659, found: 301.1659.

*8.1.2.3. tert-Butyl 4-(5-methyl-7H-pyrrolo [2,3-d]pyrimidin-4-yl)-3,6-dihydropyridine-1(2H)-carboxylate (**7**).* The reaction was carried out as

described in method **D** using the chlorinated compound **3** (0.50 g, 2.99 mmol), and *N*-Boc-1,2,3,6-tetrahydropyridine-4-boronic acid pinacol ester **5** (1.02 g, 3.29 mmol) in THF (12 mL). The crude mixture was purified by silica gel column chromatography using a gradient solvent system of CH_2Cl_2/acetone from 90/10 up to 60/40 to afford compound **7** (0.63 g, 67 %) as a beige solid. R_f (CH_2Cl_2/Acetone 60/40) 0.33. Mp: 190–192 °C. IR (ATR diamond, cm^{-1}) ν: 3101, 2977, 2867, 1688, 1561, 1408, 1361, 1164, 1109, 983, 798. ^{1}H NMR (250 MHz, $CDCl_3$) δ 10.40 (brs, 1H), 8.81 (s, 1H), 7.12 (s, 1H), 6.06–5.87 (m, 1H), 4.24–4.09 (m, 2H), 3.72 (t, J = 5.6 Hz, 2H), 2.77–2.65 (m, 2H), 2.29 (d, J = 1.1 Hz, 3H), 1.51 (s, 9H). ^{13}C NMR (63 MHz, $CDCl_3$) δ 160.9 (C), 155.1 (C), 153.1 (C), 150.8 (CH), 128.2 (CH), 123.7 (CH), 115.6 (C), 110.8 (C), 80.0 (C), 77.4 (C), 43.4 (CH_2), 40.8 (CH_2), 28.7 (3 x CH_3), 28.0 (CH_2), 13.1 (CH_3). HRMS (EI-MS) *m/z* calcd for $C_{17}H_{23}N_4O_2$ $[M+H]^+$: 315.1816, found: 315.1814.

*8.1.2.4. 4-(1,2,3,6-Tetrahydropyridin-4-yl)-7H-pyrrolo [2,3-d]pyrimidine dihydrochloride (**8**).* A 4 M solution of HCl in 1,4-dioxane (1.4 mL, 5.60 mmol, 8.0 equiv.) was added to a solution of the Boc derivative **6** (210 mg, 0.70 mmol) in CH_2Cl_2 (5.0 mL) cooled to 0 °C. The reaction mixture was then stirred at rt for 2 h and concentrated in vacuo. The residue was co-evaporated with Et_2O (3 x 10 mL) to afford compound **8** (168 mg, 89 %) as an orange solid. The product was used without further purification in the next step. Mp: >260 °C. IR (ATR diamond, cm^{-1}) ν: 3509, 3412, 3023, 2931, 2751, 1584, 1422, 1307, 892, 818, 735. ^{1}H NMR (400 MHz, DMSO-d_6) δ 12.90 (brs, 1H), 9.62 (brs, 2H), 8.88 (s, 1H), 7.84 (s, 1H), 6.98 (s, 2H), 3.91 (s, 3H), 3.35 (s, 2H), 3.00 (s, 2H). ^{13}C NMR (101 MHz, DMSO-d_6) δ 152.4 (C), 152.0 (C), 147.2 (CH), 131.3 (C), 130.2 (CH), 129.2 (CH), 113.7 (C), 101.6 (CH), 41.4 (CH_2), 39.5 (CH_2), 22.6 (CH_2). HRMS (EI-MS) *m/z* calcd for $C_{11}H_{13}N_4$ $[M+H]^+$: 201.1135, found: 201.1135.

*8.1.2.5. 5-Methyl-4-(1,2,3,6-tetrahydropyridin-4-yl)-7H-pyrrolo [2,3-d] pyrimidine dihydrochloride (**9**).* To a 4 M solution of HCl in 1,4-dioxane (3.8 mL, 15.3 mmol, 8.0 equiv.) cooled to 0 °C was added the Boc protected derivative **7** (0.60 g, 1.91 mmol) in solid form. The reaction mixture was stirred at rt for 1 h. After completion, the precipitate was filtered then washed with Et_2O (3 x 20 mL) to afford compound **9** (550 mg, quant.) as a yellow solid. The product was used without further purification in the next step. Mp: >260 °C. IR (ATR diamond, cm^{-1}) ν: 3424, 3060, 2977, 2737, 2516, 1605, 1574, 1441, 1328, 1167, 850. ^{1}H NMR (400 MHz, DMSO-d_6) δ 13.23 (brs, 1H), 9.94 (brs, 2H), 8.98 (s, 1H), 7.73 (s, 1H), 6.39–6.28 (m, 1H), 4.48–4.11 (m, 1H), 3.91–3.81 (m, 2H), 3.41–3.30 (m, 2H), 2.98–2.88 (m, 2H), 2.31 (d, J = 1.2 Hz, 3H). ^{13}C NMR (101 MHz, DMSO-d_6) δ 152.5 (C), 152.2 (C), 144.4 (CH), 129.8 (CH), 129.6 (CH), 127.6 (C), 114.4 (C), 112.7 (C), 40.9 (CH_2), 39.4 (CH_2), 24.0 (CH_2), 12.3 (CH_3). HRMS (EI-MS) *m/z* calcd for $C_{12}H_{15}N_4$ $[M+H]^+$: 215.1291, found: 215.1295.

*8.1.2.6. tert-Butyl 4-(5-chloro-7H-pyrrolo [2,3-d]pyrimidin-4-yl)-3,6-dihydro-2H-pyridine-1-carboxylate (**10**).* To a solution of compound **6** (690 mg, 2.30 mmol) in dry DMF (46 mL) was added *N*-chlorosuccinimide (338 mg, 2.53 mmol, 1.1 equiv.) by portions at rt. The reaction mixture was stirred at 40 °C for 10 h. After complete disappearance of the starting material, the reaction mixture was cooled to rt, diluted with H_2O (200 mL) then extracted with CH_2Cl_2 (3 x 100 mL). The combined organic layers were washed brine (4 x 50 mL), dried over $MgSO_4$, filtered and concentrated in vacuo. The obtained oil was co-evaporated with heptane (3 x 40 mL) to afford the desired product **10** (732 mg, 95 %) as a pale orange powder. The product was used without further purification in the next step. R_f (CH_2Cl_2/acetone 70/30) 0.41. Mp: degradation 189 °C. IR (ATR diamond, cm^{-1}) ν: 3091, 2975, 1691, 1364, 1326, 1236, 1159, 1112, 984, 797, 602.^{1}H NMR (250 MHz, MeOD-d_4) δ 8.69 (s, 1H), 7.51 (s, 1H), 6.11 (s, 1H), 4.17 (q, J = 2.8 Hz, 2H), 3.71 (t, J = 5.6 Hz, 2H), 2.66 (m, 2H), 1.50 (s, 9H). ^{13}C NMR (63 MHz, MeOD-d_4) δ 161.1 (C), 156.6 (C), 152.2 (C), 152.1 (CH), 133.6 (CH), 131.4 (C), 126.1 (CH), 113.5 (C), 104.9 (C), 81.4 (C), 44.7 (CH_2), 41.2 (CH_2), 28.7 (3 x CH_3), 28.6 (CH_2). HRMS (EI-MS) *m/z* calcd for $C_{16}H_{20}ClN_4O_2[M+H]^+$: 335.1269, found: 335.1272.

*8.1.2.7. tert-Butyl 4-(5-iodo-7H-pyrrolo [2,3-d]pyrimidin-4-yl)-5,6-dihydropyridine-1(2H)-carboxylate (**11**).* To a solution of compound **6** (1.40 g, 4.66 mmol) in anhydrous DMF (25 mL) under an argon atmosphere was added NIS (1.10 g, 4.89 mmol, 1.05 equiv.) at 0 °C. The mixture was stirred at this temperature for 20 min and was allowed to warm to room temperature. The solution was poured into ice (50 g) and the aqueous phase was extracted with EtOAc (3 x 100 mL). The combined organic layers were washed with brine (4 x 50 mL), dried over $MgSO_4$, filtered and concentrated under reduced pressure. The crude residue was dissolved in a minimum of acetone, precipitated with pentane and filtered to afford the desired product **11** (1.79 g, 90 %) as a light brown solid. R_f (CH_2Cl_2/acetone 70/30) 0.16. Mp: 151–153 °C. IR (ATR diamond, cm^{-1}) ν: 3091, 2975, 2833, 1682, 1594, 1552, 1413, 1236, 1160, 1113, 822. ^{1}H NMR (400 MHz, MeOD-d_4) δ 8.67 (s, 1H), 7.61 (s, 1H), 6.02–5.92 (m, 1H), 4.25–4.14 (m, 2H), 3.73 (t, J = 5.6 Hz, 2H), 2.62–2.52 (m, 2H), 1.49 (s, 9H). ^{13}C NMR (101 MHz, MeOD-d_4) δ 161.8 (C), 156.5 (C), 152.9 (C), 151.6 (CH), 134.7 (CH), 132.1 (CH), 132.0 (C), 116.8 (C), 81.3 (C), 53.1 (C), 44.1 (CH_2), 41.4 (CH_2), 29.2 (CH_2), 28.8 (3 x CH_3). HRMS (EI-MS) *m/z* calcd for $C_{16}H_{20}IN_4O_2$ $[M+H]^+$: 427.0625, found: 427.0626.

*8.1.2.8. tert-Butyl 4-(5-iodo-7-tosyl-7H-pyrrolo [2,3-d]pyrimidin-4-yl)-5,6-dihydro-pyridine-1(2H)-carboxylate (**12**).* NaH (60 % dispersion in mineral oil, 0.18 g, 4.50 mmol, 1.2 equiv.) was added to a solution of the iodide derivative **11** (1.60 g, 3.75 mmol) in anhydrous THF (35 mL) under an argon atmosphere at room temperature. The solution was stirred for 30 min before the addition of *p*-toluenesulfonyl chloride (0.79 g, 4.13 mmol, 1.1 equiv.). Stirring was continued overnight. After completion, the reaction was quenched with H_2O (20 mL) and the aqueous layer was extracted with EtOAc (3 x 100 mL). The combined organic layers were washed with a brine (100 mL), dried over $MgSO_4$, filtered and concentrated under reduced pressure. The crude reaction mixture was purified by silica gel column chromatography using a gradient solvent system of PE/EtOAC from 100/0 up to 50/50 to afford the tosylated derivative **12** (1.78 g, 82 %) as a white solid. R_f (CH_2Cl_2/acetone 70/30) 0.91. Mp: 183–185 °C. IR (ATR diamond, cm^{-1}) ν: 3102, 2978, 1692, 1560, 1420, 1363, 1330, 1279, 1234, 1104, 817. ^{1}H NMR (400 MHz, DMSO-d_6) δ 8.91 (s, 1H), 8.21 (s, 1H), 8.07 (d, J = 8.4 Hz, 2H), 7.47 (d, J = 8.2 Hz, 2H), 6.11–5.96 (m, 1H), 4.16–4.02 (m, 2H), 3.58 (t, J = 5.7 Hz, 2H), 2.55–2.48 (m, 2H), 2.36 (s, 3H), 1.43 (s, 9H). ^{13}C NMR (101 MHz, DMSO-d_6) δ 161.7 (C), 154.0 (C), 152.3 (CH), 150.2 (C), 146.5 (C), 133.7 (C), 132.8 (CH), 132.0 (CH), 130.3 (2 x CH), 129.4 (C), 128.0 (2 x CH), 117.1 (C), 79.1 (C), 60.8 (C), 42.78 (CH_2), 39.5 (CH_2), 28.1 (3 x CH_3), 27.1 (CH_2), 21.1 (CH_3). HRMS (EI-MS) *m/z* calcd for $C_{23}H_{26}IN_4O_4S$ $[M+H]^+$: 581.0714, found: 581.0712.

*8.1.2.9. tert-Butyl 4-(5-cyclopropyl-7-tosyl-7H-pyrrolo [2,3-d]pyrimidin-4-yl)-5,6-dihydropyridine-1(2H)-carboxylate (**13**).* A mixture of toluene (15 mL) and H_2O (1.5 mL) was degassed with argon for 30 min in a 20 mL microwave reaction vial. Compound **12** (700 mg, 1.21 mmol), cyclopropylboronic acid (260 mg, 3.03 mmol, 2.5 equiv.), K_3PO_4 (900 mg, 4.24 mmol, 3.5 equiv.), $P(Cy)_3$ (68 mg, 0.24 mmol, 0.2 equiv.) and $Pd(OAc)_2$ (27 mg, 0.12 mmol, 0.1 equiv.) were added under argon. The vial was sealed and submitted to microwave irradiation at 140 °C for 1 h. The reaction mixture was cooled to rt, diluted with H_2O (30 mL) and the aqueous layer was extracted with with CH_2Cl_2 (2 x 100 mL). The combined organic layers were dried over $MgSO_4$, filtered and concentrated in vacuo. The crude reaction mixture was purified by silica gel column chromatography using a gradient solvent system of PE/EtOAc from 80/20 up to 70/30 to afford the cyclopropyl derivative **13** (436 mg, 73 %) as

a beige powder. R_f (CH_2Cl_2/acetone 70/30) 0.90. Mp: degradation 90 °C. IR (ATR diamond, cm^{-1}) ν: 3219, 1692, 1557, 1422, 1366, 1323, 1235, 1159, 1111, 1024, 806. ^{1}H NMR (400 MHz, MeOH-d_4) δ 8.77 (s, 1H), 8.03 (d, J = 8.4 Hz, 2H), 7.55 (d, J = 1.3 Hz, 1H), 7.37 (d, J = 8.1 Hz, 2H), 6.20–6.05 (m, 1H), 4.18–4.06 (m, 2H), 3.68 (t, J = 5.6 Hz, 2H), 2.65–2.57 (m, 2H), 2.37 (s, 3H), 1.85–1.75 (m, 1H), 1.48 (s, 9H), 0.99–0.83 (m, 2H), 0.72–0.61 (m, 2H). ^{13}C NMR (101 MHz, MeOH-d_4) δ 163.1 (C), 156.5 (C), 153.4 (C), 153.0 (CH), 147.6 (C), 136.1 (C), 134.8 (C), 131.0 (2 x CH), 130.7 (CH), 129.2 (2 x CH), 124.6 (CH), 123.3 (C), 119.4 (C), 81.4 (C), 44.4 (CH_2), 41.8 (CH_2), 28.7 (3 x CH_3), 28.5 (CH_2), 21.6 (CH_3), 9.2 (CH), 7.9 (2 x CH_2). HRMS (EI-MS) *m/z* calcd for $C_{26}H_{31}N_4O_4S$ $[M+H]^+$: 495.2061, found: 495.2058.

*8.1.2.10. 5-Cyclopropyl-4-(1,2,3,6-tetrahydropyridin-4-yl)-7H-pyrrolo [2,3-d]pyrimidine (**14**).* To a solution of compound **13** (821 mg, 1.66 mmol) in a mixture of THF (28 mL) and H_2O (5 mL) was added KOH (838 mg, 14.9 mmol, 9.0 equiv.). The reaction mixture was stirred under reflux for 18 h then cooled to rt, diluted with CH_2Cl_2 (100 mL) and H_2O (10 mL). The aqueous layer was separated and extracted with CH_2Cl_2 (100 mL). The combined organic layers were dried over $MgSO_4$, filtered and concentrated in vacuo. The de-tosylated compound was further deprotected to obtain either the free amine or the dihydrochloride salt as follows:

Free base 14: The residue was dissolved in CH_2Cl_2 (40 mL), cooled to 0 °C then TFA (3.41 mL, 44.3 mmol, 26.7 equiv.) was added. The resulting solution was stirred at rt for 2 h then concentrated in vacuo. The residue was suspended in CH_2Cl_2 (20 mL), neutralized with a 2 M aqueous solution of NaOH (6 mL) and the resulting solution was left to stir at rt for 30 min. The aqueous layer was separated, extracted with CH_2Cl_2 (3 x 30 mL) then the combined organic layers were dried over $MgSO_4$, filtered and concentrated in vacuo to afford the amine **14** (216 mg, 54 %) as a yellow powder. The product was used in the next step without further purification. Mp: 184–186 °C. IR (ATR diamond, cm^{-1}) ν: 3263, 2830, 1596, 1559, 1439, 1322, 1256, 1169, 1086, 1025, 805. ^{1}H NMR (400 MHz, MeOH-d_4) δ 8.60 (s, 1H), 7.13 (d, J = 1.1 Hz, 1H), 6.25–6.15 (m, 1H), 3.58–3.51 (m, 2H), 3.14 (t, J = 5.7 Hz, 2H), 2.68–2.58 (m, 2H), 1.99–1.86 (m, 1H), 0.94–0.84 (m, 2H), 0.66–0.57 (m, 2H). ^{13}C NMR (101 MHz, MeOH-d_4) δ 162.1 (C), 153.8 (C), 151.0 (CH), 135.4 (C), 131.3 (CH), 124.3 (CH), 119.4 (C), 116.8 (C), 45.1 (CH_2), 43.5 (CH_2), 28.2 (CH_2), 9.3 (CH), 8.0 (2 x CH_2). HRMS (EI-MS) *m/z* calcd for $C_{14}H_{17}N_4$ $[M+H]^+$: 241.1448, found: 241.1447.

Dihydrochloride salt 14.HCl: To a 4 M solution of HCl in 1,4-dioxane (2.6 mL, 10.4 mmol, 8.0 equiv.) cooled to 0 °C was added the de-tosylated derivative (0.448 g, 1.31 mmol) in solid form. The reaction mixture was stirred at rt for 1 h. After completion, the precipitate was filtered then washed with Et_2O (3 x 20 mL) to afford the dihydrochloride salt **14.HCl** (405 mg, 98 %) as a beige solid. The product was used without further purification in the next step. ^{1}H NMR (250 MHz, MeOH-d_4) δ 8.99 (s, 1H), 7.63 (d, J = 1.1 Hz, 1H), 6.74–6.34 (m, 1H), 4.08 (q, J = 2.7 Hz, 2H), 3.61 (t, J = 5.9 Hz, 2H), 3.12–2.98 (m, 2H), 2.05–1.90 (m, 1H), 1.09–0.98 (m, 2H), 0.83–0.71 (m, 2H).

*8.1.2.11. 5-Chloro-4-(1,2,3,6-tetrahydropyridin-4-yl)-7H-pyrrolo [2,3-d] pyrimidine (**15**).* To a 4 M solution of HCl in 1,4-dioxane (4.4 mL, 17.5 mmol, 8.0 equiv.) cooled to 0 °C was added compound **10** (732 mg, 2.19 mmol). The reaction mixture was stirred at rt for 5 h. After completion, the precipitate was filtered then washed with Et_2O (2 x 15 mL) and dried to afford the dihydrochloride salt **15** (643 mg, 96 %) as a brown solid. The product was used without further purification in the next step. Mp: >260 °C. IR (ATR diamond, cm^{-1}) ν: 3329, 3056, 2932, 1621, 1594, 1564, 1455, 1428, 1354, 603. ^{1}H NMR (400 MHz, DMSO-d_6) δ 13.07 (s, 1H), 9.70 (s, 2H), 8.88 (s, 1H), 7.95 (s, 1H), 6.27 (s, 1H), 3.86 (s, 2H), 3.33 (s, 2H), 2.88 (s, 2H). ^{13}C NMR (101 MHz, DMSO-d_6) δ 156.0 (C), 150.9 (C), 149.2 (CH), 129.8 (C), 128.4 (CH), 127.0 (CH), 111.4 (C), 102.8 (C), 40.8 (CH_2), 39.7 (CH_2), 23.4 (CH_2). HRMS (EI-MS) *m/z* calcd for $C_{11}H_{12}ClN_4$$[M+H]^+$: 235.0745, found: 235.0743.

*8.1.2.12. tert-Butyl 4-(5,6-dimethyl-7H-pyrrolo [2,3-d]pyrimidin-4-yl)-3,6-dihydro-2H-pyridine-1-carboxylate (**17**).* The reaction was carried out as described in **method D** using 4-chloro-5,6-dimethyl-7*H*-pyrrolo [2,3-*d*]pyrimidine [24] **16** (109 mg, 0.6 mmol). The crude reaction mixture was purified by silica gel column chromatography using a gradient solvent system of CH_2Cl_2/acetone from 100/0 up to 50/50 to afford compound **17** (58 mg, 30 %) as a white solid. R_f (CH_2Cl_2/acetone 60/40): 0.26. Mp: degradation 162 °C. IR (ATR diamond, cm^{-1}) ν: 3124, 2977, 2922, 2859, 2742, 1693, 1614, 1419, 1170, 1109, 970, 793, 982. ^{1}H NMR (250 MHz, $CDCl_3$) δ 11.07 (s, 1H), 8.72 (s, 1H), 5.92 (s, 1H), 4.15 (s, 2H), 3.71 (t, J = 5.6 Hz, 2H), 2.76–2.65 (m, 2H), 2.44 (s, 3H), 2.18 (s, 3H), 1.50 (s, 9H). ^{13}C NMR (63 MHz, $CDCl_3$) δ 158.9 (C), 155.0 (C), 152.1 (C), 149.2 (CH), 135.0 (C), 133.3 (C), 127.7 (CH), 116.6 (C), 105.5 (C), 79.8 (C), 43.6 (CH_2), 40.6 (CH_2), 28.6 (CH_3), 28.6 (CH_3), 28.6 (CH_3), 27.9 (CH_2), 11.7 (CH_3), 11.1 (CH_3). HRMS (EI-MS) *m/z* calcd for $C_{18}H_{25}N_4O_2$$[M+H]^+$: 329.1972, found: 329.1973.

*8.1.2.13. 5,6-Dimethyl-4-(1,2,3,6-tetrahydropyridin-4-yl)-7H-pyrrolo [2,3-d]pyrimidine dihydrochloride (**18**).* The protected amine **17** (350 mg, 1.07 mmol) was added to a 4 M solution of HCl in 1,4-dioxane (2.1 mL, 8.5 mmol) cooled to 0 °C. The reaction mixture was stirred at rt until completion (TLC monitoring). Diethyl ether was added to precipitate the amine salt, the precipitate was filtered then washed with Et_2O (2 x 10 mL) and dried to afford compound **18** (321 mg, quant.) as a yellow solid. Mp: >260 °C. IR (ATR diamond, cm^{-1}) ν: 3373, 2921 2831, 2749, 2648, 2582, 2463, 2326, 1610, 1479, 1442, 1407, 1363, 875, 782, 673. ^{1}H NMR (400 MHz, DMSO-d_6) δ 13.27 (s, 1H), 9.95 (s, 2H), 8.92 (s, 1H), 6.28 (s, 1H), 3.86 (s, 2H), 3.35 (s, 2H), 2.92 (s, 2H), 2.43 (s, 3H), 2.21 (s, 3H). ^{13}C NMR (101 MHz, DMSO-d_6) δ 151.7 (C), 149.6 (C), 143.3 (CH), 139.5 (C), 129.4 (CH), 127.3 (C), 115.2 (C), 107.8 (C), 40.8 (CH_2), 39.5 (CH_2), 24.2 (CH_2), 11.3 (CH_3), 10.5 (CH_3). HRMS (EI-MS) *m/z* calcd for $C_{13}H_{17}N_4$$[M+H]^+$: 229.1448, found: 229.1446.

*8.1.2.14. N-(3-Chlorophenyl)-4-(7H-pyrrolo [2,3-d]pyrimidin-4-yl)-3,6-dihydropyridine-1(2H)-carboxamide (**19**).* The reaction was carried out as described in **method A** using amine **8** (70 mg, 0.26 mmol) and 3-chlorophenyl isocyanate (34 μL, 0.28 mmol). The crude reaction mixture was purified by silica gel column chromatography using a gradient solvent system of CH_2Cl_2/acetone from 100/0 up to 50/50 to afford the urea derivative **19** (64 mg, 71 %) as a white solid. R_f (CH_2Cl_2/acetone 50/50) 0.29. Mp: degradation 122 °C. IR (ATR diamond, cm^{-1}) ν: 3208, 3123, 2997, 2839, 1640, 1588, 1527, 1425, 1345, 1235, 732. ^{1}H NMR (250 MHz, MeOH-d_4) δ 8.68 (s, 1H), 7.57 (t, J = 2.0 Hz, 1H), 7.48 (d, J = 3.6 Hz, 1H), 7.33 (ddd, J = 8.2 Hz, J = 2.0 Hz, J = 1.2 Hz, 1H), 7.24 (t, J = 8.0 Hz, 1H), 7.01 (ddd, J = 7.7 Hz, J = 2.1 Hz, J = 1.2 Hz, 1H), 6.90–6.83 (m, 1H), 6.82 (d, J = 3.6 Hz, 1H), 4.41–4.28 (m, 2H), 3.82 (t, J = 5.6 Hz, 2H), 2.96–2.82 (m, 2H). ^{13}C NMR (63 MHz, MeOH-d_4) δ 158.3 (C), 157.4 (C), 153.5 (C), 151.3 (CH), 142.6 (C), 136.7 (C), 135.2 (C), 130.8 (CH), 130.7 (CH), 128.1 (CH), 123.7 (CH), 121.6 (CH), 119.9 (CH), 116.0 (C), 101.8 (CH), 45.3 (CH_2), 42.0 (CH_2), 27.8 (CH_2). HRMS (EI-MS) *m/z* calcd for $C_{18}H_{17}ClN_5O$ $[M+H]^+$: 354.1116, found: 354.1114.

8.1.2.15. 3-Aminophenyl N,N-dimethylcarbamate

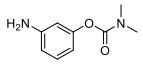

A solution of 3-nitrophenol (2.0 g, 14.4 mmol), *N,N*-dimethylchlorocarbamate (1.6 mL, 17.2 mmol, 1.2 equiv.), pyridine (3.4 ml, 43.2 mmol, 3.0 equiv.), and triethylamine (3.0 mL, 21.6 mmol, 1.5 equiv.) in CH_2Cl_2 (18 mL) was stirred for 3 days. The reaction was

quenched with H_2O (10 mL), stirred for 15 min, diluted with Et_2O, washed with sat. aq. $KHSO_4$, H_2O, sat. aq. $NaHCO_3$, and brine, then dried over $MgSO_4$, filtered, and concentrated under reduced pressure. The crude nitro compound obtained was hydrogenated with H_2 (balloon pressure) over 10 % Pd/C (400 mg) in THF (60 ml) with AcOH (0.8 mL) for 18 h at rt. The reaction was filtered through celite with EtOAc and concentrated under reduced pressure. The residue was purified by silica gel column chromatography (MeOH:CH_2Cl_2, 100/0 up to 96/4) to give 3-aminophenyl *N*,*N*-dimethylcarbamate (1.60 g, 8.9 mmol, 62 %) as a yellow powder. R_f (CH_2Cl_2/MeOH 92/8) 0.61. Mp: 80–82 °C. IR (ATR diamond, cm^{-1}) ν: 3434, 3346, 1688, 1611, 1482, 1386, 1314, 1282, 1080, 1150, 1020, 997, 882. ^{1}H NMR (250 MHz, $CDCl_3$) δ 7.08 (t, J = 8.0 Hz, 1H), 6.50–6.44 (m, 2H), 6.42 (t, J = 2.2 Hz, 1H), 3.70 (s, 2H), 3.06 (s, 3H), 2.98 (s, 3H). ^{13}C NMR (63 MHz, $CDCl_3$) δ 155.0 (C), 152.5 (C), 147.8 (C), 129.7 (CH), 112.1 (CH), 111.5 (CH), 108.6 (CH), 36.6 (CH_3), 36.4 (CH_3). HRMS (EI-MS) *m/z* calcd for $C_9H_{13}N_2O_2$ $[M+H]^+$: 181.0972, found: 181.0971. The synthesis and ^{1}H NMR spectra of this compound was described in Harrison, B. et al. Novel Class of LIM-Kinase 2 Inhibitors for the Treatment of Ocular Hypertension and Associated Glaucoma. *J. Med. Chem.* **2009**, *52*, 6515–6518.

*8.1.2.16. 3-(4-(7H-Pyrrolo [2,3-d]pyrimidin-4-yl)-1,2,3,6-tetrahydropyridine-1-carboxamido)phenyl dimethylcarbamate (**20**).* The reaction was carried out as described in **method B** using the previously synthesized 3-aminophenyl *N*,*N*-dimethylcarbamate (55 mg, 0.31 mmol) and amine **8** (100 mg, 0.37 mmol) in dry THF (4.4 mL). The crude reaction mixture was purified by silica gel column chromatography using a gradient solvent system of CH_2Cl_2/MeOH from 100 up to 96/4 to afford the urea derivative **20** (55 mg, 45 %) as a brown solid. R_f (CH_2Cl_2/MeOH 95/5) 0.23. Mp: 141–143 °C. IR (ATR diamond, cm^{-1}) ν: 3132, 2929, 2361, 2090, 1704, 1635, 1540, 1436, 1387, 1238, 1177, 751, 607. ^{1}H NMR (400 MHz, DMSO-d_6) δ 12.13 (s, 1H), 8.74–8.68 (m, 2H), 7.60–7.55 (m, 1H), 7.40–7.35 (m, 1H), 7.32 (d, J = 8.3 Hz, 1H), 7.22 (t, J = 8.1 Hz, 1H), 6.98–6.93 (m, 1H), 6.85–6.80 (m, 1H), 6.69 (d, J = 7.8 Hz, 1H), 4.32–4.26 (m, 2H), 3.72 (t, J = 5.6 Hz, 2H), 3.03 (s, 3H), 2.91 (s, 3H), 2.85–2.78 (m, 2H). ^{13}C NMR (101 MHz, DMSO-d_6) δ 155.7 (C), 154.8 (C), 154.0 (C), 152.4 (C), 151.3 (C), 150.3 (CH), 141.5 (C), 135.0 (C), 129.7 (CH), 128.7 (CH), 127.0 (CH), 116.0 (CH), 114.9 (CH), 113.6 (C), 112.9 (CH), 100.2 (CH), 44.1 (CH_2), 40.5 (CH_2), 36.2 (CH_3), 36.1 (CH_3), 26.1 (CH_2). HRMS (EI-MS) *m/z* calcd for $C_{21}H_{23}N_6O_3$ $[M+H]^+$: 407.1826, found: 407.1832.

*8.1.2.17. 4-(5-Methyl-7H-pyrrolo [2,3-d]pyrimidin-4-yl)-N-phenyl-3,6-dihydropyridine-1(2H)-carboxamide (**21**).* The reaction was carried out as described in **method A** using amine **9** (70 mg, 0.24 mmol) and phenylisocyanate (20.8 μL, 0.27 mmol) in anhydrous CH_2Cl_2 (4 mL). The crude reaction mixture was purified by silica gel column chromatography using a gradient solvent system of CH_2Cl_2/acetone from 100/0 up to 40/60 to afford compound **21** (64 mg, 80 %) as an off-white solid. R_f (CH_2Cl_2/acetone 30/70) 0.35. Mp: 245–247 °C. IR (ATR diamond, cm^{-1}) ν: 3320, 3150, 3043, 2862, 1649, 1529, 1443, 1341, 1232, 1205, 749. ^{1}H NMR (250 MHz, MeOH-d$_4$) δ 8.63 (s, 1H), 7.45–7.36 (m, 2H), 7.33–7.24 (m, 2H), 7.23 (d, J = 1.3 Hz, 1H), 7.09–6.98 (m, 1H), 6.08–6.00 (m, 1H), 4.29 (q, J = 2.8 Hz, 2H), 3.84 (t, J = 5.6 Hz, 2H), 2.80–2.68 (m, 2H), 2.30 (d, J = 1.2 Hz, 3H). ^{13}C NMR (63 MHz, MeOH-d$_4$) δ 161.2 (C), 158.1 (C), 153.8 (C), 151.0 (CH), 140.9 (C), 135.8 (C), 129.6 (2 x CH), 129.1 (CH), 126.4 (CH), 124.2 (CH), 122.4 (2 x CH), 116.6 (C), 111.6 (C), 44.9 (CH_2), 42.0 (CH_2), 29.2 (CH_2), 12.9 (CH_3). HRMS (EI-MS) *m/z* calcd for $C_{19}H_{20}N_5O$ $[M+H]^+$: 334.1662, found: 334.1661. Purity (HPLC): 95.7 %

*8.1.2.18. N-(3-Fluorophenyl)-4-(5-methyl-7H-pyrrolo [2,3-d]pyrimidin-4-yl)-3,6-dihydropyridine-1(2H)-carboxamide (**22**).* The reaction was carried out as described in **method A** using amine **9** (70 mg, 0.24 mmol) and 3-fluorophenyl isocyanate (31 μL, 0.27 mmol) in anhydrous CH_2Cl_2 (4 mL). The crude reaction mixture was purified by silica gel column chromatography using a gradient solvent system of CH_2Cl_2/acetone from 90/10 up to 60/40 to afford the urea derivative **22** (51 mg, 60 %) as an off-white solid. R_f (CH_2Cl_2/acetone 70/30) 0.28. Mp: 241–243 °C. IR (ATR diamond, cm^{-1}) ν: 3129, 2981, 2361, 1635, 1599, 1525, 1431, 1238, 1190, 1145, 772. ^{1}H NMR (400 MHz, DMSO-d_6) δ 11.83 (brs, 1H), 8.79 (brs, 1H), 8.65 (s, 1H), 7.49 (d, J = 12.4 Hz, 1H), 7.38–7.23 (m, 3H), 6.86–6.66 (m, 1H), 6.05 (s, 1H), 4.34–4.10 (m, 2H), 3.81–3.69 (m, 2H), 2.74–2.64 (m, 2H), 2.23 (s, 3H). ^{13}C NMR (101 MHz, DMSO-d_6) δ 162.2 (d, J = 239.4 Hz, C), 159.3 (C), 154.8 (C), 152.6 (C), 150.1 (CH), 142.6 (d, J = 11.1 Hz, C), 134.2 (C), 129.8 (d, J = 9.9 Hz, CH), 128.2 (CH), 125.1 (CH), 115.1 (d, J = 2.0 Hz, CH), 114.3 (C), 108.9 (C), 108.0 (d, J = 21.2 Hz, CH), 106.1 (d, J = 26.5 Hz, CH), 43.6 (CH_2), 40.6 (CH_2), 27.3 (CH_2), 12.9 (CH_3). ^{19}F NMR (376 MHz, DMSO-d_6) δ −112.84 to −112.99 (m). HRMS (EI-MS) *m/z* calcd for $C_{19}H_{19}FN_5O$ $[M+H]^+$: 352.1568, found: 352.1570.

*8.1.2.19. N-(3-Chlorophenyl)-4-(5-methyl-7H-pyrrolo [2,3-d]pyrimidin-4-yl)-3,6-dihydropyridine-1(2H)-carboxamide (**23**).* The reaction was carried out as described in **method A** using amine **9** (70 mg, 0.24 mmol) and 3-chlorophenyl isocyanate (33 μL, 0.27 mmol) in anhydrous CH_2Cl_2 (4 mL). The crude reaction mixture was purified by silica gel column chromatography using a gradient solvent system of CH_2Cl_2/acetone from 90/10 up to 60/40 to afford the urea derivative **23** (42 mg, 47 %) as an off-white solid. R_f (CH_2Cl_2/acetone 70/30) 0.29. Mp: 232–234 °C. IR (ATR diamond, cm^{-1}) ν: 3224, 3116, 2920, 1637, 1597, 1565, 1587, 1427, 1238, 1189, 758. ^{1}H NMR (400 MHz, DMSO-d_6) δ 11.84 (brs, 1H), 8.77 (brs, 1H), 8.65 (s, 1H), 7.70 (t, J = 2.1 Hz, 1H), 7.45 (dd, J = 8.2 Hz, J = 2.0 Hz, 1H), 7.32 (s, 1H), 7.27 (t, J = 8.1 Hz, 1H), 6.99 (dd, J = 8.0 Hz, J = 2.1 Hz, 1H), 6.09–6.01 (m, 1H), 4.26–4.19 (m, 2H), 3.74 (t, J = 5.6 Hz, 2H), 2.73–2.61 (m, 2H), 2.24 (s, 3H). ^{13}C NMR (101 MHz, DMSO-d_6) δ 159.2 (C), 154.7 (C), 152.6 (C), 150.0 (CH), 142.2 (C), 134.2 (C), 132.7 (C), 129.9 (CH), 128.2 (CH), 125.1 (CH), 121.3 (CH), 118.9 (CH), 117.8 (CH), 114.3 (C), 108.9 (C), 43.6 (CH_2), 40.6 (CH_2), 27.3 (CH_2), 12.9 (CH_3). HRMS (EI-MS) *m/z* calcd for $C_{19}H_{19}ClN_5O$ $[M+H]^+$: 368.1273, found: 368.1275.

*8.1.2.20. N-(3-Bromophenyl)-4-(5-methyl-7H-pyrrolo [2,3-d]pyrimidin-4-yl)-3,6-dihydropyridine-1(2H)-carboxamide (**24**).* The reaction was carried out as described in **method A** using amine **9** (70 mg, 0.24 mmol) and 3-bromophenyl isocyanate (53 mg, 0.27 mmol) in anhydrous CH_2Cl_2 (4 mL). The crude reaction mixture was purified by silica gel column chromatography using a gradient solvent system of CH_2Cl_2/acetone from 90/10 up to 60/40 to afford the urea derivative **24** (69 mg, 70 %) as a white solid. R_f (CH_2Cl_2/acetone 70/30) 0.28. Mp: 223–225 °C. IR (ATR diamond, cm^{-1}) ν: 3117, 3034, 2917, 1636, 1595, 1524, 1425, 1340, 1240, 1190, 782. ^{1}H NMR (400 MHz, DMSO-d_6) δ 11.82 (brs, 1H), 8.75 (brs, 1H), 8.65 (s, 1H), 7.83 (s, 1H), 7.50 (d, J = 8.3 Hz, 1H), 7.31 (s, 1H), 7.21 (t, J = 8.0 Hz, 1H), 7.12 (d, J = 8.0 Hz, 1H), 6.05 (s, 1H), 4.30–4.13 (m, 2H), 3.73 (t, J = 5.6 Hz, 2H), 2.75–2.62 (m, 2H), 2.23 (s, 3H). ^{13}C NMR (101 MHz, DMSO-d_6) δ 159.3 (C), 154.7 (C), 152.6 (C), 150.1 (CH), 142.3 (C), 134.2 (C), 130.3 (CH), 128.1 (CH), 125.0 (CH), 124.2 (CH), 121.7 (CH), 121.2 (C), 118.2 (CH), 114.3 (C), 108.9 (C), 43.6 (CH_2), 40.6 (CH_2), 27.3 (CH_2), 12.9 (CH_3). HRMS (EI-MS) *m/z* calcd for $C_{19}H_{19}BrN_5O$ $[M+H]^+$: 412.0767, found: 412.0766.

*8.1.2.21. N-(3-Methoxyphenyl)-4-(5-methyl-7H-pyrrolo [2,3-d]pyrimidin-4-yl)-3,6-dihydropyridine-1(2H)-carboxamide (**25**).* The reaction was carried out as described in **method A** using amine **9** (70 mg, 0.24 mmol) and 3-methoxyphenyl isocyanate (35 μL, 0.27 mmol) in anhydrous CH_2Cl_2 (4 mL). The crude reaction mixture was purified by silica gel column chromatography using a gradient solvent system of CH_2Cl_2/acetone from 90/10 up to 60/40 to afford the urea derivative **25** (40 mg, 46 %) as a white solid. R_f (CH_2Cl_2/acetone 70/30) 0.30. Mp: 212–214 °C. IR (ATR diamond, cm^{-1}) ν: 3327, 3130, 3010, 1630, 1610,

1540, 1446, 1428, 1202, 1125, 784. ^{1}H NMR (400 MHz, DMSO-d_6) δ 11.82 (brkkks, 1H), 8.65 (s, 1H), 8.56 (brs, 1H), 7.38–7.06 (m, 4H), 6.67–6.37 (m, 1H), 6.15–5.95 (m, 1H), 4.22 (s, 2H), 3.72 (brs, 5H), 2.68 (brs, 2H), 2.24 (s, 3H). ^{13}C NMR (101 MHz, DMSO-d_6) δ 159.4 (2 x C), 155.0 (C), 152.6 (C), 150.1 (CH), 141.8 (C), 134.2 (C), 129.0 (CH), 128.3 (CH), 125.0 (CH), 114.3 (C), 111.9 (CH), 108.9 (C), 107.3 (CH), 105.3 (CH), 54.9 (CH_3), 43.6 (CH_2), 40.6 (CH_2), 27.3 (CH_2), 12.9 (CH_3). HRMS (EI-MS) *m/z* calcd for $C_{20}H_{22}N_5O_2$ $[M+H]^+$: 364.1768, found: 364.1770.

*8.1.2.22. 4-(5-Methyl-7H-pyrrolo [2,3-d]pyrimidin-4-yl)-N-(3-(trifluoro methoxy)phenyl)-3,6-dihydropyridine-1(2H)-carboxamide (**26**).* The reaction was carried out as described in **method B** using 3-(trifluoromethoxy)aniline (33 μL, 0.25 mmol) and amine **9** (85 mg, 0.30 mmol) in THF (4 mL). The crude reaction mixture was purified by silica gel column chromatography using a gradient solvent system of CH_2Cl_2/acetone from 80/20 up to 20/80 to afford compound **26** (73 mg, 70 %) as a white solid. R_f (CH_2Cl_2/Acetone 60/40) 0.18. Mp: 227–229 °C. IR (ATR diamond, cm^{-1}) *ν*: 3289, 2919, 2853, 1646, 1540, 1442, 1254, 1188, 1142, 1060, 750. ^{1}H NMR (400 MHz, DMSO-d_6) δ 11.83 (brs, 1H), 8.87 (brs, 1H), 8.65 (s, 1H), 7.67 (s, 1H), 7.52 (d, J = 8.3 Hz, 1H), 7.36 (t, J = 8.3 Hz, 1H), 7.32 (s, 1H), 6.91 (d, J = 8.2 Hz, 1H), 6.05 (s, 1H), 4.33–4.13 (m, 2H), 3.75 (t, J = 5.7 Hz, 2H), 2.76–2.61 (m, 2H), 2.23 (s, 3H). ^{13}C NMR (101 MHz, DMSO-d_6) δ 159.3 (C), 154.7 (C), 152.6 (C), 150.1 (CH), 148.5 (C), 142.4 (C), 134.2 (C), 129.9 (CH), 128.1 (CH), 125.0 (CH), 120.1 (q, J = 257.6 Hz, OCF_3), 117.9 (CH), 114.3 (C), 113.6 (CH), 111.4 (CH), 108.9 (C), 43.6 (CH_2), 40.6 (CH_2), 27.3 (CH_2), 12.9 (CH_3). ^{19}F NMR (376 MHz, DMSO-d_6) δ −56.6 (s). HRMS (EI-MS) *m/z* calcd for $C_{20}H_{19}F_3N_5O_2$ $[M+H]^+$: 418.1485, found: 418.1484.

*8.1.2.23. N-(Benzo[d] [1,3]dioxol-5-yl)-4-(5-methyl-7H-pyrrolo [2,3-d] pyrimidin-4-yl)-3,6-dihydropyridine-1(2H)-carboxamide (**27**).* The reaction was carried out as described in **method A** using amine **9** (80 mg, 0.28 mmol) and phenylisocyanate (50 mg, 0.31 mmol) in anhydrous CH_2Cl_2 (4 mL). The crude reaction mixture was purified by silica gel column chromatography using a gradient solvent system of CH_2Cl_2/acetone from 80/20 up to 40/60 to afford compound **27** (37 mg, 35 %) as an off-white solid. R_f (CH_2Cl_2/Acetone 60/40) 0.13. Mp: 235–237 °C. IR (ATR diamond, cm^{-1}) *ν*: 3083, 2977, 2852, 1628, 1568, 1541, 1416, 1233, 1192, 1034, 792. ^{1}H NMR (400 MHz, DMSO-d_6) δ 11.85 (brs, 1H), 8.64 (s, 1H), 8.47 (brs, 1H), 7.38–7.24 (m, 1H), 7.22–7.11 (m, 1H), 6.93–6.69 (m, 2H), 6.09–5.81 (m, 3H), 4.28–4.05 (m, 2H), 3.79–3.59 (m, 2H), 2.73–2.58 (m, 2H), 2.23 (d, J = 17.4 Hz, 3H). ^{13}C NMR (101 MHz, DMSO-d_6) δ 159.4 (C), 155.2 (C), 152.6 (C), 150.1 (CH), 146.8 (C), 142.1 (C), 134.8 (C), 134.2 (C), 128.3 (CH), 125.0 (CH), 114.3 (C), 112.6 (CH), 108.9 (C), 107.7 (CH), 102.6 (CH), 100.7 (CH_2), 43.6 (CH_2), 40.5 (CH_2), 27.3 (CH_2), 13.0 (CH_3). HRMS (EI-MS) *m/z* calcd for $C_{20}H_{20}N_5O_3$ $[M+H]^+$: 378.1561, found: 378.1560.

8.1.2.24. N,N-Dimethylbenzene-1,3-diamine

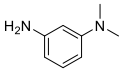

A 50 mL round bottom flask was loaded with *N,N*-dimethyl-3-nitroaniline (760 mg, 4.57 mmol), then a suspension of 10 % Pd/C (486 mg, 0.46 mmol, 0.1 equiv.) in MeOH (25 mL) was added. The flask was flushed with hydrogen then stirred at rt under hydrogen gas atmosphere until full conversion of the starting material (3h). The reaction mixture was filtered through Celite, washed with methanol then concentrated under vacuum. The crude reaction mixture was purified by silica gel column chromatography using a gradient solvent system of PE/EtOAc from 100 up to 80/20 to afford the desired aniline (122 mg, 20 %) as a dark brown oil. R_f (PE/EtOAc 80/20) 0.30. ^{1}H NMR (250 MHz, $CDCl_3$) δ 7.07–6.99 (m, 1H), 6.20 (ddd, J = 8.3, 2.3, 1.0 Hz, 1H), 6.15–6.06 (m, 2H), 3.58 (s, 2H), 2.91 (s, 6H). All spectral data corresponded to the literature values as found in Bhagwanth, S.; Adjabeng, G. M.; Hornberger, K. R. *Tetrahedron Lett.* **2009**, *50* (14), 1582–1585.

*8.1.2.25. N-(3-(Dimethylamino)phenyl)-4-(5-methyl-7H-pyrrolo [2,3-d] pyrimidin-4-yl)-3,6-dihydropyridine-1(2H)-carboxamide (**28**).* The reaction was carried out as described in **method B** using the previously prepared aniline **II** (66 mg, 0.48 mmol), and amine **9** (167 mg, 0.58 mmol) in dry THF (7.0 mL). The crude reaction mixture was purified by silica gel column chromatography using a gradient solvent system of CH_2Cl_2/MeOH from 100 up to 95/5 to afford the urea derivative **28** (86 mg, 78 %) as a brown solid. R_f (CH_2Cl_2/MeOH 95/5) 0.41. Mp: 157–159 °C. IR (ATR diamond, cm^{-1}) *ν*: 3121, 2919, 1628, 1601, 1540, 1495, 1434, 1342, 1241, 1062, 962, 830, 761, 753, 687. ^{1}H NMR (250 MHz, DMSO-d_6) δ 11.84 (s, 1H), 8.65 (s, 1H), 8.38 (s, 1H), 7.34–7.30 (m, 1H), 7.03 (t, J = 8.1 Hz, 1H), 6.94 (t, J = 2.2 Hz, 1H), 6.91–6.85 (m, 1H), 6.35 (dd, J = 8.2, 1.6 Hz, 1H), 6.11–5.99 (m, 1H), 4.21 (d, J = 3.2 Hz, 2H), 3.72 (t, J = 5.6 Hz, 2H), 2.86 (s, 6H), 2.67 (brs, 2H), 2.24 (d, J = 1.1 Hz, 3H). ^{13}C NMR (63 MHz, DMSO-d_6) δ 159.3 (C), 155.1 (C), 152.6 (C), 150.7 (C), 150.1 (CH), 141.1 (C), 134.1 (C), 128.6 (CH), 128.4 (CH), 125.1 (CH), 114.3 (C), 108.9 (C), 108.4 (CH), 106.6 (CH), 104.2 (CH), 43.6 (CH_2), 40.8 (CH_2), 40.2 (CH_3), 27.4 (CH_2), 12.9 (2 x CH_3). HRMS (EI-MS) *m/z* calcd for $C_{21}H_{25}N_6O$ $[M+H]^+$: 377.2084, found: 377.2083.

8.1.2.26. N-(3-Nitrophenyl)acetamide

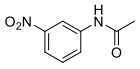

Acetic anhydride (7.24 mL, 0.5 M) was added to 3-nitroaniline (500 mg, 3.62 mmol) in a 20 mL sealed vial. The mixture was stirred for 5 h at rt. TLC monitoring (PE/EtOAc 70/30) indicated complete disappearance of 3-nitroaniline. Cold water was then added, and the solution made basic by addition of a KOH (1 M) solution to reach pH = 14. The aqueous layer was extracted with CH_2Cl_2 (3 x 35 mL). Then the combined organic layers were washed with $NaHCO_3$ and NaCl, dried over MgSO4, filtered, and concentrated under vacuum to afford the acetamide derivative **III** as a yellow solid (588 mg, 90 %) which was used without further purification in the next step. R_f (PE/EtOAc 70/30) 0.22. Mp: 151–153 °C. IR (Diamant ATR, cm^{-1}) ν: 3310, 3261, 3097, 1672, 1574, 1526, 1079, 1017, 737. ^{1}H NMR (400 MHz, DMSO-d_6) δ 10.41 (s, 1H), 8.61 (t, J = 1.9 Hz, 1H), 7.83–7.91 (m, 2H), 7.58 (t, J = 8.2 Hz, 1H), 2.09 (s, 3H). ^{13}C NMR (101 MHz, DMSO-d_6) δ 169.5 (C), 148.4 (C), 140.9 (C), 130.6 (CH), 125.3 (CH), 118.0 (CH), 113.4 (CH), 24.5 (CH_3). HRMS (EI-MS): *m/z* calc.for $C_8H_9N_2O_3$ $[M+H]^+$: 181.0608, found: 181.0611.

8.1.2.27. N-(3-Aminophenyl)acetamide

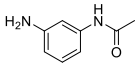

10 % Pd/C (234 mg, 0.2 mmol, 0.1 equiv.) was added to compound **III** (400 mg, 2.22 mmol) in a 50 mL round-bottomed flask in MeOH (12 mL, 0.18 M). The reaction was placed under H_2 and the mixture was stirred for 2 h at rt. TLC monitoring (PE/EtOAc 7/3) indicated the absence of the starting material.

The mixture was filtered through celite to afford the desired aniline derivative **IV** as a colorless oil (325 mg, 98 %) which was used without further purification in the next step. IR (Diamant ATR, cm^{-1}) ν: 3314, 1609, 1548, 1493, 1265, 1163, 775. ^{1}H (NMR 400 MHz, $CDCl_3$) δ 7.24 (s, 1H), 7.15 (d, J = 2.15 Hz, 1H), 7.06 (t, J = 8.0 Hz, 1H), 6.45 (d, J = 8.0 Hz, 1H) 6.42 (d, J = 8.0 Hz, 1H), 3.69 (s, 2H), 2.14 (s, 3H). ^{13}C (NMR 101 MHz, $CDCl_3$) δ 168.3 (C), 147.3 (C), 140.0 (C), 129.7 (CH), 111.1 (CH), 109.7 (CH), 106.6 (CH), 24.7 (CH_3). HRMS (EI-MS): *m/z* calc.for $C_8H_{11}N_2O$ $[M+H]^+$: 151.0866, found: 151.0869.

*8.1.2.28. 4-(5-Methyl-7H-pyrrolo [2,3-d]pyrimidin-4-yl)-3,6-dihydro-2H-pyridine-1-carboxylic acid (3-acetylaminophenyl)-amide (**29**).* The reaction was carried out as described in **method B** using aniline **IV** (0.082 mg, 0.55 mmol) and amine **9** (190 mg, 0.66 mmol, 1.2 equiv.) in dry THF (7.8 mL). The crude reaction mixture was purified by silica gel column chromatography using a gradient solvent system of CH_2Cl_2/MeOH from 100 up to 95/5 to afford the urea derivative **29** (79 mg, 37 %) as a beige solid. R_f (95/5 CH_2Cl_2/MeOH) 0.40. Mp = 123 − 125 °C. IR (Diamant ATR, cm-1) ν: 3362, 3115, 2852, 1643, 1602, 1537, 1486, 1420, 788. ^{1}H (NMR 250 MHz, DMSO-d_6) δ 11.84 (s, 1H), 9.86 (s, 1H), 8.65 (s, 1H), 8.61 (s, 1H), 7.80 (s, 1H), 7.32 (dd, J = 2.3, 1.2 Hz, 1H), 7.24–7.08 (m, 3H), 6.05 (s, 1H), 4.22 (d, J = 3.2 Hz, 2H), 3.73 (t, J = 5.5 Hz, 2H), 2.67 (s, 2H), 2.23 (d, J = 1.1 Hz, 3H), 2.02 (s, 3H). ^{13}C (NMR 101 MHz, DMSO-d_6) δ 168.3 (C), 159.5 (C), 155.2 (C), 152.6 (C), 150.2 (CH), 140.8 (C), 139.4 (C), 134.3 (C), 128.4 (CH), 128.4 (CH), 125.1 (CH), 114.9 (CH), 114.4 (C), 113.0 (CH), 111.1 (CH), 109.0 (C), 43.7 (CH_2), 40.7 (CH_2), 27.4 (CH_2), 24.0 (CH_3), 12.9 (CH_3). HRMS (EI-MS): *m/z* calc.for $C_{21}H_{23}N_6O_2$ $[M+H]^+$: 391.1877, found: 391.1880.

*8.1.2.29. 3-(4-(5-Methyl-7H-pyrrolo [2,3-d]pyrimidin-4-yl)-1,2,3,6-tetra hydropyridine-1-carboxamido)phenyl dimethylcarbamate (**30**).* The reaction was carried out as described in **method B** using previously prepared 3-aminophenyldimethyl carbamate **I** (45 mg, 0.25 mmol) and amine **9** (85 mg, 0.30 mmol) in THF (4 mL). The crude mixture was purified by silica gel column chromatography using a gradient solvent system of CH_2Cl_2/acetone from 90/10 up to 20/80 to afford the urea derivative **30** (60 mg, 57 %) as a white solid. R_f (CH_2Cl_2/Acetone 60/40) 0.21. Mp: 214–216 °C. IR (ATR diamond, cm^{-1}) ν: 3344, 3150, 2942, 2360, 1736, 1714, 1643, 1532, 1436, 1161, 611. ^{1}H NMR (400 MHz, DMSO-d_6) δ 11.83 (brs, 1H), 8.65 (brs, 2H), 7.60–7.10 (m, 4H), 6.68 (brs, 1H), 6.04 (brs, 1H), 4.22 (brs, 2H), 3.71 (s, 2H), 3.03 (s, 3H), 2.91 (s, 3H), 2.75–2.60 (m, 2H), 2.23 (s, 3H). ^{13}C NMR (101 MHz, DMSO-d_6) δ 159.3 (C), 154.9 (C), 154.0 (C), 152.6 (C), 151.4 (C), 150.1 (CH), 141.5 (C), 134.2 (C), 128.7 (CH), 128.3 (CH), 125.0 (CH), 116.0 (CH), 115.0 (CH), 114.3 (C), 113.0 (CH), 108.9 (C), 43.6 (CH_2), 40.6 (CH_2), 36.3 (CH_3), 36.1 (CH_3), 27.3 (CH_2), 12.9 (CH_3). HRMS (EI-MS) *m/z* calcd for $C_{22}H_{25}N_6O_3$ $[M+H]^+$: 421.1983, found: 421.1978.

*8.1.2.30. 4-(5-Methyl-7H-pyrrolo [2,3-d]pyrimidin-4-yl)-N-(3-(trifluoro methyl)phenyl)-3,6-dihydropyridine-1(2H)-carboxamide (**31**).* The reaction was carried out as described in **method A** using amine **9** (70 mg, 0.24 mmol) and 3-trifluorophenyl isocyanate (28 μL, 0.27 mmol) in anhydrous CH_2Cl_2 (4 mL). The crude reaction mixture was purified by silica gel column chromatography using a gradient solvent system of CH_2Cl_2/acetone from 80/20 up to 30/70 to afford the urea derivative **31** (69 mg, 72 %) as an off-white solid. R_f (CH_2Cl_2/Acetone 50/50) 0.33. Mp: degradation 231 °C. IR (ATR diamond, cm^{-1}) ν: 3285, 2978, 2833, 1632, 1535, 1443, 1333, 1239, 1123, 1066, 792. ^{1}H NMR (400 MHz, DMSO-d_6) δ 11.83 (brs, 1H), 8.93 (brs, 1H), 8.65 (s, 1H), 7.97 (s, 1H), 7.80 (d, J = 8.3 Hz, 1H), 7.48 (t, J = 8.0 Hz, 1H), 7.32 (s, 1H), 7.28 (d, J = 7.8 Hz, 1H), 6.11–5.96 (m, 1H), 4.30–4.11 (m, 2H), 3.76 (t, J = 5.6 Hz, 2H), 2.73–2.61 (m, 2H), 2.24 (s, 3H). ^{13}C NMR (101 MHz, DMSO-d_6) δ 159.3 (C), 154.8 (C), 152.6 (C), 150.1 (CH), 141.5 (C), 134.2 (C), 129.5 (CH), 129.1 (q, J = 31.3 Hz, C), 128.1 (CH), 125.0 (CH), 124.3 (q, J = 273.7 Hz, CF_3), 122.9 (CH), 117.9 (q, J = 4.0 Hz, CH), 115.5 (q, J = 4.0 Hz, CH), 114.3 (C), 108.9 (C), 43.5 (CH_2), 40.6 (CH_2), 27.3 (CH_2), 12.9 (CH_3). ^{19}F NMR (376 MHz, DMSO-d_6) δ −61.2 (s). HRMS (EI-MS) *m/z* calcd for $C_{20}H_{19}F_3N_5O$ $[M+H]^+$: 402.1536, found: 402.1536.

*8.1.2.31. N-(3-Cyanophenyl)-4-(5-methyl-7H-pyrrolo [2,3-d]pyrimidin-4-yl)-3,6-dihydropyridine-1(2H)-carboxamide (**32**).* The reaction was carried out as described in **method A** using amine **9** (70 mg, 0.24 mmol) and 3-cyanophenyl isocyanate (0.039 g, 0.27 mmol) in anhydrous CH_2Cl_2 (4 mL). The crude reaction mixture was purified by silica gel column chromatography using a gradient solvent system of CH_2Cl_2/acetone from 90/10 up to 40/60 to afford the urea derivative **32** (65 mg, 76 %) as an off-white solid. R_f (CH_2Cl_2/Acetone 50/50) 0.19. Mp: 207–209 °C. IR (ATR diamond, cm^{-1}) ν: 3369, 3116, 2872, 2230, 1672, 1584, 1543, 1429, 1289, 1232, 776. ^{1}H NMR (250 MHz, MeOH-d_4) δ 8.63 (s, 1H), 7.89–7.86 (m, 1H), 7.71 (ddd, J = 8.2, 2.3, 1.2 Hz, 1H), 7.45 (td, J = 7.6, 2.4 Hz, 1H), 7.35 (dt, J = 7.7, 1.4 Hz, 1H), 7.24 (d, J = 1.2 Hz, 1H), 6.13–5.98 (m, 1H), 4.37–4.23 (m, 2H), 3.86 (t, J = 5.6 Hz, 2H), 2.80–2.67 (m, 2H), 2.31 (d, J = 1.2 Hz, 3H). ^{13}C NMR (63 MHz, MeOH-d_4) δ 161.1 (C), 157.3 (C), 153.8 (C), 150.9 (CH), 142.4 (C), 135.8 (C), 130.8 (CH), 129.0 (CH), 127.2 (CH), 126.4 (CH), 126.0 (CH), 124.5 (CH), 119.8 (C), 116.6 (C), 113.5 (C), 111.6 (C), 44.8 (CH_2), 42.1 (CH_2), 29.2 (CH_2), 12.9 (CH_3). HRMS (EI-MS) *m/z* calcd for $C_{20}H_{19}N_6O$ $[M+H]^+$: 359.1615, found: 359.1616.

*8.1.2.32. N-(4-Chloro-3-(trifluoromethyl)phenyl)-4-(5-methyl-7H-pyrrolo [2,3-d]pyrimidin-4-yl)-3,6-dihydropyridine-1(2H)-carboxamide (**33**).* The reaction was carried out as described in **method A** using amine **9** (70 mg, 0.24 mmol) and 4-chloro-3-(trifluoromethyl)phenyl isocyanate (59 mg, 0.27 mmol) in anhydrous CH_2Cl_2 (4 mL). The crude reaction mixture was purified by silica gel column chromatography using a gradient solvent system of CH_2Cl_2/acetone from 80/20 up to 40/60 to afford the urea derivative **33** (49 mg, 47 %) as an off-white solid. R_f (CH_2Cl_2/Acetone 60/40) 0.22. Mp: 228–230 °C. IR (ATR diamond, cm^{-1}) ν: 3439, 3104, 2837, 1673, 1521, 1483, 1327, 1270, 1167, 1112, 829.^{1}H NMR (400 MHz, DMSO-d_6) δ 11.83 (brs, 1H), 9.03 (brs, 1H), 8.65 (s, 1H), 8.10 (d, J = 2.6 Hz, 1H), 7.85 (dd, J = 8.8, 2.6 Hz, 1H), 7.59 (d, J = 8.8 Hz, 1H), 7.31 (s, 1H), 6.10–6.02 (m, 1H), 4.29–4.18 (m, 2H), 3.75 (t, J = 5.6 Hz, 2H), 2.73–2.64 (m, 2H), 2.23 (s, 3H). ^{13}C NMR (101 MHz, DMSO-d_6) δ 159.2 (C), 154.5 (C), 152.6 (C), 150.1 (CH), 140.3 (C), 134.2 (C), 131.6 (CH), 128.0 (CH), 126.3 (q, J = 30.3 Hz, C) 125.1 (CH), 124.0 (CH), 122.9 (q, J = 272.9 Hz, C), 122.1 (q, J = 2.1 Hz, C), 118.0 (q, J = 5.7 Hz, CH), 114.3 (C), 108.9 (C), 43.5 (CH_2), 40.6 (CH_2), 27.2 (CH_2), 12.9 (CH_3). ^{19}F NMR (376 MHz, DMSO-d_6) δ −61.4 (s). HRMS (EI-MS) *m/z* calcd for $C_{20}H_{18}ClF_3N_5O$ $[M+H]^+$: 436.1146, found: 436.1145.

*8.1.2.33. 4-(5-methyl-7H-pyrrolo [2,3-d]pyrimidin-4-yl)-N-(3-pyridyl)-3,6-dihydro-2H-pyridine-1-carboxamide (**34**).* The reaction was carried out as described in **method B** with 3-aminopyridine (75 mg, 0.80 mmol) and amine **9** (275 mg, 0.96 mmol) in THF (12 mL). The crude reaction mixture was purified by silica gel column chromatography using a gradient solvent system of CH_2Cl_2/MeOH from 100/0 up to 95/5 to afford the urea derivative **34** (162 mg, 60 %) as a beige solid. R_f (CH_2Cl_2/MeOH 90/10) 0.24. Mp: 169–171 °C. IR (ATR diamond, cm^{-1}) ν: 3110, 1645, 1536, 1482, 1441, 1420, 1340, 1275, 1199. ^{1}H NMR (400 MHz, MeOH-d_4) δ 8.72 (brs, 1H), 8.66 (s, 1H), 8.22 (brs, 1H), 8.07–8.00 (m, 1H), 7.44 (dd, J = 8.4, 4.9 Hz, 1H), 7.28 (brs, 1H), 6.09 (s, 1H), 4.36–4.31 (m, 2H), 3.87 (t, J = 5.6 Hz, 2H), 2.78–2.71 (m, 2H), 2.32 (s, 3H). ^{13}C NMR (101 MHz MeOH-d_4) δ 160.4 (C), 157.3 (C), 153.9 (C), 150.3 (CH), 143.1 (CH), 141.6 (CH), 139.1 (C), 135.2 (C), 130.6 (CH), 129.5 (CH), 126.9 (CH), 125.5 (CH), 116.6 (C), 112.0 (C), 44.9 (CH_2), 42.1 (CH_2), 29.1 (CH_2), 12.8 (CH_3). HRMS (EI-MS): *m/z* calcd for $C_{18}H_{19}N_6O$ $[M+H]^+$: 335.1615; found: 335.1617.

*8.1.2.34. 4-(5-methyl-7H-pyrrolo [2,3-d]pyrimidin-4-yl)-N-(3-thienyl)-3,6-dihydro-2H-pyridine-1-carboxamide (**35**).* The reaction was carried out as described in **method A** with amine **9** (0.399 mg, 1.39 mmol) and 3-thienyl isocyanate (0.192 g, 1.53 mmol) in anhydrous CH_2Cl_2 (30 mL). The crude reaction mixture was purified by silica gel column chromatography using a gradient solvent system of CH_2Cl_2/acetone from 100/0 up to 50/50 to afford the urea derivative **35** (278 mg, 59 %) as a beige solid. R_f (CH_2Cl_2/Acetone 50/50) 0.57. Mp: 240–242 °C. IR (ATR diamond, cm^{-1}) ν: 3387, 3097, 2954, 2890, 1633, 1532, 1428, 1240, 772. ^{1}H NMR (400 MHz, MeOH-d_4) δ 8.62 (s, 1H), 7.28 (dd, J = 5.1, 3.2 Hz, 1H), 7.25–7.21 (m, 2H), 7.13 (dd, J = 5.1, 1.4 Hz, 1H), 6.07–6.01 (m,

1H), 4.27 (q, $J = 2.9$ Hz, 2H), 3.83 (t, $J = 5.6$ Hz, 2H), 2.76–2.68 (m, 2H), 2.30 (d, $J = 1.2$ Hz, 3H). ^{13}C NMR (101 MHz MeOH-d_4) δ 161.3 (C), 157.6 (C), 153.8 (C), 151.0 (CH), 138.9 (C), 135.9 (C), 129.1 (CH), 126.4 (CH), 124.8 (CH), 123.4 (CH), 116.6 (C), 111.7 (C), 109.4 (CH), 44.8 (CH_2), 42.0 (CH_2), 29.2 (CH_2), 12.9 (CH_3). HRMS (EI-MS): *m/z* calcd for $C_{17}H_{18}N_5OS$ $[M+H]^+$: 340.1227; found: 340.1227.

*8.1.2.35. 4-(5-Methyl-7H-pyrrolo [2,3-d]pyrimidin-4-yl)-N-(naphthalen-2-yl)-3,6-dihydropyridine-1(2H)-carboxamide (**36**).* The reaction was carried out as described in **method A** using amine **9** (70 mg, 0.24 mmol) and 2-naphthyl isocyanate (0.045 g, 0.27 mmol) in anhydrous CH_2Cl_2 (4 mL). The crude reaction mixture was purified by silica gel column chromatography using a gradient solvent system of CH_2Cl_2/acetone from 80/20 up to 30/70 to afford the urea derivative **36** (55 mg, 60 %) as an off-white solid. R_f (CH_2Cl_2/Acetone 50/50) 0.31. Mp: 233–235 °C. IR (ATR diamond, cm^{-1}) ν: 3126, 3035, 2905, 1632, 1537, 1532, 1387, 1265, 1214, 819, 748. ^{1}H NMR (250 MHz, MeOH-d_4) δ 8.64 (s, 1H), 7.91 (d, $J = 2.1$ Hz, 1H), 7.84–7.69 (m, 3H), 7.56 (dd, $J = 8.8$, 2.2 Hz, 1H), 7.47–7.30 (m, 2H), 7.24 (d, $J = 1.2$ Hz, 1H), 6.13–5.99 (m, 1H), 4.39–4.31 (m, 2H), 3.90 (t, $J = 5.6$ Hz, 2H), 2.83–2.69 (m, 2H), 2.33 (d, $J = 1.2$ Hz, 3H). ^{13}C NMR (63 MHz, MeOH-d_4) δ 161.3 (C), 158.1 (C), 151.0 (CH), 138.5 (C), 135.9 (C), 135.4 (C), 131.7 (C), 129.2 (CH), 129.1 (CH), 128.5 (CH), 128.3 (CH), 127.2 (CH), 126.4 (CH), 125.5 (CH), 122.8 (CH), 121.4 (C), 118.3 (CH), 116.7 (C), 111.7 (C), 45.0 (CH_2), 42.1 (CH_2), 29.3 (CH_2), 12.9 (CH_3). HRMS (EI-MS) *m/z* calcd for $C_{23}H_{22}N_5O$ $[M+H]^+$: 384.1819, found: 384.1815.

*8.1.2.36. N-([1,1′-Biphenyl]-3-yl)-4-(5-methyl-7H-pyrrolo [2,3-d]pyrimidin-4-yl)-3,6-dihydropyridine-1(2H)-carboxamide (**37**).* The reaction was carried out as described in **method C** using biphenyl-3-carboxylic acid (61 mg, 0.31 mmol), and the amine **9** (89 mg, 0.31 mmol). The crude reaction mixture was purified by silica gel column chromatography using a gradient solvent system of CH_2Cl_2/acetone from 100/0 up to 60/40 to afford the urea derivative **37** (43 mg, 34 %) as a white solid. R_f (CH_2Cl_2/Acetone 70/30) 0.31. Mp: 235–237 °C. IR (ATR diamond, cm^{-1}) ν: 3324, 3067, 2364, 1636, 1597, 1532, 1417, 1346, 1239, 1141, 753. ^{1}H NMR (400 MHz, DMSO-d_6) δ 11.82 (brs, 1H), 8.68 (brs, 1H), 8.65 (s, 1H), 7.83 (s, 1H), 7.71–7.18 (m, 9H), 6.17–5.97 (m, 1H), 4.33–4.15 (m, 2H), 3.83–3.67 (m, 2H), 2.78–2.62 (m, 2H), 2.25 (s, 3H). ^{13}C NMR (101 MHz, DMSO-d_6) δ 159.4 (C), 155.1 (C), 152.6 (C), 150.1 (CH), 141.1 (C), 140.4 (C), 140.3 (C), 134.3 (C), 128.9 (3 x CH), 128.3 (CH), 127.4 (CH), 126.6 (2 x CH), 125.0 (CH), 120.1 (CH), 118.7 (CH), 118.0 (CH), 114.3 (C), 108.9 (C), 43.6 (CH_2), 40.6 (CH_2), 27.3 (CH_2), 12.9 (CH_3). HRMS (EI-MS) *m/z* calcd for $C_{25}H_{24}N_5O$ $[M+H]^+$: 410.1975, found: 410.1983.

*8.1.2.37. 4-(5-Methyl-7H-pyrrolo [2,3-d]pyrimidin-4-yl)-N-(3-(pyridin-4-yl)phenyl)-3,6-dihydropyridine-1(2H)-carboxamide (**38**).* The reaction was carried out as described in **method C** using 3-(pyridin-4-yl)benzoic acid (62 mg, 0.31 mmol), and the amine **9** (89 mg, 0.31 mmol). The crude reaction mixture was purified by silica gel column chromatography using a gradient solvent system of CH_2Cl_2/acetone from 100/0 up to 50/50 to afford the urea derivative **38** (19 mg, 15 %) as a beige solid. R_f (CH_2Cl_2/Acetone 50/50) 0.24. Mp: 208–210 °C. IR (ATR diamond, cm^{-1}) ν: 3442, 2995, 2829, 2529, 1669, 1603, 1396, 1174, 1083, 877, 752. ^{1}H NMR (400 MHz, DMSO-d_6) δ 11.83 (brs, 1H), 8.77 (brs, 1H), 8.71–8.59 (m, 3H), 8.01–7.90 (m, 1H), 7.73–7.56 (m, 2H), 7.45–7.36 (m, 3H), 7.32 (s, 1H), 6.07 (s, 1H), 4.26 (s, 2H), 3.77 (s, 2H), 2.70 (s, 2H), 2.25 (s, 3H). ^{13}C NMR (101 MHz, DMSO-d_6) δ 159.4 (C), 155.0 (C), 152.6 (C), 150.2 (2 x CH), 150.1 (CH), 147.3 (C), 141.4 (C), 137.3 (C), 134.3 (C), 129.3 (CH), 128.2 (CH), 125.1 (CH), 121.1 (2 x CH), 120.4 (CH), 120.2 (CH), 117.9 (CH), 114.3 (C), 108.9 (C), 43.6 (CH_2), 40.6 (CH_2), 27.3 (CH_2), 12.9 (CH_3). HRMS (EI-MS) *m/z* calcd for $C_{24}H_{24}N_6O$ $[M+H]^+$: 411.1928, found: 411.1933.

*8.1.2.38. N-(3-(1H-Pyrrol-1-yl)phenyl)-4-(5-methyl-7H-pyrrolo [2,3-d]pyrimidin-4-yl)-3,6-dihydropyridine-1(2H)-carboxamide (**39**).* The reaction was carried out as described in **method C** using 3-(1*H*-pyrrol-1-yl) benzoic acid (58 mg, 0.31 mmol), and amine **9** (89 mg, 0.31 mmol, 1.0 equiv.). The crude reaction mixture was purified by silica gel column chromatography using a gradient solvent system of CH_2Cl_2/acetone from 100/0 up to 50/50 to afford the urea derivative **39** (61 mg, 49 %) as an off-white solid. R_f (CH_2Cl_2/Acetone 50/50) 0.28. Mp: 215–217 °C. IR (ATR diamond, cm^{-1}) ν: 3217, 3131, 2822, 1633, 1597, 1536, 1495, 1435, 1341, 1235, 725. ^{1}H NMR (400 MHz, DMSO-d_6) δ 11.85 (brs, 1H), 8.75 (brs, 1H), 8.66 (s, 1H), 7.76 (s, 1H), 7.52–7.06 (m, 6H), 6.26 (s, 2H), 6.18–5.97 (m, 1H), 4.37–4.09 (m, 2H), 3.85–3.69 (m, 2H), 2.77–2.63 (m, 2H), 2.24 (s, 3H). ^{13}C NMR (101 MHz, DMSO-d_6) δ 159.3 (C), 154.9 (C), 152.6 (C), 150.1 (CH), 141.8 (C), 140.1 (C), 134.3 (C), 129.5 (CH), 128.2 (CH), 125.1 (CH), 118.9 (2 x CH), 116.5 (CH), 114.3 (C), 113.0 (CH), 110.8 (CH), 110.3 (2 x CH), 108.9 (C), 43.6 (CH_2), 40.6 (CH_2), 27.3 (CH_2), 12.9 (CH_3). HRMS (EI-MS) *m/z* calcd for $C_{23}H_{23}N_6O$ $[M+H]^+$: 399.1928, found: 399.1928.

8.1.2.39. 3-(1H-Imidazole-1-yl)aniline

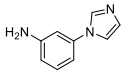

An oven-dried microwave vial was charged with a magnetic stirring bar, CuI (28 mg, 0.15 mmol, 0.05 equiv.), K_3PO_4 (1.31 g, 6.17 mmol, 2.1 equiv.), imidazole (0.20 g, 2.94 mmol, 1.0 equiv.) and 1,10-phenanthroline (52 mg, 0.29 mmol, 0.1 equiv.). The tube was then evacuated and back-filled with argon. The evacuation/backfill sequence was repeated two additional times. Under a counterflow of argon, 3-iodoaniline (0.42 mL, 3.53 mmol, 1.2 equiv.) and degassed 1,4-dioxane (1.5 mL) were added by syringe. The tube was placed in a preheated oil bath at 110 °C and the solution was stirred vigorously for 24 h. The reaction mixture was cooled to room temperature, diluted with EtOAc (2–3 mL), filtered through a plug of Celite and rinsed with EtOAc. The filtrate was concentrated under reduced pressure and the resulting residue was purified by silica gel column chromatography using a gradient solvent system of PE/EtOAc from 90/10 up to 80/20 to afford the desired 3-(1*H*-imidazole-1-yl)aniline (0.38 g, 82 %) as a beige solid. ^{1}H NMR (250 MHz, DMSO-d_6) δ 7.82 (s, 1H), 7.28–7.16 (m, 3H), 6.79–6.73 (m, 1H), 6.70–6.63 (m, 2H), 3.75 (brs, 2H). All spectral data corresponded to literature values as found in Suresh, P.; Pitchumani, K. *J. Org. Chem.* **2008**, *73*, 9121–9124.

*8.1.2.40. N-(3-(1H-Imidazole-1-yl)phenyl)-4-(5-methyl-7H-pyrrolo [2,3-d]pyrimidin-4-yl)-3,6-dihydropyridine-1(2H)-carboxamide (**40**).* The reaction was carried out as described in **method B** using aniline **V** (40 mg, 0.25 mmol) and amine **9** (85 mg, 0.30 mmol) in THF (4 mL). The crude mixture was purified by silica gel column chromatography using a gradient solvent system of CH_2Cl_2/acetone from 90/10 up to 40/60 to afford the urea derivative **40** (45 mg, 45 %) as an off-white solid. R_f (CH_2Cl_2/Acetone 50/50) 0.23. Mp: 245–247 °C. IR (ATR diamond, cm^{-1}) ν: 3349, 3109, 2843, 2360, 1654, 1600, 1504, 1434, 1207, 1063, 826. ^{1}H NMR (400 MHz, DMSO-d_6) δ 11.84 (brs, 1H), 8.83 (brs, 1H), 8.65 (s, 1H), 8.13 (s, 1H), 7.80 (s, 1H), 7.62 (s, 1H), 7.52 (d, $J = 8.0$, 1H), 7.39 (t, $J = 8.1$ Hz, 1H), 7.32 (s, 1H), 7.20 (d, $J = 7.9$ Hz, 1H), 7.11 (s, 1H), 6.06 (brs, 1H), 4.32–4.16 (m, 2H), 3.76 (t, $J = 5.5$ Hz, 2H), 2.70 (s, 2H), 2.24 (s, 3H). ^{13}C NMR (101 MHz, DMSO-d_6) δ 159.3 (C), 154.9 (C), 152.6 (C), 150.1 (CH), 142.0 (C), 137.0 (C), 135.5 (CH), 134.3 (C), 129.8 (CH), 129.7 (CH), 128.2 (CH), 125.1 (CH), 118.1 (CH), 118.0 (CH), 114.3 (C), 114.0 (CH), 111.8 (CH), 108.9 (C), 43.6 (CH_2), 40.6 (CH_2), 27.3 (CH_2), 12.9 (CH_3). HRMS (EI-MS) *m/z* calcd for $C_{22}H_{22}N_7O$ $[M+H]^+$: 400.1880, found: 400.1880.

*8.1.2.41. N-[3-(2-Methoxyphenyl)phenyl]-4-(5-methyl-7H-pyrrolo [2,3-d]pyrimidin-4-yl)-3,6-dihydro-2H-pyridine-1-carboxamide (**41**).* The reaction was carried out as described in **method B** with 2′-methoxy-[1,1′-biphenyl]-3-amine (26 mg, 0.13 mmol) and amine **9** (47 mg, 0.16 mmol) in THF (4 mL). The crude mixture was purified by silica gel column chromatography using a gradient solvent system CH_2Cl_2/acetone from 100/0 up to 40/60 to afford the urea derivative **41** (43 mg, 72 %) as a white solid. R_f (CH_2Cl_2/acetone 50/50) 0.18. Mp: degradation 205 °C. IR (ATR diamond, cm^{-1}) ν: 3211, 3120, 2999, 2852, 1633, 1548, 1437, 1239, 739. ^{1}H NMR (250 MHz, DMSO-d_6) δ 11.83 (s, 1H), 8.65 (s, 1H), 8.62 (s, 1H), 7.60 (brs, 1H), 7.49 (d, J = 8.0 Hz, 1H), 7.40–7.20 (m, 4H), 7.18–6.95 (m, 3H), 6.05 (s, 1H), 4.27–4.19 (m, 2H), 3.86–3.63 (m, 5H), 2.68 (s, 2H), 2.24 (s, 3H). ^{13}C NMR (63 MHz, DMSO-d_6) δ 159.4 (C), 156.1 (C), 155.1 (C), 152.6 (C), 150.1 (CH), 140.2 (C), 138.3 (C), 134.2 (C), 130.3 (CH), 130.1 (C), 128.7 (CH), 128.3 (CH), 127.8 (CH), 125.0 (CH), 122.9 (CH), 120.7 (CH), 120.6 (CH), 118.3 (CH), 114.3 (C), 111.7 (CH), 108.9 (C), 55.5 (OCH_3), 43.6 (CH_2), 40.5 (CH_2), 27.3 (CH_2), 12.9 (CH_3). HRMS (EI-MS) *m/z* calcd for $CH_6H_{26}N_5O_2[M+H]^+$: 440.2081, found: 440.2080.

*8.1.2.42. N-[3-(3-Methoxyphenyl)phenyl]-4-(5-methyl-7H-pyrrolo [2,3-d]pyrimidin-4-yl)-3,6-dihydro-2H-pyridine-1-carboxamide (**42**).* The reaction was carried out as described in **method B** with 3′-methoxy-[1,1′-biphenyl]-3-amine (26 mg, 0.13 mmol) and amine **9** (47 mg, 0.16 mmol) in THF (4 mL). The crude mixture was purified by silica gel column chromatography using a gradient solvent system CH_2Cl_2/acetone from 100/0 up to 40/60 to afford the urea derivative **42** (47 mg, 78 %) as a white solid. R_f (CH_2Cl_2/acetone 50/50) 0.19. Mp: degradation 224 °C. IR (ATR diamond, cm^{-1}) ν: 3291, 3119, 2831, 1631, 1601, 1539, 1437, 1235, 766, 694. ^{1}H NMR (250 MHz, DMSO-d_6) δ 11.83 (s, 1H), 8.68 (s, 1H), 8.65 (s, 1H), 7.81 (s, 1H), 7.56 (d, J = 7.9 Hz, 1H), 7.47–7.04 (m, 6H), 6.94 (d, J = 8.1 Hz, 1H), 6.07 (s, 1H), 4.26 (s, 2H), 3.82 (s, 3H), 3.76 (t, J = 4.6 Hz, 2H), 2.70 (s, 2H), 2.25 (s, 3H). ^{13}C NMR (63 MHz, DMSO-d_6) δ 159.7 (C), 159.3 (C), 155.1 (C), 152.6 (C), 150.1 (CH), 141.9 (C), 141.0 (C), 140.2 (C), 134.2 (C), 129.9 (CH), 128.8 (CH), 128.2 (CH), 125.0 (CH), 120.2 (CH), 118.9 (CH), 118.8 (CH), 118.1 (CH), 114.3 (C), 112.9 (CH), 112.1 (CH), 108.9 (C), 55.1 (OCH_3), 43.6 (CH_2), 40.6 (CH_2), 27.3 (CH_2), 12.9 (CH_3). HRMS (EI-MS) *m/z* calcd for $C_{26}H_{26}N_5O_2[M+H]^+$: 440.2081, found: 440.2083.

*8.1.2.43. N-[3-(4-Methoxyphenyl)phenyl]-4-(5-methyl-7H-pyrrolo [2,3-d]pyrimidin-4-yl)-3,6-dihydro-2H-pyridine-1-carboxamide (**43**).* The reaction was carried out as described in **method B** with 4′-methoxy-[1,1′-biphenyl]-3-amine (26 mg, 0.13 mmol) and amine **9** (47 mg, 0.16 mmol) in THF (4 mL). The crude mixture was purified by silica gel column chromatography using a gradient solvent system of CH_2Cl_2/acetone from 100/0 up to 40/60 to afford the urea derivative **43** (43 mg, 72 %) as a white solid. R_f (CH_2Cl_2/acetone 50/50) 0.25. Mp: degradation 252 °C. IR (ATR diamond, cm^{-1}) ν: 3309, 3147, 2840, 1636, 1604, 15443, 1514, 1436, 1232, 1183, 786. ^{1}H NMR (250 MHz, DMSO-d_6) δ 11.83 (s, 1H), 8.65 (s, 2H), 7.77 (s, 1H), 7.60–7.45 (m, 3H), 7.37–7.15 (m, 3H), 7.03 (d, J = 8.8 Hz, 2H), 6.06 (s, 1H), 4.25 (s, 2H), 3.85–3.71 (m, 5H), 2.69 (s, 2H), 2.25 (s, 3H). ^{13}C NMR (DEPT, 63 MHz, DMSO-d_6) δ 150.1 (CH), 128.8 (CH), 128.3 (CH), 127.6 (CH), 127.6 (CH), 125.0 (CH), 119.7 (CH), 118.0 (CH), 117.5 (CH), 114.3 (CH), 114.3 (CH), 55.1 (CH_3), 43.6 (CH_2), 40.6 (CH_2) 27.3 (CH_2), 12.9 (CH_3). HRMS (EI-MS) *m/z* calcd for $C_{26}H_{26}N_5O_2[M+H]^+$: 440.2081, found: 440.2082.

*8.1.2.44. 4-(5-Cyclopropyl-7H-pyrrolo [2,3-d]pyrimidin-4-yl)-N-phenyl-3,6-dihydropyridine-1(2H)-carboxamide (**44**).* The reaction was carried out as described in **method A** with the free amine **14** (67 mg, 0.21 mmol) and phenyl isocyanate (25 μL, 0.23 mmol) in anhydrous CH_2Cl_2 (0.7 mL). The solvent was removed under reduced pressure and the crude reaction mixture was purified by silica gel column chromatography using a gradient solvent system of CH_2Cl_2/MeOH from 100 up to 95/5 to afford the urea derivative **44** (30 mg, 0.08 mmol, 38 %) as a white solid. R_f (CH_2Cl_2/MeOH 95/5) 0.21. Mp: 231–233 °C. IR (ATR diamond, cm^{-1}) ν: 3004, 2920, 2847, 1634, 1597, 1531, 1500, 1446, 1301, 1236, 1025, 822, 757, 693, 612, 600, 575. ^{1}H NMR (250 MHz, DMSO-d_6) δ 11.80 (s, 1H), 8.60 (s, 1H), 8.52 (s, 1H), 7.44 (d, J = 7.6 Hz, 2H), 7.29–7.12 (m, 3H), 6.90 (t, J = 7.3 Hz, 1H), 6.33–6.14 (m, 1H), 4.25–4.09 (m, 2H), 3.70 (t, J = 5.6 Hz, 2H), 2.75–2.55 (m, 2H), 1.86–1.71 (m, 1H), 0.84–0.69 (m, 2H), 0.60–0.49 (m, 2H). ^{13}C NMR (63 MHz, DMSO-d_6) δ 159.5 (C), 155.1 (C), 152.5 (C), 150.2 (CH), 140.5 (C), 134.0 (C), 128.4 (CH), 128.3 (2 x CH), 123.4 (CH), 121.8 (CH), 119.8 (2 x CH), 116.4 (C), 114.6 (C), 43.7 (CH_2), 40.6 (CH_2), 27.1 (CH_2), 8.6 (CH), 7.2 (2 x CH_2). HRMS (EI-MS) *m/z* calcd for $C_{21}H_{22}N_5O$ $[M+H]^+$: 360.1819, found: 360.1821. Purity (HPLC): >99.9 %.

*8.1.2.45. 4-(5-Cyclopropyl-7H-pyrrolo [2,3-d]pyrimidin-4-yl)-N-(3-fluorophenyl)-5,6-dihydropyridine-1(2H)-carboxamide (**45**).* The reaction was carried out as described in **method A** using the free amine **14** (50 mg, 0.21 mmol) and 3-fluorophenyl isocyanate (26 μL, 0.23 mmol) in anhydrous CH_2Cl_2 (5 mL). The crude reaction mixture was purified by silica gel column chromatography using a gradient solvent system of CH_2Cl_2/acetone from 90/10 up to 30/70 to afford the urea derivative **45** (44 mg, 56 %) as a white solid. R_f (CH_2Cl_2/acetone 50/50) 0.28. Mp: 149–151 °C. IR (ATR diamond, cm^{-1}) ν: 3130, 2360, 1644, 1598, 1533, 1439, 1234, 1193, 1145, 1025, 804. ^{1}H NMR (250 MHz, MeOH-d_4) δ 8.63 (s, 1H), 7.41–7.12 (m, 4H), 6.81–6.67 (m, 1H), 6.29–6.17 (m, 1H), 4.36–4.21 (m, 2H), 3.85 (t, J = 5.6 Hz, 2H), 2.86–2.70 (m, 2H), 1.95–1.77 (m, 1H), 0.99–0.77 (m, 2H), 0.67–0.51 (m, 2H). ^{13}C NMR (63 MHz, MeOH-d_4) δ 161.3 (C), 157.5 (C), 151.1 (CH), 135.8 (C), 130.8 (d, J = 9.6 Hz, CH), 129.1 (CH), 124.9 (CH), 119.2 (C), 117.1 (d, J = 2.8 Hz, CH), 116.9 (C), 110.2 (d, J = 21.6 Hz, CH), 108.6 (d, J = 26.1 Hz, CH), 45.0 (CH_2), 42.2 (CH_2), 29.0 (CH_2), 9.2 (CH), 7.7 (2 x CH_2). ^{19}F NMR (235 MHz, MeOH-d_4) δ −114.87 to −115.04 (m). HRMS (EI-MS) *m/z* calcd for $C_{21}H_{21}FN_5O$ $[M+H]^+$: 378.1725, found: 378.1724.

*8.1.2.46. N-(3-Chlorophenyl)-4-(5-cyclopropyl-7H-pyrrolo [2,3-d]pyrimidin-4-yl)-5,6-dihydropyridine-1(2H)-carboxamide (**46**).* The reaction was carried out as described in **method A** using the free amine **14** (50 mg, 0.21 mmol) and 3-chlorophenyl isocyanate (28 μL, 0.23 mmol) in anhydrous CH_2Cl_2 (5 mL). The crude reaction mixture was purified by silica gel column chromatography using a gradient solvent system of CH_2Cl_2/acetone from 90/10 up to 30/70 to afford the urea derivative **46** (55 mg, 67 %) as a white solid. R_f (CH_2Cl_2/acetone 50/50) 0.28. Mp: 174–176 °C. IR (ATR diamond, cm^{-1}) ν: 3112, 2998, 2839, 2360, 1635, 1588, 1422, 1271, 1235, 1023, 775. ^{1}H NMR (400 MHz, MeOH-d_4) δ 8.63 (s, 1H), 7.55 (t, J = 2.1 Hz, 1H), 7.31 (d, J = 8.2 Hz, 1H), 7.24 (t, J = 8.0 Hz, 1H), 7.16 (s, 1H), 7.01 (d, J = 7.2 Hz, 1H), 6.25–6.19 (m, 1H), 4.36–4.23 (m, 2H), 3.85 (t, J = 5.6 Hz, 2H), 2.84–2.71 (m, 2H), 1.93–1.77 (m, 1H), 0.90–0.83 (m, 2H), 0.64–0.57 (m, 2H). ^{13}C NMR (101 MHz, MeOH-d_4) δ 161.3 (C), 157.5 (C), 153.8 (C), 151.1 (CH), 142.6 (C), 135.8 (C), 135.2 (C), 130.8 (CH), 129.1 (CH), 124.9 (CH), 123.7 (CH), 121.6 (CH), 119.8 (CH), 119.2 (C), 116.9 (C), 45.0 (CH_2), 42.2 (CH_2), 29.0 (CH_2), 9.3 (CH), 7.7 (2 x CH_2). HRMS (EI-MS) *m/z* calcd for $C_{21}H_{21}ClN_5O$ $[M+H]^+$: 394.1429, found: 394.1426.

*8.1.2.47. N-(3-Bromophenyl)-4-(5-cyclopropyl-7H-pyrrolo [2,3-d]pyrimidin-4-yl)-5,6-dihydropyridine-1(2H)-carboxamide (**47**).* The reaction was carried out as described in **method A** using the free amine **14** (50 mg, 0.21 mmol) and 3-bromophenyl isocyanate (29 μL, 0.23 mmol) in anhydrous CH_2Cl_2 (5 mL). The crude reaction mixture was purified by silica gel column chromatography using a gradient solvent system of CH_2Cl_2/acetone from 90/10 up to 30/70 to afford the urea derivative **47** (46 mg, 50 %) as a white solid. R_f (CH_2Cl_2/acetone 50/50) 0.28. Mp: 179–181 °C. IR (ATR diamond, cm^{-1}) ν: 3209, 3119, 2916, 2360, 1633, 1586, 1567, 1521, 1424, 1238, 774. ^{1}H NMR (250 MHz, MeOH-d_4) δ 8.63 (s, 1H), 7.74–7.66 (m, 1H), 7.40–7.32 (m, 1H), 7.23–7.11 (m, 3H),

6.25–6.19 (m, 1H), 4.34–4.23 (m, 2H), 3.85 (t, J = 5.6 Hz, 2H), 2.85–2.70 (m, 2H), 1.95–1.78 (m, 1H), 0.94–0.78 (m, 2H), 0.67–0.54 (m, 2H). ^{13}C NMR (63 MHz, MeOH-d_4) δ 161.3 (C), 157.5 (C), 153.8 (C), 151.1 (CH), 142.7 (C), 135.8 (C), 131.1 (CH), 129.1 (CH), 126.7 (CH), 124.9 (CH), 124.6 (CH), 123.1 (C), 120.3 (CH), 119.2 (C), 116.9 (C), 45.0 (CH_2), 42.2 (CH_2), 29.0 (CH_2), 9.3 (CH), 7.8 (2 x CH_2). HRMS (EI-MS) *m/z* calcd for $C_{21}H_{21}BrN_5O$ $[M+H]^+$: 438.0924, found: 438.0922.

8.1.2.48. [3-[[4-(5-Cyclopropyl-7H-pyrrolo [2,3-d]pyrimidin-4-yl)-3,6-dihydropyridine-1(2H)-carbonyl]amino] phenyl] N,N-dimethylcarbamate ***(48)***. The reaction was carried out as described in **method B** with 3-aminophenyl dimethylcarbamate (24 mg, 0.13 mmol) and the amine salt **14.HCl** (50 mg, 0.16 mmol) in anhydrous THF (4 mL). The crude reaction mixture was purified by silica gel column chromatography using a gradient solvent system of CH_2Cl_2/acetone from 100/0 up to 25/75 to afford the urea derivative **48** (35 mg, 59 %) as a white solid. R_f (CH_2Cl_2/acetone 20/80) 0.28. Mp: degradation 132 °C. IR (ATR diamond, cm^{-1}) ν: 3206, 1704, 1644, 1537, 1436, 1356, 1173, 1023, 751, 687, 642. ^{1}H NMR (400 MHz, DMSO-d_6) δ 11.83 (s, 1H), 8.67 (s, 1H), 8.64 (s, 1H), 7.35 (t, J = 2.1 Hz, 1H), 7.31 (d, J = 2.1, Hz, 1H), 7.28–7.19 (m, 2H), 6.71–6.66 (m, 1H), 6.27 (s, 1H), 4.24–4.19 (m, 2H), 3.74 (t, J = 5.6 Hz, 2H), 3.03 (s, 3H), 2.90 (s, 3H), 2.73–2.64 (m, 2H), 1.88–1.77 (m, 1H), 0.84–0.76 (m, 2H), 0.63–0.52 (m, 2H).^{13}C NMR (101 MHz, DMSO-d_6) δ 159.4 (C), 154.9 (C), 154.0 (C), 152.5 (C), 151.3 (C), 150.2 (CH), 141.5 (C), 134.0 (C), 128.7 (CH), 128.3 (CH), 123.4 (CH), 116.4 (C), 116.0 (CH), 115.0 (CH), 114.5 (C), 113.0 (CH), 43.7 (CH_2), 40.6 (CH_2), 36.3 (CH_3), 36.1 (CH_3), 27.1 (CH_2), 8.6 (CH), 7.2 (2 x CH_2). HRMS (EI-MS) *m/z* calcd for $C_{24}H_{27}N_6O_3$[M+H]$^+$: 447.2139, found: 447.2137.

8.1.2.49. 4-(5-Cyclopropyl-7H-pyrrolo [2,3-d]pyrimidin-4-yl)-N-(3-phenylphenyl)-3,6-dihydropyridine-1(2H)-carboxamide ***(49)***. The reaction was carried out as described in **method B** with 3-aminobiphenyl (23 mg, 0.14 mmol) and the amine salt **14.HCl** (53 mg, 0.17 mmol) in anhydrous THF (4 mL). The crude reaction mixture was purified by silica gel column chromatography using a gradient solvent system of CH_2Cl_2/acetone from 100/0 up to 40/60 to afford the urea derivative **49** (25 mg, 48 %) as a yellow solid. R_f (CH_2Cl_2/acetone 40/60) 0.3. Mp: degradation 145 °C. IR (ATR diamond, cm^{-1}) ν: 3290, 3115, 2848, 1632, 1537, 1420, 1238, 1024, 753, 696. ^{1}H NMR (400 MHz, DMSO-d_6) δ 11.86 (s, 1H), 8.73–8.57 (m, 2H), 7.82 (s, 1H), 7.62 (d, J = 7.6 Hz, 2H), 7.54 (d, J = 8.0 Hz, 1H), 7.47 (t, J = 7.5 Hz, 2H), 7.35 (q, J = 7.8 Hz, 2H), 7.27–7.22 (m, 2H), 6.29 (s, 1H), 4.25 (s, 2H), 3.77 (t, J = 5.5 Hz, 2H), 2.72 (s, 2H), 1.90–1.78 (m, 1H), 0.85–0.78 (m, 2H), 0.64–0.57 (m, 2H). ^{13}C NMR (101 MHz, DMSO-d_6) δ 159.5 (C), 155.1 (C), 152.5 (C), 150.2 (CH), 141.1 (C), 140.4 (C), 140.3 (C), 134.0 (C), 128.9 (CH), 128.9 (2 x CH), 128.4 (CH), 127.4 (CH), 126.6 (2 x CH), 123.4 (CH), 120.1 (CH), 118.7 (CH), 118.0 (CH), 116.4 (C), 114.6 (C), 43.7 (CH_2), 40.7 (CH_2), 27.1 (CH_2), 8.6 (CH), 7.3 (2 x CH_2). HRMS (EI-MS) *m/z* calcd for $C_{27}H_{26}N_5O$ $[M+H]^+$: 436.2132, found: 436.2130.

8.1.2.50. 3-(1H-Pyrrol-1-yl)aniline

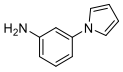

An oven-dried microwave vial was charged with a magnetic stirring bar, CuI (29 mg, 0.15 mmol, 0.05 equiv.), K_3PO_4 (1.33 g, 6.26 mmol, 2.1 equiv.) and 1,10-Phenanthroline (107 mg, 0.60 mmol, 0.2 equiv.). The tube was then evacuated and back-filled with argon. The evacuation/backfill sequence was repeated two additional times. Under a counter-flow of argon, 3-iodoaniline (0.43 mL, 3.58 mmol, 1.2 equiv.), pyrrole (0.21 mL, 2.98 mmol) and degassed 1,4-dioxane (1.5 mL) were added by syringe. The tube was placed in a preheated oil bath at 110 °C and the solution was stirred vigorously for 24 h. The reaction mixture was cooled to room temperature, diluted with EtOAc (2–3 mL), filtered through a plug of Celite and eluted with EtOAc. The filtrate was concentrated under reduced pressure and the resulting residue was purified by silica gel column chromatography using a gradient solvent system PE/EtOAc from 90/10 up to 80/20 to afford the intermediate aniline **VI** (0.41 g, 87 %) as a brown solid. ^{1}H NMR (250 MHz, $CDCl_3$) δ 7.22 (t, J = 8.0 Hz, 1H), 7.11 (t, J = 2.2 Hz, 2H), 6.83 (ddd, J = 8.0, 2.1 Hz, J = 0.9 Hz, 1H), 6.71 (t, J = 2.2 Hz, 1H), 6.57 (ddd, J = 8.0, 2.3, 0.9 Hz, 1H), 6.40 (t, J = 2.2 Hz, 2H), 3.76 (brs, 2H). All spectral data corresponded to literature values as found in *Tetrahedron* **2011**, *67*, 898–903.

8.1.2.51. 4-(5-Cyclopropyl-7H-pyrrolo [2,3-d]pyrimidin-4-yl)-N-(3-pyrrol-1-ylphenyl)-3,6-dihydropyridine-1(2H)-carboxamide ***(50)***. The reaction was carried out as described in **method B** with 3-(1*H*-pyrrol-1-yl) aniline **VI** (22 mg, 0.14 mmol) and the amine salt **14.HCl** (53 mg, 0.17 mmol) in anhydrous THF (4 mL). The crude reaction mixture was purified by silica gel column chromatography using a gradient solvent system of CH_2Cl_2/acetone from 100/0 up to 50/50 to afford the urea derivative **50** (42 mg, 70 %) as a white solid. R_f (CH_2Cl_2/acetone 70/30) 0.25. Mp: degradation 140 °C. IR (ATR diamond, cm^{-1}) ν: 3275, 3208, 3110, 3007, 2846, 1636, 1602, 1537, 1497, 1444, 1343, 1239, 722. ^{1}H NMR (400 MHz, DMSO-d_6) δ 11.84 (s, 1H), 8.72 (s, 1H), 8.65 (s, 1H), 7.74 (s, 1H), 7.41 (d, J = 7.9 Hz, 1H), 7.32 (t, J = 8.0 Hz, 1H), 7.27–7.21 (m, 3H), 7.13 (d, J = 7.7 Hz, 1H), 6.43–6.07 (m, 3H), 4.31–4.16 (m, 2H), 3.77 (t, J = 5.4 Hz, 2H), 2.77–2.68 (m, 2H), 1.91–1.77 (m, 1H), 0.86–0.75 (m, 2H), 0.66–0.53 (m, 2H). ^{13}C NMR (101 MHz, DMSO-d_6) δ 159.5 (C), 155.0 (C), 152.5 (C), 150.2 (CH), 141.8 (C), 140.1 (C), 134.1 (C), 129.5 (CH), 128.3 (CH), 123.4 (CH), 118.9 (2 x CH), 116.5 (CH), 116.4 (C), 114.6 (C), 113.0 (CH), 110.8 (CH), 110.3 (2 x CH), 43.7 (CH_2), 40.7 (CH_2), 27.1 (CH_2), 8.6 (CH), 7.2 (2 x CH_2). HRMS (EI-MS) *m/z* calcd for $C_{25}H_{24}N_6O$[M+H]$^+$: 425.2084, found: 425.2084.

8.1.2.52. 4-(5-Cyclopropyl-7H-pyrrolo [2,3-d]pyrimidin-4-yl)-N-[3-(2-methoxyphenyl)phenyl]-3,6 dihydropyridine-1(2H)-carboxamide ***(51)***. The reaction was carried out as described in **method B** with 2′-methoxy-[1,1′-biphenyl]-3-amine (25 mg, 0.12 mmol) and the amine salt **14.HCl** (48 mg, 0.15 mmol) in anhydrous THF (4 mL). The crude reaction mixture was purified by silica gel column chromatography using a gradient solvent system of CH_2Cl_2/acetone from 100/0 up to 30/70 to afford the urea derivative **51** (35 mg, 58 %) as a white solid. R_f (CH_2Cl_2/acetone 30/70) 0.43. Mp: degradation 140 °C. IR (ATR diamond, cm^{-1}) ν: 3128, 2836, 1636, 1591, 1538, 1421, 1239, 1207, 1025, 789, 752, 699, 643. ^{1}H NMR (400 MHz, DMSO-d_6) δ 11.96 (s, 1H), 8.68 (s, 1H), 8.61 (s, 1H), 7.59 (s, 1H), 7.48 (d, J = 8.2 Hz, 1H), 7.33 (t, J = 8.2 Hz, 1H), 7.31–7.21 (m, 3H), 7.10 (d, J = 8.3 Hz, 1H), 7.08–6.98 (m, 2H), 6.30 (s, 1H), 4.24 (s, 2H), 3.76 (s, 5H), 2.71 (s, 2H), 1.84 (m, 1H), 0.85–0.78 (m, 2H), 0.64–0.57 (m, 2H). ^{13}C NMR (101 MHz, DMSO-d_6) δ 158.9 (C), 156.1 (C), 155.1 (C), 152.5 (C), 149.7 (CH), 140.2 (C), 138.3 (C), 133.5 (C), 130.3 (CH), 130.1 (C), 128.8 (CH), 128.7 (CH), 127.8 (CH), 123.8 (CH), 122.9 (CH), 120.8 (CH), 120.6 (CH), 118.3 (CH), 116.7 (C), 114.5 (C), 111.7 (CH), 55.5 (OCH_3), 43.7 (CH_2), 40.6 (CH_2), 27.2 (CH_2), 8.5 (CH), 7.2 (2 x CH_2). HRMS (EI-MS) *m/z* calcd for $C_{28}H_{28}N_5O_2$[M+H]$^+$: 466.2238, found: 466.2234.

8.1.2.53. 4-(5-Cyclopropyl-7H-pyrrolo [2,3-d]pyrimidin-4-yl)-N-[3-(3-methoxyphenyl)phenyl]-3,6-dihydropyridine-1(2H)-carboxamide ***(52)***. The reaction was carried out as described in **method B** with 3′-methoxy-[1,1′-biphenyl]-3-amine (25 mg, 0.12 mmol) and the amine salt **14.HCl** (48 mg, 0.15 mmol) in anhydrous THF (4 mL). The crude reaction mixture was purified by silica gel column chromatography using a gradient solvent system of CH_2Cl_2/acetone from 100/0 up to 40/60 to afford the urea derivative **52** (40 mg, 67 %) as a white solid. R_f (CH_2Cl_2/acetone 30/70) 0.67. Mp: degradation 199 °C. IR (ATR diamond, cm^{-1}) ν: 3084, 2995, 2868, 1643, 1594, 1557, 1435, 1323, 1238, 1205, 1025,

780, 698. ^{1}H NMR (400 MHz, DMSO-d_6) δ 11.86 (s, 1H), 8.66 (s, 2H), 7.80 (s, 1H), 7.55 (d, J = 8.1 Hz, 1H), 7.38 (t, J = 7.9 Hz, 1H), 7.33 (t, J = 7.9 Hz, 1H), 7.29–7.22 (m, 2H), 7.18 (d, J = 7.7 Hz, 1H), 7.16–7.11 (m, 1H), 6.94 (dd, J = 8.2, 2.6 Hz, 1H), 6.29 (s, 1H), 4.30–4.20 (m, 2H), 3.82 (s, 3H), 3.77 (t, J = 5.7 Hz, 2H), 2.72 (s, 2H), 1.91–1.78 (m, 1H), 0.86–0.76 (m, 2H), 0.65–0.52 (m, 2H). ^{13}C NMR (101 MHz, DMSO-d_6) δ 159.7 (C), 159.4 (C), 155.1 (C), 152.5 (C), 150.1 (CH), 141.9 (C), 141.0 (C), 140.2 (C), 133.9 (C), 129.9 (CH), 128.8 (CH), 128.4 (CH), 123.4 (CH), 120.2 (CH), 118.9 (2 x CH), 118.1 (CH), 116.4 (C), 114.5 (C), 112.9 (CH), 112.1 (CH), 55.1 (OCH_3), 43.7 (CH_2), 40.6 (CH_2), 27.1 (CH_2), 8.6 (CH), 7.2 (2 x CH_2). HRMS (EI-MS) *m/z* calcd for $C_{28}H_{28}N_5O_2[M+H]^+$: 466.2238, found: 466.2235. Purity (HPLC): 99 %.

*8.1.2.54. 4-(5-Cyclopropyl-7H-pyrrolo [2,3-d]pyrimidin-4-yl)-N-[3-(4-methoxyphenyl)phenyl]-3,6-dihydropyridine-1(2H)-carboxamide (**53**).* The reaction was carried out as described in **method B** with 4′-methoxy-[1,1′-biphenyl]-3-amine (25 mg, 0.12 mmol) and the amine salt **14.HCl** (48 mg, 0.15 mmol) in anhydrous THF (4 mL). The crude reaction mixture was purified by silica gel column chromatography using a gradient solvent system of CH_2Cl_2/acetone from 100/0 up to 40/60 to afford the urea derivative **53** (40 mg, 67 %) as a light beige solid. R_f (CH_2Cl_2/acetone 30/70) 0.4. Mp: degradation 149 °C. IR (ATR diamond, cm^{-1}) ν: 3292, 3113, 2999, 2837, 1634, 1607, 1538, 1511, 1437, 1404, 1245, 1180, 1026, 830, 784. ^{1}H NMR (400 MHz, DMSO-d_6) δ 11.89 (s, 1H), 8.67 (s, 1H), 8.64 (s, 1H), 7.77 (s, 1H), 7.55 (d, J = 8.6 Hz, 2H), 7.48 (d, J = 8.1 Hz, 1H), 7.33–7.24 (m, 2H), 7.19 (d, J = 7.6 Hz, 1H), 7.03 (d, J = 8.5 Hz, 2H), 6.30 (s, 1H), 4.31–4.19 (m, 2H), 3.84–3.71 (m, 5H), 2.72 (s, 2H), 1.90–1.78 (m, 1H), 0.82 (d, J = 7.0 Hz, 2H), 0.61 (d, J = 4.2 Hz, 2H). ^{13}C NMR (101 MHz, DMSO-d_6) δ 159.3 (C), 158.8 (C), 155.1 (C), 152.5 (C), 150.0 (CH), 141.0 (C), 140.0 (C), 133.8 (C), 132.7 (C), 128.8 (CH), 128.6 (CH), 127.6 (2 x CH) 123.5 (CH), 119.7 (CH), 118.1 (CH), 117.6 (CH), 116.5 (C), 114.5 (C), 114.3 (2 x CH), 55.1 (OCH_3), 43.7 (CH_2), 40.6 (CH_2), 27.1 (CH_2), 8.5 (CH), 7.2 (2 x CH_2). HRMS (EI-MS) *m/z* calcd for $C_{28}H_{28}N_5O_2[M+H]^+$: 466.2238, found: 466.2234.

*8.1.2.55. 4-(5-Chloro-7H-pyrrolo [2,3-d]pyrimidin-4-yl)-N-(3-chlorophenyl)-3,6-dihydropyridine-1(2H)-carboxamide (**54**).* The reaction was carried out as described in **method B** using 3-chloroaniline (40 μL, 0.38 mmol) and amine **15** (141 mg, 0.46 mmol) in dry THF (5.4 mL). The crude reaction mixture was purified by silica gel column chromatography using a gradient solvent system of CH_2Cl_2/MeOH from 100 up to 97/3 to afford the urea derivative **54** (121 mg, 82 %) as a white powder. R_f (CH_2Cl_2/MeOH 95/5) 0.26. Mp: 140–142 °C. IR (ATR diamond, cm^{-1}) ν: 3119, 2988, 2361, 2090, 1635, 1587, 1521, 1424, 1337, 1236, 995, 773, 680, 599. ^{1}H NMR (400 MHz, DMSO-d_6) δ 12.53 (s, 1H), 8.82–8.72 (m, 2H), 7.79 (s, 1H), 7.72–7.67 (m, 1H), 7.45 (d, J = 8.2 Hz, 1H), 7.27 (t, J = 8.1 Hz, 1H), 6.99 (d, J = 7.8 Hz, 1H), 6.27–6.19 (m, 1H), 4.31–4.20 (m, 2H), 3.74 (t, J = 5.6 Hz, 2H), 2.77–2.67 (m, 2H). ^{13}C NMR (101 MHz, DMSO-d_6) δ 158.8 (C), 154.7 (C), 151.1 (CH), 150.8 (C), 142.1 (C), 132.7 (C), 132.1 (C), 130.7 (CH), 129.9 (CH), 125.3 (CH), 121.3 (CH), 118.9 (CH), 117.8 (CH), 111.3 (C), 101.9 (C), 43.6 (CH_2), 40.5 (CH_2), 26.9 (CH_2). HRMS (EI-MS) *m/z* calcd for $C_{18}H_{16}Cl_2N_5O$ $[M+H]^+$: 388.0726, found: 388.0726. Purity (HPLC): 97.2 %.

*8.1.2.56. N-(3-Bromophenyl)-4-(5-chloro-7H-pyrrolo [2,3-d]pyrimidin-4-yl)-3,6-dihydropyridine-1(2H)-carboxamide (**55**).* The reaction was carried out as described in **method B** using 3-bromoaniline (33 μL, 0.30 mmol) and amine **15** (111 mg, 0.36 mmol) in dry THF (4.3 mL). The crude reaction mixture was purified by silica gel column chromatography using a gradient solvent system of CH_2Cl_2/MeOH from 100 up to 96/4 to afford the urea derivative **55** (79 mg, 60 %) as a white powder. R_f (CH_2Cl_2/MeOH 95/5) 0.28. Mp: 131–133 °C. IR (ATR diamond, cm^{-1}) ν: 3114, 2979, 2838, 1636, 1583, 1520, 1477, 1421, 1335, 1233, 994, 772, 677, 599. ^{1}H NMR (400 MHz, DMSO-d_6) δ 12.53 (s, 1H), 8.77 (s, 1H), 8.75 (s, 1H), 7.83 (t, J = 2.0 Hz, 1H), 7.79 (s, 1H), 7.50 (d, J = 8.2 Hz, 1H), 7.21 (t, J = 8.0 Hz, 1H), 7.12 (d, J = 7.8 Hz, 1H), 6.25–6.17 (m, 1H), 4.26 (d, J = 2.9 Hz, 2H), 3.73 (t, J = 5.6 Hz, 2H), 2.76–2.68 (m, 2H). ^{13}C NMR (101 MHz, DMSO-d_6) δ 158.8 (C), 154.6 (C), 151.0 (CH), 150.8 (C), 142.3 (C), 132.1 (C), 130.7 (CH), 130.2 (CH), 125.3 (CH), 124.2 (CH), 121.7 (CH), 121.2 (C), 118.2 (CH), 111.3 (C), 101.9 (C), 43.6 (CH_2), 40.5 (CH_2), 26.9 (CH_2). HRMS (EI-MS) *m/z* calcd for $C_{18}H_{16}BrClN_5O$ $[M+H]^+$: 432.0221, found: 432.0224. Purity (HPLC): 91.4 %

*8.1.2.57. [3-[[4-(5-Chloro-7H-pyrrolo [2,3-d]pyrimidin-4-yl)-3,6-dihydro-2H-pyridine-1-carbonyl]amino] phenyl] N,N-dimethylcarbamate (**56**).* The reaction was carried out as described in **method B** using 3-aminophenyl dimethylcarbamate (24 mg, 0.14 mmol) and amine **15** (50 mg, 0.16 mmol). The crude reaction mixture was purified by silica gel column chromatography using a gradient solvent system CH_2Cl_2/acetone from 10/0 up to 60/40 to afford the urea derivative **56** (42 mg, 70 %) as a white solid. R_f (CH_2Cl_2/acetone 50/50) 0.25. Mp: degradation 132 °C. IR (ATR diamond, cm^{-1}) ν: 3123, 1703, 1643, 1599, 1538, 1435, 1386, 1335, 1276, 1173, 993, 751, 687, 599. ^{1}H NMR (250 MHz, DMSO-d_6) δ 12.53 (s, 1H), 8.77 (s, 1H), 8.69 (s, 1H), 7.79 (t, J = 2.1 Hz, 1H), 7.42–7.28 (m, 2H), 7.22 (t, J = 8.0 Hz, 1H), 6.69 (d, J = 8.3 Hz, 1H), 6.22 (s, 1H), 4.25 (s, 2H), 3.73 (t, J = 5.5 Hz, 2H), 3.03 (s, 3H), 2.90 (s, 3H), 2.71 (s, 2H). ^{13}C NMR (63 MHz, DMSO-d_6) δ 158.9 (C), 154.8 (C), 154.0 (C), 151.3 (CH), 151.0 (C), 150.8 (C), 141.5 (C), 132.0 (C), 130.9 (CH), 128.7 (CH), 125.3 (CH), 116.0 (CH), 115.0 (CH), 113.0 (CH), 111.3 (C), 101.9 (C), 43.6 (CH_2), 40.1 (CH_2), 36.3 (CH_3), 36.1 (CH_3), 26.9 (CH_2). HRMS (EI-MS) *m/z* calcd for $C_{21}H_{22}ClN_6O_3[M+H]^+$: 441.1436, found: 441.1436.

*8.1.2.58. 4-(5,6-dimethyl-7H-pyrrolo [2,3-d]pyrimidin-4-yl)-N-phenyl-3,6-dihydro-2H-pyridine-1-carboxamide (**57**).* The reaction was carried out as described in **method A** using the amine salt **18** (52 mg, 0.17 mmol) and phenyl isocyanate (21 μL, 0.19 mmol). The crude reaction mixture was purified by silica gel column chromatography using a gradient solvent system of CH_2Cl_2/acetone from 100/0 up to 50/50 to afford the urea derivative **57** (43 mg, 72 %) as a white solid. R_f (CH_2Cl_2/acetone 70/30) 0.48. Mp: >260 °C. IR (ATR diamond, cm^{-1}) ν: 3332, 3151, 3042, 2928, 2839, 1632, 1596, 1533, 1500, 1482, 1444, 1409, 1233, 1211, 747, 695. ^{1}H NMR (400 MHz, DMSO-d_6) δ 11.77 (s, 1H), 8.59–8.53 (m, 2H), 7.50 (d, J = 8.0 Hz, 2H), 7.24 (t, J = 7.7 Hz, 2H), 6.94 (t, J = 7.3 Hz, 1H), 5.98 (s, 1H), 4.21 (s, 2H), 3.73 (t, J = 5.5 Hz, 2H), 2.66 (s, 2H), 2.33 (s, 3H), 2.14 (s, 3H). ^{13}C NMR (101 MHz, DMSO-d_6) δ 157.4 (C), 155.1 (C), 151.8 (C), 149.1 (CH), 140.5 (C), 134.1 (C), 133.9 (C), 128.3 (2 x CH), 127.8 (CH), 121.8 (CH), 119.8 (2 x CH), 115.2 (C), 104.1 (C), 43.6 (CH_2), 40.6 (CH_2), 27.5 (CH_2), 11.1 (CH_3), 11.0 (CH_3). HRMS (EI-MS) *m/z* calcd for $C_{20}H_{22}N_5O[M+H]^+$: 348.1819, found: 348.1821.

*8.1.2.59. 4-(5,6-dimethyl-7H-pyrrolo [2,3-d]pyrimidin-4-yl)-N-(3-methoxyphenyl)-3,6-dihydro-2H-pyridine-1-carboxamide (**58**).* The reaction was carried out as described in **method A** using the amine salt **18** (48 mg, 0.16 mmol) and 3-methoxyphenyl isocyanate (23 μL, 0.18 mmol). The crude reaction mixture was purified by silica gel column chromatography using a gradient solvent system of CH_2Cl_2/acetone from 100/0 up to 40/60 to afford the urea derivative **58** (33 mg, 55 %) as a white solid. R_f (CH_2Cl_2/acetone 30/70) 0.36. Mp: >260 °C. IR (ATR diamond, cm^{-1}) ν: 3140, 3056, 2929, 2837, 1640, 1604, 1537, 1450, 1429, 1236, 1206, 1159, 1047, 769, 687. ^{1}H NMR (400 MHz, DMSO-d_6) δ 11.80 (s, 1H), 8.60–8.53 (m, 2H), 7.20 (s, 1H), 7.17–7.06 (m, 2H), 6.52 (d, J = 7.5 Hz, 1H), 5.98 (s, 1H), 4.20 (s, 2H), 3.72 (s, 5H), 2.66 (s, 2H), 2.33 (s, 3H), 2.13 (s, 3H). ^{13}C NMR (101 MHz, DMSO-d_6) δ 159.3 (C), 157.4 (C), 155.0 (C), 151.8 (C), 149.0 (CH), 141.8 (C), 134.0 (C), 133.9 (C), 129.0 (CH), 127.8 (CH), 115.2 (C), 111.9 (CH), 107.2 (CH), 105.3 (CH), 104.1 (C), 54.9 (CH_3), 43.6 (CH_2), 40.6 (CH_2), 27.4 (CH_2), 11.1 (CH_3), 11.0

(CH_3). HRMS (EI-MS) *m/z* calcd for $C_{21}H_{24}N_5O_2$ $[M+H]^+$: 378.1925, found: 378.1922.

*8.1.2.60. N-(3-Bromophenyl)-4-(5,6-dimethyl-7H-pyrrolo [2,3-d]pyrimidin-4-yl)-3,6-dihydro-2H-pyridine-1-carboxamide (**59**).* The reaction was carried out as described in **method A** using the amine salt **18** (42 mg, 0.14 mmol) and 3-bromophenyl isocyanate (30 mg, 0.15 mmol). The crude mixture was purified by silica gel column chromatography using a gradient solvent system of CH_2Cl_2/acetone from 100/0 up to 50/50 to afford the urea derivative **59** (45 mg, 75 %) as a white solid. R_f (CH_2Cl_2/acetone 50/50): 0.25. Mp: >260 °C. IR (ATR diamond, cm^{-1}) ν: 3304, 3318, 3024, 2915, 2853, 1634, 1525, 1478, 1417, 1234, 775, 674.^{1}H NMR (400 MHz, DMSO-d_6) δ 11.76 (s, 1H), 8.75 (s, 1H), 8.55 (s, 1H), 7.83 (s, 1H), 7.50 (d, J = 8.6 Hz, 1H), 7.21 (t, J = 8.1 Hz, 1H), 7.12 (d, J = 8.0 Hz, 1H), 5.97 (s, 1H), 4.21 (s, 2H), 3.73 (t, J = 5.6 Hz, 2H), 2.66 (s, 2H), 2.33 (s, 3H), 2.13 (s, 3H). ^{13}C NMR (101 MHz, DMSO-d_6) δ 157.5 (C), 154.7 (C), 151.8 (C), 149.2 (CH), 142.3 (C), 134.2 (C), 133.8 (C), 130.2 (CH), 127.5 (CH), 124.2 (CH), 121.7 (CH), 121.2 (C), 118.2 (CH), 115.2 (C), 104.0 (C), 43.5 (CH_2), 40.6 (CH_2), 27.4 (CH_2), 11.1 (CH_3), 11.0 (CH_3). HRMS (EI-MS) *m/z* calcd for $C_{20}H_{21}BrN_5O[M+H]^+$: 426.0924, found: 426.0919.

*8.1.2.61. [3-[[4-(5,6-Dimethyl-7H-pyrrolo [2,3-d]pyrimidin-4-yl)-3,6-dihydro-2H-pyridine-1-carbonyl]amino] phenyl] N,N-dimethylcarbamate (**60**).* The reaction was carried out as described in **method B** using 3-aminophenyldimethyl carbamate **I** (25 mg, 0.14 mmol) and the amine salt **18** (50 mg, 0.17 mmol) in THF (4 mL). The crude mixture was purified by silica gel column chromatography using a gradient solvent system CH_2Cl_2/acetone from 100/0 up to 50/50 to afford the urea derivative **60** (35 mg, 58 %) as a pale-yellow solid. R_f (CH_2Cl_2/acetone 30/70): 0.41. Mp: degradation 142 °C. IR (ATR diamond, cm^{-1}) ν: 3233, 2929, 1704, 1644, 1601, 1529, 1436, 1386, 1236, 1175, 1059, 773, 752, 686. ^{1}H NMR (400 MHz, DMSO-d_6) δ 11.81 (s, 1H), 8.69 (s, 1H), 8.57 (s, 1H), 7.38 (s, 1H), 7.32 (d, J = 8.2 Hz, 1H), 7.22 (t, J = 8.1 Hz, 1H), 6.69 (d, J = 7.4 Hz, 1H), 5.99 (s, 1H), 4.21 (s, 2H), 3.73 (t, J = 5.4 Hz, 2H), 3.04 (s, 3H), 2.91 (s, 3H), 2.65 (s, 2H), 2.33 (s, 3H), 2.13 (s, 3H). ^{13}C NMR (101 MHz, DMSO-d_6) δ 157.2 (C), 155.4 (C), 154.8 (C), 154.0 (C), 151.7 (C), 151.3 (C), 148.9 (CH), 141.5 (C), 134.0 (C), 128.7 (CH), 127.8 (CH), 116.0 (CH), 115.2 (C), 114.9 (CH), 112.9 (CH), 104.1 (C), 43.5 (CH_2), 40.6 (CH_2), 36.3 (CH_3), 36.1 (CH_3), 27.4 (CH_2), 11.1 (CH_3), 11.0 (CH_3). HRMS (EI-MS) *m/z* calcd for $C_{23}H_{27}N_6O_3$ $[M+H]^+$: 435.2136, found: 435.2139.

*8.1.2.62. 4-(5,6-dimethyl-7H-pyrrolo [2,3-d]pyrimidin-4-yl)-N-(3-phenylphenyl)-3,6-dihydro-2H-pyridine-1-carboxamide (**61**).* The reaction was carried out as described in **method B** with 1,1′-biphenyl]-3-amine (16 mg, 0.14 mmol) and the amine salt **18** (51 mg, 0.17 mmol) in THF (4 mL). The crude reaction mixture was purified by silica gel column chromatography using a solvent system of CH_2Cl_2/acetone 70/30 to afford the urea derivative **61** (29 mg, 48 %) as a white solid. R_f (CH_2Cl_2/acetone 50/50) 0.35. Mp: degradation 144 °C. IR (ATR diamond, cm^{-1}) ν: 3139, 3056, 2919, 2859, 1637, 1606, 1538, 1479, 1450, 1419, 1237, 755, 698. ^{1}H NMR (400 MHz, DMSO-d_6) δ 11.78 (s, 1H), 8.68 (s, 1H), 8.57 (s, 1H), 7.83 (s, 1H), 7.62 (d, J = 7.6 Hz, 2H), 7.55 (d, J = 8.0 Hz, 1H), 7.47 (t, J = 7.6 Hz, 2H), 7.35 (q, J = 7.8 Hz, 2H), 7.24 (d, J = 7.7 Hz, 1H), 5.99 (s, 1H), 4.24 (s, 2H), 3.76 (t, J = 4.9 Hz, 2H), 2.68 (s, 2H), 2.33 (s, 3H), 2.14 (s, 3H). ^{13}C NMR (101 MHz, DMSO-d_6) δ 157.4 (C), 155.1 (C), 151.8 (C), 149.1 (CH), 141.1 (C), 140.4 (C), 140.3 (C), 134.2 (C), 133.8 (C), 128.9 (2 x CH), 128.9 (CH), 127.7 (CH), 127.4 (CH), 126.5 (2 x CH), 120.1 (CH), 118.7 (CH), 118.0 (CH), 115.2 (C), 104.0 (C), 43.6 (CH_2), 40.6 (CH_2), 27.4 (CH_2), 11.1 (CH_3), 11.0 (CH_3). HRMS (EI-MS) *m/z* calcd for $C_{26}H_{26}N_5O$ $[M+H]^+$: 424.2132, found: 424.2128.

*8.1.2.63. 4-(5,6-Dimethyl-7H-pyrrolo [2,3-d]pyrimidin-4-yl)-N-[3-(4-methoxyphenyl)phenyl]-3,6-dihydropyridine-1(2H)-carboxamide (**62**).* The reaction was carried out as described in **method B** using 4′-methoxy-[1,1′-biphenyl]-3-amine (26 mg, 0.13 mmol) and the amine salt **18** (48 mg, 0.16 mmol) in THF (4 mL). The crude mixture was purified by silica gel column chromatography using a gradient solvent system CH_2Cl_2/acetone from 100/0 up to 40/60 to afford the urea derivative **62** (30 mg, 50 %) as a white solid R_f (CH_2Cl_2/acetone 30/70) 0.53. Mp: degradation 248 °C. IR (ATR diamond, cm-1) ν: 3299, 3140, 2939, 1637, 1607, 1549, 1434, 1410, 1241, 794, 782. 1H NMR (400 MHz, DMSO-d_6) δ 11.77 (s, 1H), 8.64 (s, 1H), 8.56 (s, 1H), 7.77 (s, 1H), 7.55 (d, J = 8.4 Hz, 2H), 7.49 (d, J = 7.9 Hz, 1H), 7.30 (t, J = 7.8 Hz, 1H), 7.19 (d, J = 7.7 Hz, 1H), 7.03 (d, J = 8.3 Hz, 2H), 5.99 (s, 1H), 4.23 (s, 2H), 3.80 (s, 3H), 3.79–3.71 (m, 2H), 2.67 (s, 2H), 2.33 (s, 3H), 2.14 (s, 3H). 13C NMR (101 MHz, DMSO-d_6) δ 158.8 (C), 157.2 (C), 155.1 (C), 151.7 (C), 148.9 (CH), 141.0 (C), 140.0 (C), 134.0 (C), 134.0 (C), 132.8 (C), 128.8 (CH), 127.9 (CH), 127.6 (2 x CH), 119.7 (CH), 118.1 (CH), 117.6 (CH), 115.2 (C), 114.3 (2 x CH), 104.1 (C), 55.1 (CH3), 43.6 (CH2), 40.6 (CH2), 27.5 (CH2), 11.1 (CH3), 11.0 (CH3). HRMS (EI-MS) *m/z* calcd for C27H28N5O2[M+H]+: 454.2238, found: 454.2238.

8.1.2.64. tert-butyl N-[3-(3-bromophenoxy)propyl]carbamate (64). *tert*-Butyl *N*-(3-hydroxypropyl)carbamate (912 mg, 5.20 mmol, 1.5 equiv.) and triphenylphosphine (1.0 g, 3.81 mmol, 1.1 equiv.). was added to a solution of 3-bromophenol **63** (600 mg, 3.47 mmol) in THF (12 mL) in a microwave tube. A solution of diisopropyl azodicarboxylate (DIAD) (768 mg, 3.81 mmol, 1.1 equiv.) in THF (5 mL) was added dropwise and the tube was sealed and the mixture heated in the microwave at 120 °C for 1 h. After cooling, an additional amount of triphenylphosphine and DIAD were added (1 equiv.) and the tube heated at 120 °C for 30 min. The mixture was concentrated, and the residue taken up in EtOAc, washed with brine (30 mL), dried with $MgSO_4$ and concentrated under reduced pressure. The crude reaction mixture was purified by silica gel column chromatography using a gradient solvent system of PE/Et_2O from 100/0 up to 50/50 to afford the desired compound **64** (874 mg, 77 %) as a white solid. R_f (PE/Et_2O 50/50) 0.51. Mp: 77–79 °C. IR (ATR diamond, cm^{-1}) ν: 3325, 3003, 2969, 2932, 1675, 1527, 1280, 993, 859, 773, 654. ^{1}H NMR (400 MHz, $CDCl_3$) δ 7.18–7.01 (m, 3H, 3 x CH), 6.85–6.79 (m, 1H, CH), 4.72 (s, 1H, NH), 4.00 (t, J = 6.2 Hz, 2H, CH_2), 3.31 (q, J = 6.3 Hz, 2H, CH_2), 1.97 (p, J = 6.2 Hz, 2H, CH_2), 1.44 (s, 9H, 3 x CH_3). ^{13}C NMR (101 MHz, $CDCl_3$) δ 159.7 (C), 156.1 (C), 130.7 (CH), 124.1 (CH), 122.9 (C), 117.9 (CH), 113.6 (CH), 79.5 (C), 66.1 (CH_2), 38.0 (CH_2), 29.6 (CH_2), 28.5 (3 x CH_3). HRMS (EI-MS) *m/z* calcd for $C_{14}H_{21}BrNO_3$ $[M+H]^+$: 330.0699, found: 330.0695.

*8.1.2.65. tert-Butyl N-[3-[3-(3-aminophenyl)phenoxy]propyl]carbamate (**65**).* This compound was obtained in a two-step sequence:

Compound **64** (300 mg, 0.91 mmol), 3-nitrophenylboronic acid (304 mg, 1.82 mmol, 2.0 equiv.) and K_2CO_3 (377 mg, 2.73 mmol, 3.0 equiv.) were suspended in a mixture of DME/EtOH/H_2O (1.8 mL, 1.2 mL and 0.6 mL). The solution was degassed for 20 min under Ar and Pd(PPh_3)$_4$ (53 mg, 0.045 mmol, 0.05 equiv.) was added. The reaction was heated in the microwave at 160 °C for 15 min. After cooling, the mixture was extracted with CH_2Cl_2 (3 x 10 mL). The combined organic layers were dried ($MgSO_4$), filtered and evaporated under reduced pressure. The crude reaction mixture was purified by silica gel column chromatography using a gradient solvent system of PE/Et_2O from 100/0 up to 70/30 to afford the nitro derivative *tert*-butyl *N*-[3-[3-(3-nitrophenyl) phenoxy] propyl]carbamate (267 mg, 79 %) as a yellow solid. R_f (PE/Et_2O 80/20) 0.26. Mp: 93–95 °C. IR (ATR diamond, cm^{-1}) ν: 3368, 2981, 2880, 1678, 1521, 1299, 1166, 1064, 783, 738, 685. ^{1}H NMR (400 MHz, MeOD-d_4) δ 8.41 (t, J = 1.9 Hz, 1H, CH), 8.20 (ddd, J = 8.2, 2.2, 0.8 Hz, 1H, CH), 8.03–7.98 (m, 1H, CH), 7.67 (t, J = 8.0 Hz, 1H, CH), 7.39 (t, J = 7.9 Hz, 1H, CH), 7.24 (d, J = 7.7 Hz, 1H, CH), 7.22–7.19 (m, 1H, CH), 6.99 (dd, J = 8.2, 1.8 Hz, 1H, CH), 4.09 (t, J = 6.2 Hz, 2H, CH_2), 3.26 (t, J = 6.8 Hz, 2H, CH_2), 1.97 (p, J = 6.5 Hz, 2H, CH_2), 1.42 (s, 9H, 3 x CH_3). ^{13}C NMR (101 MHz, MeOD-d_4) δ 161.1 (C), 158.6 (C),

150.1 (C), 144.1 (C), 141.4 (C), 134.2 (CH), 131.3 (CH), 131.1 (CH), 123.1 (CH), 122.5 (CH), 120.5 (CH), 115.6 (CH), 114.5 (CH), 80.0 (C), 66.8 (CH_2), 38.4 (CH_2), 30.8 (CH_2), 28.8 (3 x CH_3). HRMS (EI-MS) *m/z* calcd for $C_{20}H_{24}NaN_2O_5$ $[M+Na]^+$: 395.1577, found: 395.1575.

The intermediate nitro derivative (377 mg, 1.01 mmol) was suspended in EtOAc (30 mL) in a hydrogenation reactor. 10 % Pd/C (11 mg, 0.10 mmol, 0.1 equiv.) was then added and the reaction was stirred under 20 bars of hydrogen for 24 h. The reaction mixture was then filtered over Celite and concentrated under reduced pressure to give the aniline **65** as a yellow oil (0.345 g, quant.) which was used in the next step without further purification. R_f (PE/Et_2O 80/20) 0.11. IR (ATR diamond, cm^{-1}) ν: 3359, 2974, 2874, 1693, 1575, 1245, 1162, 773, 694. ^1H NMR (400 MHz, MeOD-d_4) δ 7.29 (t, $J = 7.9$ Hz, 1H, CH), 7.18–7.07 (m, 3H, CH), 6.98 (t, $J = 1.8$ Hz, 1H, CH), 6.95–6.90 (m, 1H, CH), 6.89–6.85 (m, 1H, CH), 6.73–6.67 (m, 1H, CH), 4.03 (t, $J = 6.3$ Hz, 2H, CH_2), 3.23 (q, $J = 6.3$ Hz 2H, CH_2), 1.93 (p, $J = 6.3$ Hz, 2H, CH_2), 1.44 (s, 9H, 3 x CH_3). ^{13}C NMR (101 MHz, MeOD-d_4) δ 160.7 (C), 158.5 (C), 149.0 (C), 144.4 (C), 143.3 (C), 130.6 (CH), 130.4 (CH), 120.4 (CH), 118.1 (CH), 115.7 (CH), 115.1 (CH), 114.3 (CH), 114.2 (CH), 80.0 (C), 66.6 (CH_2), 38.5 (CH_2), 30.8 (CH_2), 28.8 (3 x CH_3). HRMS (EI-MS) *m/z* calcd for $C_{20}H_{27}N_2O_3$ $[M+H]^+$: 343.2016, found: 343.2011.

*8.1.2.66. tert-butyl N-[3-[3-[3-[[4-(5-methyl-7H-pyrrolo [2,3-d]pyrimidin-4-yl)-3,6-dihydro -2H-pyridine-1-carbonyl]amino]phenyl]phenoxy] propyl]carbamate **(66)**.* The reaction was carried out as described in **method B** using the aniline **65** (300 mg, 0.88 mmol) and amine **9** (263 mg, 1.05 mmol, 1.2 equiv.) in THF (13 mL). The crude reaction mixture was purified by silica gel column chromatography using a gradient solvent system of CH_2Cl_2/acetone from 90/10 up to 50/50 to afford the urea derivative **66** (294 mg, 58 %) as a beige solid. R_f (CH_2Cl_2/acetone 50/50) 0.32. Mp: degradation 105 °C. IR (ATR diamond, cm^{-1}) ν: 3269, 2975, 1686, 1575, 1234, 1167, 1058, 777, 695. ^1H NMR (250 MHz, DMSO-d_6) δ 11.83 (s, 1H, NH), 8.67 (s, 1H, NH), 8.65 (s, 1H, CH), 7.81 (s, 1H, CH), 7.57 (d, $J = 7.9$ Hz, 1H, CH), 7.42–7.08 (m, 6H, 6 x CH), 6.97–6.84 (m, 2H, CH + NH), 6.06 (s, 1H, CH), 4.35–4.20 (m, 2H, CH_2), 4.04 (t, $J = 6.0$ Hz, 2H, CH_2), 3.76 (t, $J = 5.5$ Hz, 2H, CH_2), 3.21–3.02 (m, 2H, CH_2), 2.77–2.63 (m, 2H, CH_2), 2.25 (s, 3H, CH_3), 1.87 (p, $J = 6.6$ Hz, 2H, CH_2), 1.37 (s, 9H, 3 x CH_3). ^{13}C NMR (101 MHz, DMSO-d_6) δ 159.4 (C), 159.1 (C), 155.6 (C), 155.1 (C), 152.6 (C), 150.1 (CH), 141.9 (C), 141.0 (C), 140.2 (C), 134.3 (C), 129.9 (CH), 128.8 (CH), 128.3 (CH), 125.0 (CH), 120.2 (CH), 118.8 (CH), 118.8 (CH), 118.0 (CH), 114.3 (C), 113.3 (CH), 112.7 (CH), 108.9 (C), 77.5 (C), 65.3 (CH_2), 43.6 (CH_2), 40.6 (CH_2), 36.9 (CH_2), 29.3 (CH_2), 28.2 (3 x CH_3), 27.3 (CH_2), 12.9 (CH_3). HRMS (EI-MS) *m/z* calcd for $C_{33}H_{39}N_6O_4$ $[M+H]^+$: 583.3027, found: 583.3018.

*8.1.2.67. tert-butyl N-[3-[3-[3-[[4-(5-cyclopropyl-7H-pyrrolo [2,3-d]pyrimidin-4-yl)-3,6-dihydro-2H-pyridine-1-carbonyl]amino]phenyl]phenoxy] propyl]carbamate **(67)**.* The reaction was carried out as described in **method B** using the aniline **65** (210 mg, 0.61 mmol) and amine **14.HCl** (205 mg, 0.74 mmol, 1.2 equiv.) in THF (13 mL). The crude reaction mixture was purified by silica gel column chromatography using a gradient solvent system of CH_2Cl_2/acetone from 90/10 up to 50/50 to afford the urea derivative **67** (152 mg, 41 %) as a beige solid. R_f (CH_2Cl_2/acetone 50/50) 0.36. Mp: degradation 113 °C. IR (ATR diamond, cm^{-1}) ν: 3218, 2974, 1683, 1640, 1537, 1442, 1235, 1166, 1025, 776, 695. ^1H NMR (400 MHz, DMSO-d_6) δ 11.84 (s, 1H, NH), 8.65 (s, 2H, NH + CH), 7.80 (s, 1H, CH), 7.55 (d, $J = 8.0$ Hz, 1H, CH), 7.40–7.29 (m, 2H, CH), 7.26–7.22 (m, 2H, 2 x CH), 7.18 (d, $J = 7.8$ Hz, 1H, CH), 7.12 (s, 1H, CH), 6.96–6.86 (m, 2H, NH + CH), 6.32–6.26 (m, 1H, CH), 4.30–4.20 (m, 2H, CH_2), 4.04 (t, $J = 6.3$ Hz, 2H, CH_2), 3.77 (t, $J = 5.6$ Hz, 2H, CH_2), 3.11 (q, $J = 6.5$ Hz, 2H, CH_2), 2.81–2.66 (m, 2H, CH_2), 1.93–1.80 (m, 3H, CH + CH_2), 1.37 (s, 9H, 3 x CH_3), 0.86–0.76 (m, 2H, CH_2), 0.66–0.57 (m, 2H, CH_2). ^{13}C NMR (101 MHz, DMSO-d_6) δ 159.5 (C), 159.0 (C), 155.6 (C), 155.1 (C), 152.5 (C), 150.2 (CH), 141.8 (C), 141.0 (C), 140.1 (C), 134.1 (C), 129.9 (CH), 128.8 (CH), 128.3 (CH), 123.3 (CH), 120.1 (CH), 118.8 (CH), 118.0 (CH), 116.4 (C), 115.8 (CH), 114.5 (C), 113.3 (CH), 112.7 (CH), 77.5 (C), 65.3 (CH_2), 43.7 (CH_2), 40.6 (CH_2), 36.9 (CH_2), 29.3 (CH_2), 28.2 (3 x CH_3), 27.1 (CH_2), 8.6 (CH), 7.2 (2 x CH_2). HRMS (EI-MS) *m/z* calcd for $C_{35}H_{41}N_6O_4$ $[M+H]^+$: 609.3184, found: 609.3180.

*8.1.2.68. Bodipy probe **(68)**.* A solution of HCl (4 M in 1,4-dioxane, 0.34 mL, 8 equiv.) was slowly added to a solution of urea **66** (100 mg, 0.17 mmol) in CH_2Cl_2 (4 mL) at 0 °C and stirred at rt until the reaction was complete by TLC. The solvent was then evaporated under reduced pressure and the crude amine salt was used in the next step without further purification. Anhydrous DMF (12 mL) was added and the reaction placed under Ar. DIPEA (0.18 mL, 1.03 mmol, 6.0 equiv.), HOBt (70 mg, 0.52 mmol, 3.0 equiv.), and Bodipy FL [28] (55 mg, 0.19 mmol, 1.1 equiv.) were then added followed by EDC (91 μL, 0.52 mmol, 3.0 equiv.). The reaction was stirred at rt overnight. The reaction mixture was diluted with water (4 mL) and the aqueous layer extracted with EtOAc (3 x 15 mL). The combined organic layers were washed with brine, dried over $MgSO_4$, and the solvent removed under reduced pressure. The crude reaction mixture was purified by silica gel column chromatography using a gradient solvent system of CH_2Cl_2/MeOH from 100/0 up to 90/10 to afford the desired probe **68** (37 mg, 28 % two steps) as a red solid. R_f (CH_2Cl_2/acetone 95/5) 0.25. Mp: 129–131 °C. IR (ATR diamond, cm^{-1}) ν: 3268, 2918, 1643, 1600, 1529, 1132, 969, 728. ^1H NMR (400 MHz, $CDCl_3$) δ 9.70 (s, 1H, NH), 8.80 (s, 1H, CH), 7.60–7.55 (m, 1H, CH), 7.52–7.48 (m, 1H, CH), 7.34 (t, $J = 7.9$ Hz, 1H, CH), 7.30–7.23 (m, 2H, CH), 7.19–7.14 (m, 1H, CH), 7.08 (brs, 1H, CH), 7.04 (t, $J = 2.1$ Hz, 1H, CH), 6.95 (brs, 1H, CH), 6.86 (brs, 1H, NH), 6.80 (dd, $J = 8.2$, 2.5 Hz, 1H, CH), 6.75 (d, $J = 4.0$ Hz, 1H, CH), 6.23 (d, $J = 4.0$ Hz, 1H, CH), 6.16 (t, $J = 5.9$ Hz, 1H, NH), 6.06 (s, 1H, CH), 5.99 (s, 1H, CH), 4.27 (d, $J = 2.9$ Hz, 2H, CH_2), 3.93 (t, $J = 6.2$ Hz, 2H, CH_2), 3.82 (t, $J = 5.6$ Hz, 2H, CH_2), 3.42 (q, $J = 6.3$ Hz, 2H, CH_2), 3.26 (t, $J = 7.4$ Hz, 2H, CH_2), 2.87–2.77 (m, 2H, CH_2), 2.65 (t, $J = 7.4$ Hz, 2H, CH_2), 2.48 (s, 3H, CH_3), 2.26 (s, 3H, CH_3), 2.17 (s, 3H, CH_3), 1.92 (p, $J = 6.3$ Hz, 2H, CH_2). ^{13}C NMR (101 MHz, $CDCl_3$) δ 172.1 (C), 160.5 (C), 160.2 (C), 159.1 (C), 157.1 (C), 155.3 (C), 153.1 (C), 151.0 (CH), 144.2 (C), 142.4 (C), 141.7 (C), 139.7 (C), 135.5 (C), 135.3 (C), 133.4 (C), 129.8 (CH), 129.4 (CH), 128.4 (CH), 127.4 (CH), 123.9 (CH), 123.8 (CH), 122.0 (CH), 120.6 (CH), 119.8 (CH), 119.3 (CH), 118.9 (CH), 117.6 (CH), 115.4 (C), 113.6 (CH), 113.4 (CH), 110.8 (C), 65.9 (CH_2), 43.9 (CH_2), 41.1 (CH_2), 37.1 (CH_2), 36.2 (CH_2), 29.1 (CH_2), 28.1 (CH_2), 25.1 (CH_2), 15.0 (CH_3), 13.2 (CH_3), 11.4 (CH_3). HRMS (EI-MS): *m/z* calcd for $C_{42}H_{44}BF_2N_8O_3$ $[M+H]^+$: 757.3593; found: 757.3592.

*8.1.2.69. Bodipy probe **(69)**.* A solution of HCl (4 M in 1,4-dioxane, 0.26 mL, 8 equiv.) was slowly added to a solution of urea **67** (81 mg, 0.13 mmol) in CH_2Cl_2 (3 mL) at 0 °C and stirred at rt until the reaction was complete by TLC. The solvent was then evaporated under reduced pressure and the crude amine salt was used in the next step without further purification. Anhydrous DMF (10 mL) was added and the reaction placed under Ar. DIPEA (0.140 mL, 0.80 mmol, 6.0 equiv.), HOBt (54 mg, 0.40 mmol, 3.0 equiv.), and Bodipy FL [28] (43 mg, 0.15 mmol, 1.1 equiv.) were then added followed by EDC (71,2 μL, 0.40 mmol, 3.0 equiv.). The reaction was stirred at rt overnight. The reaction mixture was diluted with water (3 mL) and the aqueous layer extracted with EtOAc (3 x 10 mL). The combined organic layers were washed with brine, dried over $MgSO_4$, and the solvent removed under reduced pressure. The crude reaction mixture was purified by silica gel column chromatography using a gradient solvent system of CH_2Cl_2/MeOH from 100/0 up to 90/10 to afford the desired probe **69** (25 mg, 24 % two steps) as a red solid. R_f (CH_2Cl_2/acetone 90/10) 0.52. Mp: degradation 138 °C. IR (ATR diamond, cm^{-1}) ν: 3291, 2922, 1644, 1601, 1530, 1485, 1440, 1246, 1173, 1134, 1084, 970. ^1H NMR (250 MHz, $CDCl_3$) δ 10.18 (brs, 1H, NH), 8.80 (s, 1H, CH), 7.60–7.54 (m, 1H, CH), 7.50 (d, $J = 8.0$

Hz, 1H, CH), 7.33 (t, $J = 7.8$ Hz, 1H, CH), 7.26 (t, $J = 7.9$ Hz, 2H, 2 x CH), 7.15 (d, $J = 7.8$ Hz, 1H, CH), 7.04–7.01 (m, 1H, CH), 7.01–6.95 (m, 2H, CH + NH), 6.94 (s, 1H, CH), 6.82–6.73 (m, 2H, 2 x CH), 6.28–6.15 (m, 3H, 2 x CH, NH), 6.05 (s, 1H, CH), 4.32–4.18 (m, 2H, CH_2), 3.91 (t, $J = 6.1$ Hz, 2H, CH_2), 3.82 (t, $J = 5.5$ Hz, 2H, CH_2), 3.41 (q, $J = 6.3$ Hz, 2H, CH_2), 3.26 (t, $J = 7.3$ Hz, 2H, CH_2), 2.84 (s, 2H, CH_2), 2.65 (t, $J = 7.3$ Hz, 2H, CH_2), 2.48 (s, 3H, CH_3), 2.16 (s, 3H, CH_3), 1.91 (p, $J = 6.0$ Hz, 2H, CH_2), 1.85–1.74 (m, 1H, CH), 0.91–0.78 (m, 2H, CH_2), 0.62–0.51 (m, 2H, CH_2). ^{13}C NMR (101 MHz, $CDCl_3$) δ 172.1 (C), 160.5 (C), 160.4 (C), 159.1 (C), 157.1 (C), 155.4 (C), 153.0 (C), 150.8 (CH), 144.2 (C), 142.4 (C), 141.7 (C), 139.7 (C), 135.2 (C), 135.2 (C), 133.4 (C), 129.8 (CH), 129.4 (CH), 128.4 (CH), 127.7 (CH), 123.9 (CH), 122.5 (CH), 121.9 (CH), 120.6 (CH), 119.8 (CH), 119.4 (CH), 118.9 (CH), 118.2 (C), 117.5 (CH), 115.7 (C), 113.6 (CH), 113.4 (CH), 65.9 (CH_2), 44.0 (CH_2), 41.2 (CH_2), 37.1 (CH_2), 36.1 (CH_2), 29.1 (CH_2), 27.8 (CH_2), 25.1 (CH_2), 15.0 (CH_3), 11.4 (CH_3), 8.7 (CH), 7.5 (2 x CH_2). HRMS (EI-MS) *m/z* calcd for $C_{44}H_{46}BF_2N_8O_3$ $[M+H]^+$: 783.3749, found: 783.3755.

8.2. Biology

8.2.1. Cytotoxicity

HeLa cells were seeded at 10^3 cells per well in a 96 well plates. 24 h later, inhibitors at different concentrations were added. Forty-eight-hours later, cell cytotoxicity was assessed using CellTiter Glo® Luminescent cell viability assay from Promega following manufacturer's recommendations. Alternatively, for U-2 OS cells, cell viability was assessed using CellTiter A_{queous} One Solution Cell Proliferation Assay (Promega). For KHOS cells, cell viability was assessed using crystal violet staining as previously described [29].

For cell viability of the cancerous cell lines reported in Appendix A Table 1: Skin normal fibroblastic cells were purchased from Lonza (Basel, Switzerland), HuH7, Caco-2, MDA-MB-231, HCT116, PC3, MCF7 and NCI-H727 cancer cell lines were obtained from the ECACC collection (Porton Down, UK). Cells were grown at 37 °C, 5 % CO2 in ECACC recommended media: DMEM for HuH7, MDA-MB-231 and fibroblast, EMEM for MCF7 and CaCo-2, McCoy's for HCT116 and RPMI for PC3. All culture media were supplemented by 10 % of FBS, 1 % of penicillin-streptomycin and 2 mM glutamine.

Cytotoxic assays were performed as follows: Chemicals were solubilized in DMSO at a concentration of 10 mM (stock solution) and diluted in culture medium to the desired final concentrations. The dose effect cytotoxic assays (Ic50 determination) were performed by increasing concentrations of each chemical (final well concentrations: 0.1 μM–0.3 μM – 0.9 μM–3 μM – 9 μM - 25 μM). Cells were plated in 96 wells plates (4000 cells/well). Twenty-four hours after seeding, cells were exposed to chemicals. After 48h of treatment, cells were washed in PBS and fixed in cooled 90 % ethanol/5 % acetic acid for 20 min and the nuclei were stained with Hoechst 33342 (B2261 Sigma). Image acquisition and analysis was performed using a Cellomics ArrayScan VTI/HCS Reader (ThermoScientific). The survival percentages were calculated as the percentage of cell number after compound treatment over cell number after DMSO treatment. The relative Ic50 were calculated using the curve fitting XLfit 5.5.0.5 (idbs) integrates in Microsoft Excel as an add on. The 4 Parameter Logistic Model or Sigmoidal Dose-Response Model was used (fit = (A+((B-A)/(1+((C/x)^D))))).

8.2.2. Cell staining

HeLa cells were incubated with 10 μM of fluorescent inhibitors for 30 min. Then, cells were washed three times with PBS, fixed with CytoFix/CytoPerm™ from BD Biosciences, mounted on glass slides, and analyzed on a Carlzeiss Axio Observer Z1 videomicroscope.

For actin cytoskeleton labelling, HeLa cells were fixed in 4 % paraformaldehyde in PBS, permeabilized with 0.5 % Triton-X100 in PBS for 10 min at room temperature and incubated with mouse anti-acetyltubulin antibody followed with co-incubation of anti-mouse antibody conjugated with Alexa Fluor 488 and phalloidin conjugated with AlexaFluor568 for 1 h. Cells were then washed three times with PBS, mounted on glass slides, and analyzed on a Carlzeiss Axio Observer Z1 videomicroscope.

8.2.3. Cofilin phosphorylation measurement

HeLa cells were cultured under 5 % CO_2 at 37 °C in high glucose Dulbecco's modified Eagle's medium supplemented with 10 % fetal calf serum. They were seeded at 2.10^5 cells per well in a 6 well plates. 48 h later, inhibitors were added at a final concentration of 25 μM for 2 h as previously described [27]. Cells were lysed in 150 μl of 0.1 % Triton X-100 lysis buffer (50 mM Tris–HCl, pH 7.5, 100 mM NaCl, 5 mM EDTA, 50 mM NaF, 10 mM sodium pyrophosphate, 1 mM Na_3VO_4, 20 mM *p*-nitrophenyl phosphate, 20 mM β-glycerophosphate, 10 mg/ml aprotinin, 0.05 mg/ml okaidic acid, 1 mg/ml leupeptin, and 1 mM PMSF) and incubated on ice for 10 min. After centrifugation, the supernatants were analyzed by western blotting using anti-phospho-Ser3-cofilin, and anti-cofilin antibodies. Membranes were visualized with PXi imaging system (Syngene). Band quantification was performed with GeneTools software from Syngene. Antibodies anti-cofilin (#5175) and anti-phospho-Ser3-cofilin (#3313) are from Cell Signaling Technology.

8.2.4. Wound healing

U-2 OS, KHOS and HeLa cells were plated in 96-well plates (ZOOM-image Lock, Essen Bioscience) with DMEM medium containing 0.5 % FBS (fetal bovine serum). To create cell-free zones, scratch wounds were made in the cell monolayers, followed by gentle washing. Compounds or DMSO (used as control) were added to the cultures, with experiments conducted in eight copies. The migration assay was initiated by capturing images in real time using an IncuCyte system (Essen Bioscience) at hourly intervals for 48 h. The Relative Wound Density (RWD) served as the parameter for assessing cellular migration.

9. Crystallization and structure determination

The LIMK2 kinase domain (residues 330 to 632) was expressed and purified as previously described [30]. 100 nL of a solution containing $LIMK2_{330\text{-}632}$ (14 mg/mL) and compound **52** (500 μM) were transferred to a 3-well crystallization plate (Swissci), mixed with 50 nL of precipitant solution (0.04 M potassium phosphate, 20 % glycerol, 16 % PEG8000), and incubated at 20 °C. Crystals were spotted after 24 h and did not change appearance after 3 days. They were mounted in precipitant solution cryoprotected with additional 25 % ethylene glycol. Data were collected at Swiss Light Source (SLS) X06SA and analyzed, scaled, and merged with the SLS automated data processing (adp) pipeline [31]. The structure was solved by molecular replacement with Phaser [32] using a LIMK2 model as a template (PDB code 7QHG) [10] and refined with Phenix [33]. The model and structure factors have been deposited to the PDB with the code 8S3X (crystallographic parameters are included in Appendix A Table 3).

CRediT authorship contribution statement

Anthony Champiré: Validation, Investigation. **Rayan Berabez:** Validation, Investigation. **Abdennour Braka:** Methodology, Formal analysis. **Aurélie Cosson:** Validation, Investigation. **Justine Corret:** Validation, Investigation. **Caroline Girardin:** Validation, Investigation. **Amandine Serrano:** Validation, Investigation. **Samia Aci-Sèche:** Writing – review & editing, Methodology, Formal analysis. **Pascal Bonnet:** Supervision, Resources, Methodology. **Béatrice Josselin:** Methodology, Investigation, Formal analysis. **Pierre Brindeau:** Investigation. **Sandrine Ruchaud:** Writing – review & editing, Formal analysis. **Rémy Leguevel:** Investigation, Formal analysis. **Deep Chatterjee:** Validation, Investigation. **Sebastian Mathea:** Investigation, Formal analysis. **Stefan Knapp:** Formal analysis. **Régis Brion:** Validation, Resources, Investigation. **Franck Verrecchia:** Resources. **Béatrice**

Vallée: Writing – review & editing, Methodology, Formal analysis. **Karen Plé:** Writing – review & editing, Methodology, Data curation. **Hélène Bénédetti:** Writing – review & editing, Project administration. **Sylvain Routier:** Writing – original draft, Project administration, Conceptualization.

Declaration of competing interest

The authors declare that they have no known competing financial interests or personal relationships that could have appeared to influence the work reported in this paper.

Data availability

Data will be made available on request.

Acknowledgments

The authors would like to thank the "Région Centre Val de Loire" Licorne program, the C Valo and CNRS Innovation Pelican program, and the CNRS pre-maturation program for financing this research project. The ANR CliNeF1 (ANR_19_CE18) is gratefully acknowledged for PhD funding (R.B.). We would also like to thank the Cancéropôle Grand Ouest "marine molecules, metabolism and cancer network", IBiSA (French Infrastructure in Life Science: Biology, health and agronomy and the "Ligue contre le Cancer du Grand-Ouest" (comités des Deux Sèvres, du Finistère, de l'Ile et Villaine, du Loir et Cher, de Loire Atlantique, du Loiret, de la Vienne) for their financial support. The following projects contributed to funding of our Institute (ICOA): **CHemBio (FEDER-FSE 2014–2020-EX003677), Techsab (FEDER-FSE 2014–2020-EX011313), QUALICHIM (APR-IA-PF 2021–00149467), CPER FEDER ESTIM and RTR Motivhealth (2019–00131403) along with the Labex programs SYNORG (ANR-11-LABX-0029) and IRON (ANR-11-LABX-0018–01).** We thank M. Sainjeon, T. Lelievre, J. Chatelier and G. Bourdeau for their support during the synthesis of the chemical library, and the SALSA platform for spectroscopic measurements (IR, UV–Vis, Fluorimetry, Polarimetry), spectrometric and chromatographic analyses (NMR, HPTLC, HPLC, MS, HRMS), and analytical chemistry instrumentation.

Appendix A. Supplementary data

Supplementary data to this article can be found online at https://doi.org/10.1016/j.ejmech.2024.116391.

References

[1] K.M. Yamada, M. Sixt, Mechanisms of 3D cell migration, Nat. Rev. Mol. Cell Biol. 20 (2019) 738–752, https://doi.org/10.1038/s41580-019-0172-9.
[2] V. DesMarais, M. Ghosh, R. Eddy, J. Condeelis, Cofilin takes the lead, J. Cell Sci. 118 (2005) 19–26, https://doi.org/10.1242/jcs.01631.
[3] E. Villalonga, C. Mosrin, T. Normand, C. Girardin, A. Serrano, B. Žunar, M. Doudeau, F. Godin, H. Bénédetti, B. Vallée, L.I.M. Kinases, LIMK1 and LIMK2, are crucial Node Actors of the cell fate: molecular to Pathological features, Cells 12 (2023) 805, https://doi.org/10.3390/cells12050805.
[4] D. Chatterjee, F. Preuss, V. Dederer, S. Knapp, S. Mathea, Structural aspects of LIMK regulation and pharmacology, Cells 11 (2022) 142, https://doi.org/10.3390/cells11010142.
[5] C. Ruggiero, E. Lalli, Targeting the cytoskeleton against metastatic dissemination, Cancer Metastasis Rev. 40 (2021) 89–140, https://doi.org/10.1007/s10555-020-09936-0.
[6] J. Xu, Y. Huang, J. Zhao, L. Wu, Q. Qi, Y. Liu, G. Li, J. Li, H. Liu, H. Wu, Cofilin: a promising protein implicated in cancer metastasis and apoptosis, Front. Cell Dev. Biol. 9 (2021) 599065, https://doi.org/10.3389/fcell.2021.599065.
[7] F. Manetti, LIM kinases are attractive targets with many macromolecular partners and only a few small molecule regulators, Med. Res. Rev. 32 (2012) 968–998, https://doi.org/10.1002/med.20230.
[8] F. Manetti, Recent advances in the rational design and development of LIM kinase inhibitors are not enough to enter clinical trials, Eur. J. Org. Chem. 155 (2018) 445–458, https://doi.org/10.1016/j.ejmech.2018.06.016.
[9] R. Berabez, S. Routier, H. Bénédetti, K. Plé, B. Vallée, L.I.M. Kinases, Promising but reluctant therapeutic targets: chemistry and preclinical validation in vivo, Cells 11 (2022) 2090.
[10] T. Hanke, S. Mathea, J. Woortman, E. Salah, B.-T. Berger, A. Tumber, R. Kashima, A. Hata, B. Kuster, S. Müller, S. Knapp, Development and characterization of type I, type II, and type III LIM-kinase chemical probes, J. Med. Chem. 65 (2022) 13264–13287, https://doi.org/10.1021/acs.jmedchem.2c01106.
[11] L. He, S.P. Seitz, G.L. Trainor, D. Tortolani, W. Vaccaro, M. Poss, C.M. Tarby, J. S. Tokarski, B. Penhallow, C.-Y. Hung, R. Attar, T.-A. Lin, Modulation of cofilin phosphorylation by inhibition of the Lim family kinases, Bioorg. Med. Chem. Lett. 22 (2012) 5995–5998, https://doi.org/10.1016/j.bmcl.2012.07.002.
[12] P. Ross-Macdonald, H. de Silva, Q. Guo, H. Xiao, C.-Y. Hung, B. Penhallow, J. Markwalder, L. He, R.M. Attar, T.-a. Lin, S. Seitz, C. Tilford, J. Wardwell-Swanson, D. Jackson, Identification of a nonkinase target mediating cytotoxicity of novel kinase inhibitors, Mol. Cancer Therapeut. 7 (2008) 3490–3498, https://doi.org/10.1158/1535-7163.mct-08-0826.
[13] S.T. Wrobelski, S. Lin, K. Leftheris, L. He, S.P. Seitz, T.-A. Lin, W. Vaccaro, Phenyl-substituted Pyrimidine Compounds Useful as Kinase Inhibitors, 2006. WO 2006/084017 A2.
[14] S. Gory-Fauré, R. Powell, J. Jonckheere, F. Lanté, E. Denarier, L. Peris, C. H. Nguyen, A. Buisson, L. Lafanechère, A. Andrieux, Pyr1-Mediated pharmacological inhibition of LIM kinase restores synaptic plasticity and normal behavior in a mouse model of schizophrenia, Front. Pharmacol. 12 (2021), https://doi.org/10.3389/fphar.2021.627995.
[15] C. Prunier, R. Prudent, R. Kapur, K. Sadoul, L. Lafanechère, LIM kinases: cofilin and beyond, Oncotarget 8 (2017), https://doi.org/10.18632/oncotarget.16978.
[16] S. Boland, A. Bourin, J. Alen, J. Geraets, P. Schroeders, K. Castermans, N. Kindt, N. Boumans, L. Panitti, J. Vanormelingen, S. Fransen, S. Van de Velde, O. Defert, Design, synthesis and biological characterization of selective LIMK inhibitors, Bioorg. Med. Chem. Lett. 25 (2015) 4005–4010, https://doi.org/10.1016/j.bmcl.2015.07.009.
[17] B.A. Harrison, Z.Y. Almstead, H. Burgoon, M. Gardyan, N.C. Goodwin, J. Healy, Y. Liu, R. Mabon, B. Marinelli, L. Samala, Y. Zhang, T.R. Stouch, N.A. Whitlock, S. Gopinathan, B. McKnight, S. Wang, N. Patel, A.G.E. Wilson, B.D. Hamman, D. S. Rice, D.B. Rawlins, Discovery and development of LX7101, a dual LIM-kinase and ROCK inhibitor for the treatment of glaucoma, ACS Med. Chem. Lett. 6 (2015) 84–88, https://doi.org/10.1021/ml500367g.
[18] B.A. Harrison, N.A. Whitlock, M.V. Voronkov, Z.Y. Almstead, K.-j. Gu, R. Mabon, M. Gardyan, B.D. Hamman, J. Allen, S. Gopinathan, B. McKnight, M. Crist, Y. Zhang, Y. Liu, L.F. Courtney, B. Key, J. Zhou, N. Patel, P.W. Yates, Q. Liu, A.G. E. Wilson, S.D. Kimball, C.E. Crosson, D.S. Rice, D.B. Rawlins, Novel class of LIM-kinase 2 inhibitors for the treatment of ocular hypertension and associated glaucoma, J. Med. Chem. 52 (2009) 6515–6518, https://doi.org/10.1021/jm901226j.
[19] E. Amin, B.N. Dubey, S.-C. Zhang, L. Gremer, R. Dvorsky, J.M. Moll, M.S. Taha, L. Nagel-Steger, R.P. Piekorz, A.V. Somlyo, M.R. Ahmadian, Rho-kinase: regulation, (dys)function, and inhibition, Biol. Chem. 394 (2013) 1399–1410, https://doi.org/10.1515/hsz-2013-0181.
[20] N.C. Goodwin, G. Cianchetta, H.A. Burgoon, J. Healy, R. Mabon, E.D. Strobel, J. Allen, S. Wang, B.D. Hamman, D.B. Rawlins, Discovery of a type III inhibitor of LIM kinase 2 that binds in a DFG-out conformation, ACS Med. Chem. Lett. 6 (2015) 53–57, https://doi.org/10.1021/ml500242y.
[21] H. Djamai, J. Berrou, M. Dupont, A. Kaci, J.E. Ehlert, H. Weber, A. Baruchel, F. Paublant, R. Prudent, C. Gardin, H. Dombret, T. Braun, Synergy of FLT3 inhibitors and the small molecule inhibitor of LIM kinase1/2 CEL_Amide in FLT3-ITD mutated Acute Myeloblastic Leukemia (AML) cells, Leuk. Res. 100 (2021) 106490, https://doi.org/10.1016/j.leukres.2020.106490.
[22] J. Berrou, M. Dupont, H. Djamai, E. Adicéam, V. Parietti, A. Kaci, E. Clappier, J.-M. Cayuela, A. Baruchel, F. Paublant, R. Prudent, J. Ghysdael, C. Gardin, H. Dombret, T. Braun, Preclinical evaluation of a novel small molecule inhibitor of LIM kinases (LIMK) CEL_amide in philadelphia-chromosome positive (BCR::ABL+) acute lymphoblastic leukemia (ALL), J. Clin. Med. 11 (2022) 6761, https://doi.org/10.3390/jcm11226761.
[23] P. Malvi, D.S. Reddy, R. Kumar, S. Chava, S. Burela, K. Parajuli, X. Zhang, N. Wajapeyee, LIMK2 promotes melanoma tumor growth and metastasis through G3BP1-ESM1 pathway-mediated apoptosis inhibition, Oncogene (2023), https://doi.org/10.1038/s41388-023-02658-x.
[24] S. Routier, H. Bénédetti, B. Vallée-Meheust, P. Bonnet, K. Plé, S. Aci-Sèche, S. Ruchaud, A. Braka, A. Champiré, C. Andrès, P. Vourc'h, 4-(7H-pyrrolo[2,3-D] pyrimidin-4-yl)-3,6-dihydropyridine-(2H)-carboxamide Derivatives as Limk And/or Rock Kinases Inhibitors for Use in the Treatment of Cancer, 2021. WO2021239727 A1.
[25] R.C. Kanamarlapudi, M. Bednarz, W. Wu, P. Keyes, One-pot synthesis of 5-methyl-3H-pyrrolo[2,3-d]pyrimidin-4(7H)-one, Org. Process Res. Dev. 11 (2007) 86–89, https://doi.org/10.1021/op060207y.
[26] S. Routier, F. Buron, F. Suzenet, N. Rodrigues, S. Chalon, J. Vercouillie, D. Guilloteau, P. Emond, H. Marzag, Radiolabelled Compounds for Diagnosing Cholinergic Neurodegenerative Diseases, 2022. WO2022106714.
[27] R Prudent, E Vassal-Stermann, C.-H. Nguyen, C. Pillet, A Martinez, C. Prunier, et al., Pharmacological inhibition of LIM kinase stabilizes microtubules and inhibits neoplastic growth, Cancer Res. 72 (17) (2012) 4429–4439, https://doi.org/10.1158/0008-5472.can-11-3342.
[28] K. Gießler, H. Griesser, D. Göhringer, T. Sabirov, C. Richert, Synthesis of 3′-BODIPY-labeled active esters of nucleotides and a chemical primer extension assay on beads, Eur. J. Org. Chem. (2010) 3611–3620, https://doi.org/10.1002/ejoc.201000210, 2010.

[29] M. Mullard, M. Cadé, S. Morice, M. Dupuy, G. Danieau, J. Amiaud, S. Renault, F. Lézot, R. Brion, R.A. Thepault, B. Ory, F. Lamoureux, I. Corre, B. Brounais-LeRoyer, F. Rédini, F. Verrecchia, Sonic hedgehog signature in pediatric primary bone tumors: effects of the GLI antagonist GANT61 on ewing's sarcoma tumor growth, Cancers 12 (2020) 3438, https://doi.org/10.3390/cancers12113438.

[30] E. Salah, D. Chatterjee, A. Beltrami, A. Tumber, F. Preuss, P. Canning, A. Chaikuad, P. Knaus, S. Knapp, A.N. Bullock, S. Mathea, Lessons from LIMK1 enzymology and their impact on inhibitor design, Biochem. J. 476 (2019) 3197–3209, https://doi.org/10.1042/bcj20190517.

[31] W. Kabsch, XDS, Acta Crystallogr. D 66 (2010) 125–132, https://doi.org/10.1107/S0907444909047337.

[32] A.J. McCoy, R.W. Grosse-Kunstleve, L.C. Storoni, R.J. Read, Likelihood-enhanced fast translation functions, Acta Crystallogr. D 61 (2005) 458–464, https://doi.org/10.1107/S0907444905001617.

[33] D. Liebschner, P.V. Afonine, M.L. Baker, G. Bunkóczi, V.B. Chen, T.I. Croll, B. Hintze, L.W. Hung, S. Jain, A.J. McCoy, N.W. Moriarty, R.D. Oeffner, B.K. Poon, M.G. Prisant, R.J. Read, J.S. Richardson, D.C. Richardson, M.D. Sammito, O. V. Sobolev, D.H. Stockwell, T.C. Terwilliger, A.G. Urzhumtsev, L.L. Videau, C. J. Williams, P.D. Adams, Macromolecular structure determination using X-rays, neutrons and electrons: recent developments in Phenix, Acta Crystallogr D Struct Biol 75 (2019) 861–877, https://doi.org/10.1107/s2059798319011471.